BC-667
Dan-2012

xx(182698.1)

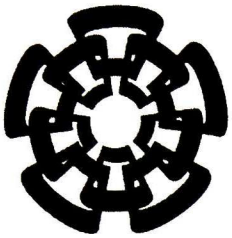

Centro de Investigación y de Estudios Avanzados
del Instituto Politécnico Nacional
Unidad Guadalajara

Control robusto por modos deslizantes de un sistema ABS

Tesis que presenta:

Juan Diego Sánchez Torres

para obtener el grado de:

Maestro en Ciencias

en la especialidad de:

Ingeniería Eléctrica

Directores de Tesis

Dr. Alexander Georgievich Loukianov
Dr. Jorge Rivera Dominguez

CINVESTAV del IPN Unidad Guadalajara, Guadalajara, Jalisco, Agosto de 2011.

BC-667
20 Loi/2012
Dec 2012

JD. 181209-1001

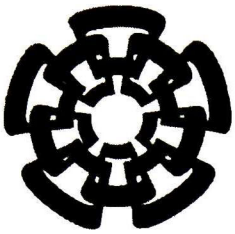

Centro de Investigación y de Estudios Avanzados

del Instituto Politécnico Nacional

Unidad Guadalajara

Robust sliding mode control of Antilock Brake System

A thesis presented by:
Juan Diego Sánchez Torres

to obtain the degree of:
Master in Science

in the subject of:
Electrical Engineering

Thesis Advisors:
Dr. Alexander Georgievich Loukianov
Dr. Jorge Rivera Dominguez

CINVESTAV del IPN Unidad Guadalajara,Guadalajara, Jalisco, August 2011

Control robusto por modos deslizantes de un sistema ABS

Tesis de Maestría en Ciencias
Ingeniería Eléctrica

Por:
Juan Diego Sánchez Torres
Ingeniero de Control
Universidad Nacional de Colombia 2001-2008

Becario de Conacyt, expediente no. 347739

Directores de Tesis
Dr. Alexander Georgievich Loukianov
Dr. Jorge Rivera Dominguez

CINVESTAV del IPN Unidad Guadalajara, Agosto de 2011

Robust sliding mode control of Antilock Brake System

Master of Science Thesis
In Electrical Engineering

By:
Juan Diego Sánchez Torres
Control Engineer
Universidad Nacional de Colombia 2001-2008

Scholarship granted by CONACYT, No. 347739

Thesis Advisors:
Dr. Alexander Georgievich Loukianov
Dr. Jorge Rivera Dominguez

CINVESTAV del IPN Unidad Guadalajara, August, 2011.

Agradecimientos

En primer lugar a mis papá, mi mamá, mis descendientes y mis hermanos. A mi abuela Marta y mi tío Iván, por todo su apoyo al momento de mi viaje de venida.

A mis asesores Dr. Alexander G. Loukianov y al Dr. Jorge Rivera por su conocimiento, su paciencia, sus opurtunas correcciones y buenas ideas.

A los sinodales Dr. Edgar Sánchez y Dr. Javier Ruiz por sus enseñanzas y por las correcciones que han ayudado a mejorar la calidad de este documento.

A mis compañeros de la generación 2009 (Incluye a Perla). Qué es líneal, completo, normado, y amarillo? Un espacio de Bananach!! Debo admitir que los voy a extrañar.

A las demás personas y profesores del CINVESTAV, muy especialmente a el Dr. Antonio Ramírez Treviño, al Dr. Juan Manuel Ramírez Arredondo y a Marcos Galicia. Muchas gracias!!

A las personas de la Universidad Nacional, mis compañeros de la generación de ingreso 2001 (Sin olvidar a Richard), a mis compañeros de inicio de maestría, a los profesores Héctor Botero, Jairo Espinosa, Gerard Olivar y, aunque fuera de la escuela, al profesor Hubertus Von Bremmen.

A todos mis amigos! Al Omar!

A México y a su gente buena y generosa.

A Diana Paola: *Básicamente la teoría de las catástrofes representa la propensión de los sistemas estructuralmente estables a manifestar discontinuidad (pueden producirse cambios repentinos del comportamiento o de los resultados), divergencia (tendencia de las pequeñas divergencias a crear grandes divergencias) e histéresis (el estado depende de su historia previa pero si los comportamientos se invierten conducen a que no se vuelva a la situación inicial).* Así eres tú para mi. Gracias por todo, por aparecer! Te adoro!

Finalmente, un agradecimiento muy especial CONACyT por otorgarme la beca que me ha permitido desarrollar esta tesis.

Dedicado:
A mis padres

" *The scientist does not study nature because it is useful;*
he studies it because he delights in it,
and he delights in it because it is beautiful.
If nature were not beautiful,
it would not be worth knowing,
and if nature were not worth knowing,
life would not be worth living. "

Henri Poincaré

Control robusto por modos deslizantes de un sistema ABS

Resumen

Se proponen un controlador basado en control por bloques con modos deslizantes y un controlador basado en modos deslizantes integrales anidados para un sistema antibloquéo de frenos (ABS). El problema de control es lograr seguimiento de referencia para de la tasa de deslizamiento de la llanta. De esta forma, la fricción entre el neumático y la calzada es suficiente para controlar el coche. Además, se propone el diseño de un regulador basado en control por bloques para asegurar asintóticamente seguimiento de la referencia y la estabilización de la dinámica residual, que consiste en la velocidad lineal del vehículo.

Adicionalmente se acopla una suspensión activa con el freno con el objetivo de garantizar la mejora de la calidad de marcha y la comodidad de los pasajeros. Para la suspensión activa, se propone un controlador basado modos deslizantes. Para el diseño de la superficie de deslizante se propone el uso de la forma regular y de métodos geométricos de control lineal con el fin de asegurar el seguimiento de la referencia y el rechazo de perturbaciones.

Todos estos controladores maximizan la fuerza de fricción en la rueda y evitan el bloquéo del freno y dan robustez ante perturbaciones *matched* y *unmatched*. Se consideran los casos de deformación y no deformación de los neumáticos También se muestran análisis detallados de estabilidad y robustez. El sistema de lazo cerrado es robusto en presencia de perturbaciones e incertidumbre. Para mostrar el desempeño de la estrategia de control propuesta, se lleva a cabo un estudio de simulación , donde los resultados muestran un buen comportamiento del ABS en las variaciones en la fricción de la carretera.

Robust Sliding Mode Control of Antilock Brake System

Abstract

A sliding mode block control and sliding mode based on the technique of integral nested sliding controllers are proposed to control an Antilock Brake System (ABS). The control problem is to achieve reference tracking for the slip rate, such that, the friction between tyre and road surface is good enough to control the car. Moreover, the design of a sliding mode block control regulator to ensure asymptotically output tracking with the stabilization of the residual dynamic consisting of the vehicle velocity for the brake system.

In addition, an active suspension is coupled with the brake with objective to guarantee the improvement of the ride quality and comfort for the passengers. For the active suspension, a controller based on the regular form, sliding mode control and geometric linear control methods for the sliding surface design is proposed in order to ensure output tracking.

All these controllers maximize the friction force in the wheel and avoids brake locking and provide robustness to matched, and unmatched perturbations. The cases of no deformation on the tire and with deformation are considered. Detailed stability and robustness analysis are presented. The closed-loop system is robust in presence of matched and unmatched perturbations. To show the performance of the proposed control strategy, a simulation study is carried on, where results show good behaviour of the ABS under variations of the road friction.

Contents

List of Figures

Chapter 1

Introduction

1.1 Preliminaries

The anti-lock brake systems (ABS) were originally developed to prevent wheels from locking up during hard braking [1], [2], [3]. Modern ABS systems not only try to prevent wheels from locking but also try to maximize the breaking forces generated by the tires to prevent that the longitudinal slip ratio exceeds an optimal value [4], [5].

First, note that locking of the wheels reduces the braking forces generated by the tires and causes the vehicle takes a longer time to stop. Further, locking of the front wheels prevents the driver from being able to steer the vehicles while it is coming to a stop. If the driver presses hard on the brakes, the wheels will slow down considerable faster than the vehicle slows down, resulting in a big slip ratio value. However, as described above, slip ratios higher than an optimal value actually result in reduced breaking forces. The vehicle would take longer to a stop if the slip ratio exceeds the optimal value. Then, the ABS goal is to prevent excessive brake torque from being applied on the wheels, so that the slip ratio does not exceed the optimal value. This fact would also prevent or delay the wheels from locking up and increase steerability of the vehicle during braking.

The ABS control problem consists in imposing a desired vehicle motion and as a consequence, providing adequate vehicle stability. On the other hand, active suspension are designed with the objective to improve the ride quality and comfort for the passengers. The main difficulties arising in the ABS design and control are due to its high non-linearities and uncertainties presented in the mathematical model. For the active suspension control design is necessary to cope with the disturbance due to road friction, which is unknown. Therefore, the ABS and active suspension have become two attractive examples for research in area of robust control.

There are several works reported in the literature in order to solve the problem of

automotive modelling, simulation, control, parameter identification and state observation.

A good introduction to automotive modelling is presented in [4], [5] and [6]. A research based in bond graph approach incorporating sensors, actuators, and vehicle dynamics is given in [7] and for modelling and estimation for tire-road system [8], this approach also allows the developing of controllers for vehicle safety. References [9], [10] present energy based techniques to obtain models of vehicle with tire-road interaction and for brake system. In [11] a further study in tire and vehicle dynamics is found. Reference [12] discusses an object oriented modelling and simulation of a pneumatic brake system with ABS. The modelling of ABS solenoid valves is also studied in [13].

For the case of braking system design, important challenges are associated with the estimation of the velocity and vehicle parameters. The friction coefficient estimation based on an extended Kalman filter is given in [14]; reference [15] presents the use of observers for tire/road contact friction using only wheel angular velocity information, and real-time identification of tire/road friction conditions and maximum tire/road friction coefficient are presented in [16] and [17], respectively. The use of longitudinal and lateral tire/road friction for vehicle motion control is presented in [18]. Triangular observers for road profiles inputs estimation [19], virtual sensors design in vehicle sideslip angle and velocity of the centre of gravity estimation [20] and the nonlinear estimation of longitudinal tire stiffness and effective radius [21] has been also studied; its principal applications are: adaptive emergency braking control with underestimation of friction coefficient [22], PI controllers for longitudinal slip control [23] and nonlinear adaptive tracking for ground vehicles [24].

So many solutions have been proposed as solutions for the design of control algorithms for antilock brake system (ABS) in order to obtain minimum time braking and increase steerability of the vehicle [25], [26]. Examples are based on the well known PID [27]; robust controllers [28], [29], [30] and approaches based on LMI [31]; optimal control based algorithms [32]; self-tuning control strategies [33]; minimum energy control laws [34]; control logics [35]. Besides, due to presence of high nonlinearities, solutions based in fuzzy and neural modelling and control are widely spread; neuro-adaptive control methods for ABS [36], [37], [38], [39]; fuzzy control [40], [41], [42], [43], [44], [45]; fuzzy PI controller [46]; neural network control [47], [48], [49], [50]; feedback linearization control using neural networks [51], [52] and [53]. Another important issue in design of braking systems and, particularly, ABS, is the development of control algorithms which maximize the tire/road friction; reference [54] presents an extremum seeking control strategy for ABS system and the paper [55] considers a time delay; a non-gradient extremum seeking control of feedback linearizable systems is given in [56] and a numerical optimization-based extremum seeking control is presented in [57]; [58] presents an ABS with a continuous wheel slip control to maximize the braking performance and, finally a dynamic method to forecast the wheel slip for ABS and its Experimental evaluation is presented in [59].

Sliding mode techniques arise as an attractive approach to deal with automotive problems due to its robustness and simplicity in design, examples of sliding mode controllers for vehicle traction control is presented in [60]; the use of high-order sliding control for mechanical systems is shown in [61] and observers in automotive systems is given in [62]. Particularly, sliding mode observers [63] have been illustrated to give very good results for observation and identification of mechanical systems [64], [65]; the papers [66], [67] present sliding mode observers for the estimation of velocities, wheel slip, radius, stiffness vehicle parameters, forces and states of the center of gravity; in [68] the use of second order sliding modes for observation and estimation of dynamics performance of heavy vehicle is shown and an experimental evaluation of a sliding mode observer for tire-road forces and an extended Kalman filter for vehicle sideslip angle is presented in [69]. Finally, a further research in sliding mode based analysis and identification of vehicle dynamics is given in [70].

The ABS design have also been dealt using the sliding mode technique; the wheel-slip sliding mode control with ABS [71], [72], [73]; direct measurement feedback sliding mode control [74], [75], [76], [77], [78]; sliding mode controller design with usage of sluggish actuators [79]; ABS control using optimum search via sliding modes [80] and optimal braking and estimation of tyre friction in automotive vehicles using sliding modes [81] are well-known proposed approaches. Other solutions are based on adaptive sliding mode control [82]; sliding mode-like fuzzy logic control considering uncertainties and disturbances [83]; sliding mode control with disturbance observer [84]; a sliding surface design to improve the performance of sliding mode controller [85]; a hybrid electric brake system with a sliding mode controller [86] and ABS sliding mode control for electric vehicles; sliding-mode PWM control of hydraulic ABS [87] and the use of second order sliding mode wheel slip control [88]. Finally, there are approaches that includes the joint analysis of the braking system and active suspension in order to improve vehicle performance [89]; for this problem a proportional integral sliding mode control is designed for an active suspension system in [90] and for the whole active suspension and brake system a fuzzy neural controllers for uncertain active suspension system with ABS is presented in [91] and a nonlinear control design based on backstepping for an ABS with assistance of active suspension is given in [92].

The majority of the mentioned above works does not consider real situations, as:

- For most of cases, the control input can take only two values "0" or "1" depending on the corresponding valve to be open or closed.
- For the joint case of analysis for the braking system and the active suspension, the road disturbances are assumed know in order to propose the control law.
- No further stability and robustness, specially for unmatched perturbations, is done.
- The actuator dynamics, the brake valve, it is not considered.

1.2 Objective

The main objective of this thesis is design of controllers on the basis of the block control approach and sliding mode for antilock brake system, providing a detailed analysis of stability and robustness.

The related tasks to accomplish this objective are:

- The design of a controller on the basis of the block control principle, sliding mode and the technique of integral nested sliding mode to ensure asymptotically tracking of the relative slip.
- The design of a sliding mode block control regulator to ensure asymptotically output tracking with the stabilization of the residual dynamic consisting of the vehicle velocity for the brake system.
- In addition, an active suspension is coupled with the brake to improve ride quality and comfort for the passengers. For the active suspension, a controller based on the regular form, sliding mode control and geometric linear control methods for the sliding surface design is proposed in order to achieve and ensure output tracking.

All these controllers must maximize the friction force in the wheel and avoid brake locking and provide robustness to matched, and unmatched perturbations. The cases of no deformation on the tire and with deformation are considered. Moreover, stability and robustness analysis are presented.

Throughout the development of the controller, we assume that all the state variables are available for measurement.

1.3 Contributions

This thesis presents the following contributions:

1. For the case of no tire deformation and the control input can taking only two values "0" or "1" for the valve being open or closed, as a first approach for the ABS problem, the joint application of sliding mode control and block control principle is proposed. The block control technique is used to design the sliding surface and to provide linear dynamics on the sliding nonlinear manifold.

2. Again, for the case of no tire deformation, we consider two situations. Firstly, it is supposed that the control input can only take only the values "0" and "1" for the two valve positions. Subsequently, the use of integral nested sliding mode is considered. The integral nested sliding mode control can guarantee robustness of the system throughout the entire response starting from the initial time instance, and reduces the sliding functions gains in comparison with standard sliding mode.

3. For the case of tire deformation, and assuming that the control input can only take only the values "0" and "1", for the two valve positions. The use of integral nested sliding mode is considered. The integral nested sliding mode control can guarantee the robustness of the system throughout the entire response starting from the initial time instance and reduce the sliding functions gains in comparison with standard sliding mode.

4. For the case of no tire deformation and the control input can take only two values "0" or "1" for the two valve positions, a sliding mode block control regulator for the asymptotically tracking of the relative slip to a desired trajectory is designed. To solve this problem, we propose to use the block control technique combined with the SM control algorithm to achieve robustness for perturbations, and to ensure asymptotic output tracking along with the stabilization of the residual dynamic consisting of the vehicle velocity. In order to accomplish such tasks, we follow:

   - first, the block control is used to linearize and asymptotically stabilize the output error dynamics, and derive a standard sliding variable,
   - second, it is defined the velocity error as a difference between real vehicle velocity and an auxiliary integral variable which estimates the vehicle velocity steady state value on the central manifold; finally,
   - following this procedure a sliding manifold is formed as a linear combination of the standard sliding variable and the velocity error and the SM control is implemented to ensure this manifold to be attractive.

   As a result, the vehicle dynamic, i.e., the vehicle velocity, on the designed SM manifold becomes asymptotically stable, ensuring an stable tracking error.

5. Finally, brake control with active suspension is presented. An ABS control based on integral nested sliding mode is designed in order to impose a desired vehicle motion and as a consequence, provides adequate vehicle stability. In the other hand, active suspension are designed with the objective to guarantee the improvement of the ride quality and comfort for the passengers. For the active suspension, another new controller based on the regular form, sliding mode control and geometric linear control methods for the sliding surface design is proposed in order to achieve robustness to

matched, and unmatched perturbations and ensure output tracking. As a result the vehicle dynamic, i.e., the vehicle velocity and horizontal position, on the designed SM manifolds becomes asymptotically stable with disturbance attenuation, ensuring an stable tracking error. The deformation on the tire is not considered and for both subsystems a Super-Twisting control is used.

1.4 Thesis structure

This thesis is organized as follows: The mathematical model for the longitudinal movement of a vehicle, including the brake system and the active suspension is presented in Chapter 2. In Chapter 3 a revision of the control methods to be applied is presented in detail. The proposed controllers with their stability and robustness analysis are presented in Chapter 4. Simulation results are presented in Chapter 5 to verify the robustness and performance of the proposed control strategy. Finally, conclusions and recommendations are presented in Chapter 6.

Chapter 2

Mathematical models

In this chapter, three dynamic models of a vehicle are discussed. The first one is presented in the section 2.1. We use a model which only regards one wheel, the so-called *quarter of vehicle model*; this model includes considers the pneumatic brake system dynamics, the wheel motion dynamics and the vehicle motion dynamics. In the section 2.2, the second model is presented; here, we use a quarter of vehicle model, this model considers the pneumatic brake system, the wheel motion, tire deformation and the vehicle motion. Finally, the third model is presented in section 2.3; this model considers the pneumatic brake system, the wheel motion, the vehicle motion and the dynamics of an active suspension.

2.1 Pneumatic brake system equations without tire deformation

In this section a model for pneumatic brake system, which does not consider tire deformation, is presented. The equations for the valve, the wheel and the vehicle motion are obtained from Newton mechanics.

2.1.1 Pneumatic brake system equations

The specific configuration of this system considers brake disks, which stop the wheels, as a result of the increment of the air pressure in the brake cylinder (Figure 2.1). The entrance of the air trough the pipes, from the central reservoir and the expulsion from the brake cylinder to the atmosphere is regulated by a common valve. This valve allows only one pipe to be open, when pipe 1 is open, pipe 2 is closed and vice versa. The time response of the valve is considered small, compared with the time constant of the pneumatic system. Let consider the Figure 2.1; we assume that the brake torque T_b is proportional to the pressure P_b inside

the brake cylinder

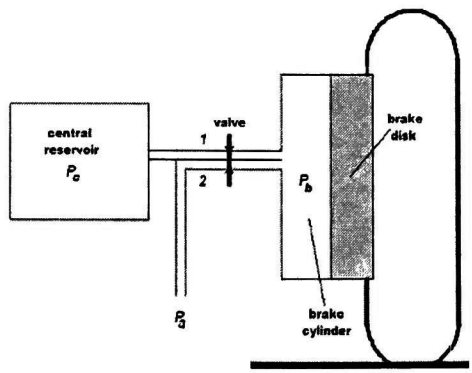

Figure 2.1: Pneumatic brake scheme

$$T_b = k_b P_b \tag{2.1.1}$$

with $k_b > 0$. For the brake system we use an approximated model, it considers pressure changes in the brake cylinder due to the opening of the valve with a first order relation [93]; this relation can be represented as

$$\tau \dot{P}_b + P_b = P_c u \tag{2.1.2}$$

where τ is the time constant of the pipelines, P_c is the pressure inside the central reservoir, u is the valve input signal. We consider two cases:

- When the control valve position is a continuous variable, the parameter τ of the equation (2.1.2) is constant.
- When the control input can take only two values "0" or "1", the opening and closing of the valve is momentary and the parameter τ of the equation (2.1.2) are given by the following rules:
  - If the pipe 1 is opened and 2 is closed, then $u = 1$ and $\tau = \tau_{in}$
  - If the pipe 2 is opened and 1 is closed, then $u = 0$ and $\tau = \tau_{out}$

For both cases, the atmospheric pressure P_a is considered equal to zero.

2.1.2 Wheel motion equations

To describe the wheels motion, we will use a partial mathematical model of the dynamic system as is done in [94], [95], [96] and [97].

Consider Figure 2.2, the dynamics of the angular momentum change relative to the rotation axis are given by

$$J\dot{\omega} = rf(s) - B_b\omega - T_b \tag{2.1.3}$$

where ω is the wheel angular velocity, J is the wheel inertia moment, r is the wheel radius, B_b is a viscous friction due to bearings coefficient and $f(s)$ is the wheel contact force .

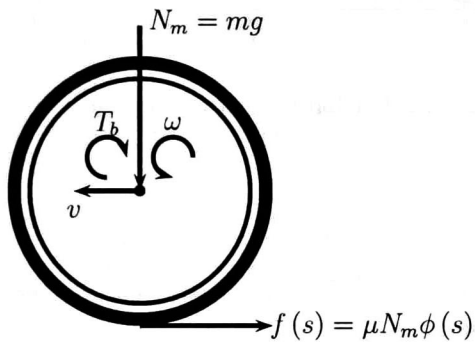

Figure 2.2: Wheel forces and torques

The expression for the contact force longitudinal component in the motion plane is

$$f(s) = \mu N_m \phi(s) \tag{2.1.4}$$

where μ is the nominal friction coefficient between the wheel and the road, N_m is the normal reaction force in the wheel

$$N_m = mg \tag{2.1.5}$$

with m equal to the mass supported by the wheel and g the gravity acceleration. Function $\phi(s)$ represents a friction/slip characteristic relation between the tire and road surface. Here, we use the Pacejka model [98], defined as follows:

$$\phi(s) = D\sin(C\arctan(Bs - E(Bs - \arctan(Bs)))) \tag{2.1.6}$$

With the following parameters $B = 10$, $C = 1.9$, $D = 1$ and $E = 0.97$ that function represents the friction relation under a dry surface condition. A plot of this function is shown in Figure 2.3. In general, this model produces a good approximation of the tire/road friction interface.

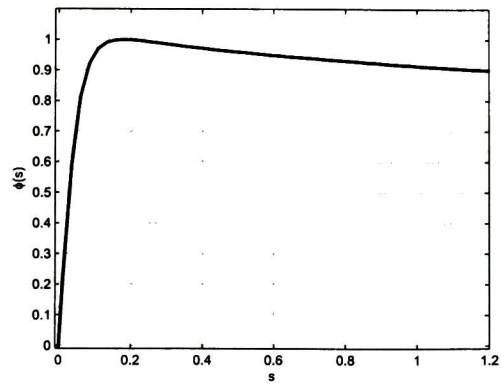

Figure 2.3: Characteristic function $\phi(s)$

The slip rate s is defined as

$$s = \frac{v - r\omega}{v} \tag{2.1.7}$$

where v is the longitudinal velocity of the wheel mass center. The equations (2.1.3)-(2.1.6) characterize the wheel motion.

2.1.3 The vehicle motion equation

The vehicle longitudinal dynamics without lateral motion considered is represented as

$$M\dot{v} = -F(s) - F_a(v) \tag{2.1.8}$$

where M is the vehicle mass; $F_a(v)$ is the aerodynamic drag force, which is proportional to the square of relative to wind vehicle velocity and is defined as:

$$F_a(v) = \frac{1}{2}\rho C_d A_f (v + v_w)^2$$

where ρ is the air density, C_d is the aerodynamic coefficient, A_f is the frontal area of vehicle, v_w is the wind velocity; the contact force of the vehicle F is modelled as:

$$F(s) = \mu\phi(s) N_M \tag{2.1.9}$$

where

$$N_M = Mg \tag{2.1.10}$$

is the normal reaction force of the vehicle, with M equal to the vehicle mass.

2.1.4 State space model

The dynamic equations of the whole system (2.1.1)-(2.1.8) can be rewritten using the state variables

$$\mathbf{x} = [x_1, x_2, x_3]^T = [\omega, P_b, v]^T$$

with initial conditions $x_0 = x(0)$ results as:

$$\begin{aligned} \dot{x}_1 &= -a_0 x_1 + a_1 f(s) - a_2 x_2 \\ \dot{x}_2 &= -a_3 x_2 + bu \\ \dot{x}_3 &= -a_4 F(s) - f_w(x_3) \\ y = s = h(x) &= 1 - r\frac{x_1}{x_3} \end{aligned} \tag{2.1.11}$$

Where $a_0 = B_b/J$, $a_1 = r/J$, $a_2 = k_b/J$, $a_3 = 1/\tau$, $a_4 = 1/M$, $b = P_c/\tau$ and $f_w(x_3) = \frac{1}{2M}(\rho C_d A_f)(x_3 + v_w)^2$

2.2 Pneumatic brake system equations with tire deformation

In this section, a model for pneumatic brake system considering tire deformation, is presented. The equations for the valve, the wheel and the vehicle motion are the same that the presented ones in the last section in equations (2.1.2), (2.1.3) and (2.1.8), respectively. To introduce the dynamics of the tire deformation, we will use a partial mathematical model of the dynamic system as is done in [94], [95], [96] and [97].

2.2.1 Tire deformation equations

Let consider Figure 2.4, the motion equation of the contact element with mass M_c is described by the tire longitudinal deformation. The interaction between this element and the rigid part of the wheel can be described by the following visco-elastic forces model

$$M_c \frac{d}{dt}\left(v - r\omega + \frac{d\hat{\xi}}{dt}\right) = f(s) - c_x \frac{d}{dt}\hat{\xi} - k_x \hat{\xi} \tag{2.2.1}$$

and the slip rate is

$$s = \frac{v - r\omega - \frac{d\hat{\xi}}{dt}}{v} \tag{2.2.2}$$

where c_x and k_x are the longitudinal constants of viscous and elastic behaviour of tire model, respectively.

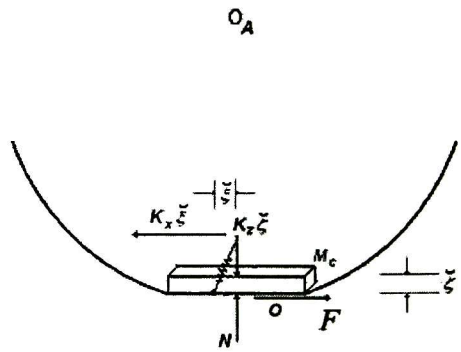

Figure 2.4: Deformation in the tire scheme

The dynamic equations of the whole system (2.1.2), (2.1.3), (2.1.8) and (2.2.1) can be rewritten in a more useful form as:

$$\begin{aligned} \tau \dot{P}_b + P_b &= P_c u \\ J\dot{\omega} &= rf(s) - B_b\omega - T_b \\ M\dot{v} &= -F(s) - F_a(v) \\ M_c\frac{d^2\hat{\xi}}{dt^2} + c_x\frac{d\hat{\xi}}{dt} + k_x\hat{\xi} &= \left(\frac{M_c r^2}{J} + 1\right) f(s) - \frac{M_c r}{J}T_b - \frac{M_c B_b r}{J}\omega + \frac{M_c}{M}F(s) + \frac{1}{M}F_a(v) \end{aligned} \tag{2.2.3}$$

with the slip defined in (2.2.2).

2.2.2 State space model

The system (2.2.3) is represented using the state variables $x = [x_1, x_2, x_3, x_4, x_5]^T = \left[\omega, P_b, \hat{\xi}, \frac{d\hat{\xi}}{dt}, v\right]^T$ with initial conditions $x_0 = x(0)$ as:

$$\begin{aligned}
\dot{x}_1 =& c_1 (r f(s) - B_b x_1 - k_b x_2) \\
\dot{x}_2 =& -c_2 x_2 + bu \\
\dot{x}_3 =& x_4 \\
\dot{x}_4 =& -a_{41} x_1 - a_{42} x_2 - a_{43} x_3 - a_{44} x_4 + f_4(x_1, x_4) \\
\dot{x}_5 =& -c_3 F(s) - f_w(x_5)
\end{aligned} \tag{2.2.4}$$

with output

$$y = s = h(x) = 1 - r\frac{x_1}{x_5} - \frac{x_4}{x_5}$$

where $b = c_2 k_b P_c$, $c_1 = 1/J$, $c_2 = 1/\tau$, $c_3 = 1/M$, $a_{41} = (B_b r)/J$, $a_{42} = (r k_b)/J$, $a_{43} = k_x/M_c$, $a_{44} = c_x/M_c$, $f_4(x_1, x_4) = \left(\frac{r^2}{J} + \frac{1}{M_c}\right) f(s) + \frac{1}{M} F(s) + \frac{1}{M M_c} F_a(v)$ and $f_w(x_5) = \frac{1}{2M}(x_5 + v_{wind})^2$

2.3 Active suspension model

In this section, the dynamic model of a vehicle active suspension and ABS subsystems is discussed. Here we consider a quarter of vehicle model, this model includes the active suspension, the pneumatic brake system, the wheel motion and the vehicle motion.The equation for the active suspension are obtained in the following subsection.

2.3.1 Suspension

The quarter-car active suspension is a 2-DOF mechanical system shown in Figure 2.5.

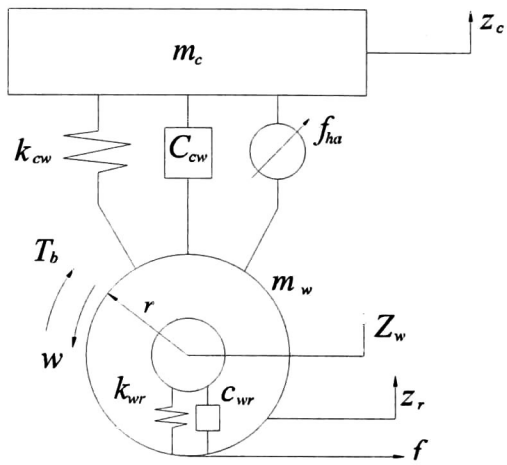

Figure 2.5: Pneumatic brake scheme

This system connects the car body and the wheel masses and is modelled as a linear viscous damper and a spring elements, whereas the tire is represented as a linear spring and damping elements. The motion equations for this system are governed by

$$\begin{aligned} m_c\ddot{z}_c &= -K_{cw}(z_c - z_w) - C_{cw}(\dot{z}_c - \dot{z}_w) + f_{ha} \\ m_w\ddot{z}_w &= K_{cw}(z_c - z_w) + C_{cw}(\dot{z}_c - \dot{z}_w) \\ &\quad -K_{wr}(z_w - z_r) - C_{wr}(\dot{z}_w - \dot{z}_r) - f_{ha} \end{aligned} \tag{2.3.1}$$

where m_c and m_w are the mass of the car an the wheel, respectively, z_c is the car vertical displacement, z_w is the wheel vertical displacement, K_{cw} and K_{wr} are the spring coefficients, C_{cw} and C_{wr} are the damping coefficients, z_r is the disturbance due to road and f_{ha} is the force of the hydraulic actuator.

The equations for the valve, the wheel and the vehicle motion are similar to the presented in equations (2.1.2), (2.1.3) and (2.1.8), respectively. But, instead of the definition of normal reaction forces N_m and N_M given in (2.1.5) and (2.1.10), respectively, and considering the equation (2.3.1) we have that the normal reaction of the wheel is defined by:

$$N_m = mg - K_{wr}(z_w - z_r) - C_{wr}(\dot{z}_w - \dot{z}_r)$$

and the normal reaction force of the vehicle is defined by:

$$N_M = Mg - K_{wr}(z_w - z_r) - C_{wr}(\dot{z}_w - \dot{z}_r)$$

2.3.2 State space equations

The dynamic equations of the whole system (2.1.2), (2.1.3), (2.1.8) and (2.3.1), can be rewritten using the state variables $x = [x_1, x_2, x_3, x_4, x_5, x_6, x_7]^T = [z_c, \dot{z}_c, z_w, \dot{z}_w, \omega, P_b, v]^T$ as:

$$\begin{aligned}
\dot{x}_1 &= x_2 \\
\dot{x}_2 &= -a_1(x_1 - x_3) - a_2(x_2 - x_4) + b_1 u_s \\
\dot{x}_3 &= x_4 \qquad (2.3.2) \\
\dot{x}_4 &= a_3(x_1 - x_3) + a_4(x_2 - x_4) - a_5(x_3 - z_r) - a_6(x_4 - \dot{z}_r) - b_2 u_s \\
\dot{x}_5 &= -a_7 x_5 + a_8 f(s) - a_9 x_6 \\
\dot{x}_6 &= -a_{10} x_6 + b_3 u_b \qquad (2.3.3) \\
\dot{x}_7 &= -a_{11} F(s) - f_w(x_7)
\end{aligned}$$

with the outputs

$$y_1 = x_1 \text{ and } y_2 = x_5$$

where $a_1 = K_{cw}/m_c$, $a_2 = C_{cw}/m_c$, $a_3 = K_{cw}/m_w$, $a_4 = C_{cw}/m_w$, $a_5 = K_{wr}/m_w$, $a_6 = C_{wr}/m_w$, $a_7 = b_b/J$, $a_8 = r/J$, $a_9 = k_b/J$, $a_{10} = 1/\tau$, $a_{11} = 1/M$, $b_1 = 1/m_c$, $b_2 = 1/m_w$, $b_3 = 1/\tau$, $u_s = f_{ha}$, $u_b = P_c$ and $f_w(x_7) = \frac{1}{2M}(\rho C_d A_f)(x_7 + v_w)^2$

2.4 Conclusions

In this chapter we have presented three models for the wheel-brake system with their state space representations, the last one including an active suspension. It is worth to noticing that the first two models represent the same situation, the difference is that the second one is a detailed version of the first and includes equations of the tire deformation. All these models will be used in the design and simulation of the control algorithms proposed in the following chapters.

Chapter 3

Control methods

The sliding mode control (SMC) technique is known as a suitable control method for handling nonlinear systems with uncertain dynamics and disturbances [99], [100], [101]. Control design for nonlinear multivariable systems has been widely studied, while the design procedure of high order nonlinear control systems can be complicated and varies from case to case. [102] suggest a decomposition design approach transforming the original plant into the so-called *regular form*, which facilitates the controller design. The SMC of the regular form has been well established for a class of linear systems. For a high order linear system, the block control approach [103], [104] can be incorporated into the design of the SMC.

Several approaches based on block control have been proposed. Here, we empathize on the so-called Integral Sliding Modes with Block Control; this technique is based on integral Sliding Mode (SM) [101] in combination with nested SM [105] and allows to achieve robustness to matched, and unmatched perturbations, and to ensure output tracking. Theoretically, this integral nested SM control can guarantee the robustness of the system throughout the entire response starting from the initial time instance and reduce the sliding functions gains in comparison with standard SM.

The Regular Form is presented in Section 3.1. It provides a convenient interpretation of the reduced order dynamics given by sliding mode control, decoupling the system into two subsystems of lower dimensions. In Section 3.2 Block Control is introduced as a method for decomposition and design robust controllers for dynamical systems. In Section 3.3, Integral Sliding Mode with Block Control is presented. Finally, chapter conclusions are given in Section 3.4.

3.1 The regular form

In this section a particular canonical for, the so-called *regular form* is presented to obtain a convenient interpretation of the reduced order dynamics provided by sliding mode control, decoupling the system into two subsystems of lower dimensions.

3.1.1 The regular form representation of a class of dynamical systems

Consider an affine system,

$$\dot{\mathbf{x}} = \mathbf{f}(x) + \mathbf{B}(x)\,\mathbf{u} \tag{3.1.1}$$

where $\mathbf{x} \in \mathbb{R}^n$, $\mathbf{u} \in \mathbb{R}^m$, $\mathbf{B} \in \mathbb{R}^{n\times m}$, and $\operatorname{rank}(\mathbf{B}) = m < n$. Following the regular form design approach, a nonlinear transformation should be found such that the system is decoupled into two subsystems of lower dimensions $(n-m)$ and m:

$$\begin{cases} \dot{\mathbf{x}}_1 = \mathbf{f}_1(\mathbf{x}_1, \mathbf{x}_2) \\ \dot{\mathbf{x}}_2 = \mathbf{f}_2(\mathbf{x}_1, \mathbf{x}_2) + \mathbf{B}_2(\mathbf{x}_1, \mathbf{x}_2)\,\mathbf{u} \end{cases} \tag{3.1.2}$$

where $\mathbf{x}_1 \in \mathbb{R}^{n-m}$, $\mathbf{x}_2 \in \mathbb{R}^m$, $\mathbf{u} \in \mathbb{R}^m$ and $\det(\mathbf{B}_2) \neq 0$. The system (3.1.2), where the dimension of the lower equation coincides with that of the control input $\mathbf{u}$ and the upper equation does not depend on the real control, is referred to as a *regular form* [102].

The idea of transformation is formulated in the following way: Let $y^T = \left[y_1^T, y_2^T\right]$ be a vector of new state variables defined by the nonlinear transformation

$$\mathbf{y}_1 = \phi(\mathbf{x}), \quad y_2 = \mathbf{x}_2, \tag{3.1.3}$$

where the vector function $\phi(x)$ is continuous and continuously differentiable with respect to x. The equations with respect to y_1,

$$\dot{y}_1 = \frac{\partial \phi(\mathbf{x})}{\partial \mathbf{x}} f(\mathbf{x}) + \frac{\partial \phi(\mathbf{x})}{\partial \mathbf{x}} \mathbf{B}(\mathbf{x})\,\mathbf{u}, \tag{3.1.4}$$

will be independent of the control if the vector function $\phi(x)$ is a solution to the matrix partial differential equation

$$\frac{\partial \phi(\mathbf{x})}{\partial \mathbf{x}} \mathbf{B}(x) = 0. \tag{3.1.5}$$

Necessary and sufficient conditions for solving the equation (3.1.5) may be found based on the theory of Pfaffian's form in the text book of Rashevskii [106]. It should be noticed that partial differential equations of this type need strong solvability conditions. In [102] authors have investigated this problem and proposed a design regularization algorithm. It

has been established that the regularization problem is solvable only for one class of systems which fulfills the Frobenius' theorem conditions. The reader is referred to [99] for a complete overview of this approach applied to both single-input and multiple-input.

According to system (3.1.2), the sliding mode control approach assumes that u is a discontinuous control enforcing sliding mode in the manifold $S(x) = 0$ with m selected switching surfaces denoted by the vector $S(\mathbf{x}) = [s_1(\mathbf{x}), s_2(\mathbf{x}), \ldots, s_m(\mathbf{x})]^T$ After sliding mode occurs on $S(\mathbf{x}) = 0$, m components of the state vector are function of the remaining $(n - m)$ ones: $\mathbf{x}_2 = S_0(\mathbf{x}_1)$. As a result, the sliding mode equation along the manifold $S(\mathbf{x}) = \mathbf{x}_2 - S_0(\mathbf{x}_1) = 0$ is

$$\dot{\mathbf{x}}_1 = \mathbf{f}_1(\mathbf{x}_1, S_0(\mathbf{x}_1)). \tag{3.1.6}$$

In other words, the evolution of the upper subsystem in (3.1.2) is determined by equation (3.1.6). The desired dynamics of sliding mode can be designed by a proper choice of the function $S_0(\mathbf{x}_1)$ which takes part of the reduced order system dynamics(3.1.6).

To confine the state trajectory to the preselected manifold $S(\mathbf{x})$, the discontinuous control $\mathbf{u} = -\mathbf{M}\text{sign}(S(\mathbf{x}))$ can be directly employed. If the existence condition of sliding mode [101] is satisfied by proper selection of the input gain matrix $\mathbf{M}$, the state trajectory is driven to reach the manifold $S(x)$ in finite time. Accordingly, sliding mode takes place in the switching manifold and follows the desired system dynamics. It can be seen that the order of the system is reduced from n to $(n - m)$. In addition, due to the equal dimension of the control inputs and state vectors, the controller design for the lower subsystem is very simple. Therefore, the original problem is decomposed into two independent sub-problems of lower dimension, and both of them can be solved individually.

Repeating the above control design procedure to the upper subsystem of (3.1.2), and decoupling it into subsystems of lower dimensions is the core idea of the block control approach [107]; details will be discussed in the following section.

3.1.2 The regular form representation of linear system

The consideration is given to control in the multidimensional linear system, as a particular case of the system (3.1.1)

$$\dot{\mathbf{x}} = \mathbf{A}\mathbf{x} + \mathbf{B}\mathbf{u}, \tag{3.1.7}$$

with $\mathbf{x} \in \mathbb{R}^n$, $\mathbf{u} \in \mathbb{R}^m$ and without loss of generality it is assumed that the rank of matrix $\mathbf{B}$ or control space dimensionality coincides with the control dimensionality, namely $\text{rank}\mathbf{B} = m$.

Indeed, if the column vectors of matrix $\mathbf{B}$ are linearly dependent, then

$$\mathbf{B}\mathbf{u} = \mathbf{B}_1\Lambda\mathbf{u} = \mathbf{B}_1\mathbf{u}_1, \quad \mathbf{u}_1 = \Lambda\mathbf{u}, \quad \mathbf{u}_1 \in \mathbb{R}^{m_1}$$

where $\mathbf{B}_1$ is $(n \times m_1)$-dimensional matrix, $m_1 < m$, consisting control space base vectors, $\mathbf{\Lambda}$ is constant $(m_1 \times m)$-dimensional matrix whose column elements are the coefficients of the matrix columns expansion $\mathbf{B}$ with respect to base vectors. As the result, there is a system with a new control $\mathbf{u}_1$ having lower dimensionality coincides with that of the control space.

From the condition

$$\text{rank}\mathbf{B} = m_1$$

follows that

$$\text{rank}\mathbf{\Lambda} = m_1.$$

The original control $\mathbf{u}$ can be determined after designing the control $\mathbf{u}'$

Thus,

$$\text{rank}\mathbf{B} = m. \tag{3.1.8}$$

The control vector components have discontinuities on some planes $S_i(\mathbf{x}) = 0$, $i = 1, \ldots, m$, which should be chosen such that sliding mode motion on their intersection

$$\mathbf{s} = \mathbf{C}\mathbf{x} = \mathbf{0}, \quad \mathbf{s}^T = (s_1(\mathbf{x}), \ldots, s_m(\mathbf{x})) \tag{3.1.9}$$

have a equation with dynamics given by the allocation of characteristic equation roots.

This problem will be solved in the space of new variables related to the original ones by a non-singular linear transformation

$$\mathbf{x}' = \mathbf{M}\mathbf{x}, \quad \mathbf{x}' \in \mathbb{R}^n \tag{3.1.10}$$

such that

$$\mathbf{M}\mathbf{B} = \begin{pmatrix} 0 \\ \mathbf{B}_2 \end{pmatrix} \tag{3.1.11}$$

where $\mathbf{B}_2$ is quadratic $(m \times m)$-dimensional matrix.

In order to satisfy condition (3.1.11), the first $(n - m)$ rows of matrix $\mathbf{M}$ should be composed of the base of $(n - m)$-dimensional subspace orthogonal to the control subspace. The remaining m rows are chosen so that $\text{rank}\mathbf{M} = n$ and the $\mathbf{B}_2$ is non-singular. For example, $\mathbf{B}^T$ can be taken as these rows, then

$$\mathbf{B}_2 = \mathbf{B}^T\mathbf{B} \quad \text{and} \quad \det \mathbf{B}_2 \neq 0$$

The behaviour of (3.1.7) in the space $\mathbf{x}'$ is described by

$$\dot{\mathbf{x}}' = \mathbf{M}^{-1}\mathbf{A}\mathbf{M}\mathbf{x} + \mathbf{M}\mathbf{B}\mathbf{u}$$

or

$$\dot{\mathbf{x}}_1 = \mathbf{A}_{11}\mathbf{x}_1 + \mathbf{A}_{12}\mathbf{x}_2 \tag{3.1.12}$$

$$\dot{\mathbf{x}}_2 = \mathbf{A}_{21}\mathbf{x}_1 + \mathbf{A}_{22}\mathbf{x}_2 + \mathbf{B}_2\mathbf{u} \tag{3.1.13}$$

where $\mathbf{x}_1$ and $\mathbf{x}_2$ are vectors consisting of $(n-m)$ and m components of vector $\mathbf{x}'$ and

$$\mathbf{M}^{-1}\mathbf{A}\mathbf{M} = \begin{pmatrix} \mathbf{A}_{11} & \mathbf{A}_{12} \\ \mathbf{A}_{21} & \mathbf{A}_{22} \end{pmatrix}$$

The equation of the manifold $\mathbf{s} = 0$ with respect to the new variables, correspondingly, has the form

$$\mathbf{s} = \mathbf{C}_1\mathbf{x}_1 + \mathbf{C}_2\mathbf{x}_2$$

where $\mathbf{C}\mathbf{M}^{-1} = (\mathbf{C}_1, \mathbf{C}_2)$, $\mathbf{C}_1 \in \mathbb{R}^{m\times n}$ and $\mathbf{C}_2 \in \mathbb{R}^{m\times m}$ Below, consideration will be given only for discontinuity surfaces for which

$$\det \mathbf{C}\mathbf{B} \neq \mathbf{0}$$

i.e. the sliding equation can be written unambiguously.

Since $\mathbf{C}\mathbf{B} = \mathbf{C}_2\mathbf{B}_2$ this requirement amounts to the condition

$$\det \mathbf{C}_2 \neq \mathbf{0}$$

Without loss of generality, one can confine oneself to the case of

$$\mathbf{C}_2 = \mathbf{I}_m$$

which is due to the invariance property to linear transformation of the vector $\mathbf{s}$.

3.2 Block control

The problem of decomposition and design robust controllers for dynamical systems is one of interesting problem in the control theory. A fruitful and relatively simple approach to solve this problem, especially when dealing with multivariable nonlinear uncertain ones, is based on the use of Variable Structure Control approach with sliding mode, Utkin [108]. This approach enables high accuracy and robustness to disturbances and system parameter variations to be obtained. Second, the control design problem is conveniently divided into two sub-problems: (a) the design of nonlinear sliding surfaces enforcing motion according to the specified closed-loop performance, and (b) determination of a control law providing stable motion in the sub-state space of the surface.

In order to illustrate the decomposition potential with the use of the above technique, consider the following system subject to uncertainty:

$$\dot{\mathbf{x}} = \mathbf{f}(\mathbf{x}, t) + \mathbf{B}(\mathbf{x}, \mathbf{t})\,\mathbf{u} + \mathbf{g}(\mathbf{x}, \mathbf{t}) \tag{3.2.1}$$

where $\mathbf{x} \in \mathbf{X} \subset \mathbb{R}^n$ is the state vector, $\mathbf{u} \in \mathbf{U} \subset \mathbb{R}^m$ is the control vector to be bounded by

$$|u_i| \leq M \quad \text{with} \quad M > 0, \quad \mathbf{u} = (u_1, \ldots, u_m)^T \tag{3.2.2}$$

The unknown mapping $\mathbf{g}(\mathbf{x}, t)$ characterizes external disturbances and parameter variations which should not affect the feedback systems. It is assumed the vector fields $\mathbf{f}(\mathbf{x}, t)$ and $\mathbf{g}(\mathbf{x}, t)$, and the columns of $\mathbf{B}(\mathbf{x}, t)$ are smooth and bounded mappings of class $C^{\infty}_{[0,\infty)}$, $\mathbf{f}(\mathbf{0}, t) = 0$, and $\operatorname{rank}(\mathbf{B}(\mathbf{x}, t)) = m$ for all $\mathbf{x} \in \mathbf{X}$ and $t \geq 0$. The standard sliding mode design procedure comprises two sub-problems.

$$\mathbf{s}(\mathbf{x}) = 0, \quad \mathbf{s} = (s_1, \ldots, s_m)^T \tag{3.2.3}$$

must to selected such that the matrix $\mathbf{GB}$ $(\mathbf{G} = \partial \mathbf{s}/\partial \mathbf{x})$ has full rank for $\mathbf{x} \in \mathbf{X}$ and $t \geq 0$, and the sliding mode (SM) equation

$$\dot{\mathbf{x}} = \mathbf{f}_s(\mathbf{x}, t) + \mathbf{g}_s(\mathbf{x}, \mathbf{t}), \quad \mathbf{g}(\mathbf{x}) = \mathbf{0} \tag{3.2.4}$$

where $\mathbf{f}_s = \left(\mathbf{I}_n - \mathbf{B}(\mathbf{GB})^{-1}\mathbf{G}\right)\mathbf{f}$ and $\mathbf{g}_s = \left(\mathbf{I}_n - \mathbf{B}(\mathbf{GB})^{-1}\mathbf{G}\right)\mathbf{g}$, has the desired properties, including stability. Secondly, a discontinuous control

$$\mathbf{u}_i(\mathbf{x}, t) = \begin{cases} \mathbf{u}_i^+(\mathbf{x}, t) & \text{if } s_i(x) > 0, \quad i = 1, \ldots, m \\ \mathbf{u}_i^-(\mathbf{x}, t) & \text{if } s_i(x) < 0, \end{cases} \tag{3.2.5}$$

is introduced to guarantees convergence of the closed-loop system projection motion in the subspace $\mathbf{s}$, described by

$$\dot{\mathbf{s}} = \mathbf{Gf} + \mathbf{GBu} + \mathbf{Gg}$$

where $\mathbf{u}_i^+(\mathbf{x}, t)$ and $\mathbf{u}_i^-(\mathbf{x}, t)$, are smooth functions to be selected. If $\mathbf{g}(\mathbf{x}, t)$ satisfies the so called *matching condition*, [109], $\mathbf{g}(\mathbf{x}, t) \in \operatorname{span}\mathbf{B}(\mathbf{x}, t)$, i.e. there exists vector $\mu(\mathbf{x}, t)$ such that

$$\mathbf{g}(\mathbf{x}, t) = \mathbf{B}(\mathbf{x}, t)\,\mu(\mathbf{x}, t) \qquad \forall \mathbf{x} \in \mathbf{X} \text{ and } t \geq 0 \tag{3.2.6}$$

then $\mathbf{g}_s(\mathbf{x}, t) = \left(\mathbf{I}_n - \mathbf{B}(\mathbf{GB})^{-1}\mathbf{G}\right)\mathbf{B}\mu = 0$. In this case, SM equation (3.2.4) reduces to:

$$\dot{\mathbf{x}} = \mathbf{f}_s(\mathbf{x}, t), \quad \mathbf{s}(\mathbf{x}) = 0 \tag{3.2.7}$$

Note this equation has the reduced order $(n - m)$; however, it is still nonlinear and non-autonomous. One possible approach to ensuring stability of the nominal system (3.2.7),

is connected with the input-output linearization technique, [110]. Another approach is the *Backstepping* that is based on the use step by step of Lyapunov functions, [111].

Here, the universal decomposition block control method is adopted to design a nonlinear time-varying sliding manifold (3.2.3) which stabilizes the perturbed SM equation (3.2.4). Another important goal is to provide robustness of the sliding mode motion with respect to non vanishing perturbation, $\mathbf{g}(\mathbf{x}, t)$ in cases where it does *not* satisfy the matching condition (3.2.6). A solution for the control of nonlinear, time-varying plants with both matched and unmatched uncertainties is offered here. A solution is achieved by a combination of three techniques:

First, the block control method is applied to decompose the control law synthesis problem into a number of sub-problems of lower order which can be solved independently of one another. A special state representation of the system must be used, this representation is referred as *Block Controllable form (BC-form).* This is achieved either by multiple decomposition of the original system under structural conditions on unmatched uncertainties, employing the integral method, [102]. After the first step of the transformation procedure described above, the original system is represented as two blocks

$$\dot{\bar{\mathbf{x}}}_2 = \bar{\mathbf{f}}_2(\bar{\mathbf{x}}_2, \mathbf{x}_1, t) \tag{3.2.8}$$

$$\dot{\mathbf{x}}_1 = \bar{\mathbf{f}}_1(\bar{\mathbf{x}}_2, \mathbf{x}_1, t) + \mathbf{B}_1(\bar{\mathbf{x}}_2, \mathbf{x}_1, t)\, u, \tag{3.2.9}$$

with an additional tie

$$u = \mathbf{B}_1^{+} v. \tag{3.2.10}$$

For the case where $n_1 = m$ and the inverse matrix $\mathbf{B}_1^{-1}$ exists, the tie (3.2.10) can be omitted, and an additional transformation $\bar{\mathbf{x}}_2 = \bar{\mathbf{x}}_2$; $\bar{\mathbf{x}}_1 = \int_0^{\mathbf{x}_1} \mathbf{B}_1^{-1}(\bar{\mathbf{x}}_2, \gamma, t)\, d\gamma$, can be introduced instead, such that the control matrix in the block (3.2.9) is transformed to the identity matrix $\dot{\bar{\mathbf{x}}}_1 = \bar{\mathbf{f}}_1(\bar{\mathbf{x}}_2, \bar{\mathbf{x}}_1, t) + u$.

Next, we will consider the class of nonlinear systems for which the map $\bar{\mathbf{f}}_2(\bar{\mathbf{x}}_2, \mathbf{x}_1, t)$ in the block (3.2.8) is linear with respect to x_1, that is,

$$\bar{\mathbf{f}}_2(\bar{\mathbf{x}}_2, \mathbf{x}_1, t) = \bar{\mathbf{f}}_2(\bar{\mathbf{x}}_2, t) + \bar{\mathbf{B}}_2(\bar{\mathbf{x}}_2, t)\, \mathbf{x}_1, \tag{3.2.11}$$

where $\bar{\mathbf{B}}_2$ is a matrix of dimension $(n - n_1) \times n_1$. Note that the map

$$\bar{\mathbf{f}}_2(\bar{\mathbf{x}}_2, t) = \bar{\mathbf{f}}_2(\bar{\mathbf{x}}_2, t) + \bar{\mathbf{B}}_2(\bar{\mathbf{x}}_2, t)\, \phi(\mathbf{x}_1). \quad \phi \in \mathbb{R}^{n_1} \quad \operatorname{rank}\left\{\frac{\partial \phi_1}{\partial \mathbf{x}_1}\right\} \neq 0,$$

where $\phi(\mathbf{x}_1)$ is a vector-function, can also be transformed to the form (3.2.11). The following cases are possible:

1. $\bar{\mathbf{B}}_2(\bar{\mathbf{x}}_2, t) \equiv 0$, $\forall x; t \geq 0$. This means that the subsystem (3.2.8), and hence the original system (3.2.1) are not controllable;

2. $\mathrm{rank}\bar{\mathbf{B}}_2(\bar{\mathbf{x}}_2,t)=n-n_1$, $\forall x;t\geq 0$. In this case, the system

$$\begin{aligned}\dot{\bar{\mathbf{x}}}_2 &= \bar{\mathbf{f}}_2(\bar{\mathbf{x}}_2,t)+\bar{\mathbf{B}}_2(\bar{\mathbf{x}}_2,t)\,\mathbf{x}_{1,}, &(3.2.12)\\ \dot{\mathbf{x}}_1 &= \bar{\mathbf{f}}_1(\bar{\mathbf{x}}_2,\mathbf{x}_1,t)+\mathbf{B}_1(\bar{\mathbf{x}}_2,\mathbf{x}_1,t)\,u, &(3.2.13)\end{aligned}$$

is the block-controlled form for the original system (3.2.1), and the transformation procedure is over;

3. $\mathrm{rank}\bar{\mathbf{B}}_2(\bar{\mathbf{x}}_2,t)=n_2<n-n_1$, $\forall x;t\geq 0$. In this case, we pass to the second step, where the vector $\mathbf{x}_1$ in the subsystem (3.2.12) is taken as a dummy control. This subsystem is split as

$$\begin{aligned}\bar{\mathbf{x}}_2 &= \begin{bmatrix}\tilde{\mathbf{x}}_3\\ \tilde{\mathbf{x}}_2\end{bmatrix} \qquad \bar{\mathbf{f}}_2(\tilde{\mathbf{x}}_3,\tilde{\mathbf{x}}_2,t)=\begin{bmatrix}\tilde{\mathbf{f}}_3(\tilde{\mathbf{x}}_3,\tilde{\mathbf{x}}_2,t)\\ \tilde{\mathbf{f}}_2(\tilde{\mathbf{x}}_3,\tilde{\mathbf{x}}_2,t)\end{bmatrix}\\ \bar{\mathbf{B}}_2(\tilde{\mathbf{x}}_3,\tilde{\mathbf{x}}_2,t) &= \begin{bmatrix}\tilde{\mathbf{B}}_3(\tilde{\mathbf{x}}_3,\tilde{\mathbf{x}}_2,t)\\ \tilde{\mathbf{B}}_2(\tilde{\mathbf{x}}_3,\tilde{\mathbf{x}}_2,t)\end{bmatrix} \qquad \begin{pmatrix}n-n_1-n_2\\ n_2\end{pmatrix}\end{aligned}$$

in order to fulfill the condition $\mathrm{rank}\tilde{\mathbf{B}}_2=\mathrm{rank}\bar{\mathbf{B}}_2=n_2$, $\forall x,t\geq 0$.

Next, similar to (3.2.10), a constraint on the quasicontrol $\mathbf{x}_1$ is imposed in the block (3.2.12): $\mathbf{x}_1=\tilde{\mathbf{B}}_2^{+}v_2$, $\tilde{\mathbf{B}}_2^{+}=\tilde{\mathbf{B}}_2^{T}\left(\tilde{\mathbf{B}}_2\tilde{\mathbf{B}}_2^{T}\right)^{-1}{}_2\in\mathbb{R}^{n_2}$

The corresponding Pfaff system [106] of order $(n-n_1-n_2)$ is written:

$$d\tilde{\mathbf{x}}_3+\mathbf{A}_2(\tilde{\mathbf{x}}_3,\tilde{\mathbf{x}}_2,t)\,d\tilde{\mathbf{x}}_2=0, \qquad \mathbf{A}_2=-\tilde{\mathbf{B}}_3\tilde{\mathbf{B}}_2^{+}. \tag{3.2.14}$$

Under the condition of complete integrability of the Pfaff system (3.2.14), we find its integral manifold $\tilde{\varphi}(\tilde{\mathbf{x}}_3,\tilde{\mathbf{x}}_2,t)=\tilde{\mathbf{c}}$, $\tilde{\varphi}=\mathrm{col}\,(\tilde{\varphi}_1,\ldots,\tilde{\varphi}_{n-n_1-n_2})$, $\tilde{\mathbf{c}}=\mathrm{col}\,(\tilde{\mathbf{c}}_1,\ldots,\tilde{\mathbf{c}}_{n-n_1-n_2})$ and introduce the change of coordinates

$$\begin{aligned}\dot{\tilde{\mathbf{x}}}_3 &= \bar{\mathbf{f}}_3(\bar{\mathbf{x}}_3,\tilde{\mathbf{x}}_2,t),\\ \dot{\tilde{\mathbf{x}}}_2 &= \tilde{\mathbf{f}}_2(\bar{\mathbf{x}}_3,\tilde{\mathbf{x}}_2,t)+\tilde{\mathbf{B}}_2(\bar{\mathbf{x}}_3,\tilde{\mathbf{x}}_2,t).\\ \dot{\tilde{\mathbf{x}}}_1 &= \tilde{\mathbf{f}}_1(\bar{\mathbf{x}}_3,\tilde{\mathbf{x}}_2,\tilde{\mathbf{x}}_1,t)+\tilde{\mathbf{B}}_1(\bar{\mathbf{x}}_3,\tilde{\mathbf{x}}_2,\tilde{\mathbf{x}}_1,t)\,u,\end{aligned} \tag{3.2.15}$$

where $\mathrm{rank}\tilde{\mathbf{B}}_2=n_2$ and $\mathrm{rank}\tilde{\mathbf{B}}_1=n_1,\forall x,t\geq 0$.

If the linearity condition $\tilde{\mathbf{f}}_3(\bar{\mathbf{x}}_3,\tilde{\mathbf{x}}_2,t)$ holds with respect to $\tilde{\mathbf{x}}_2$,

$$\tilde{\mathbf{f}}_3(\bar{\mathbf{x}}_3,\tilde{\mathbf{x}}_2,t)=\bar{\mathbf{f}}_3(\bar{\mathbf{x}}_3,t)+\bar{\mathbf{B}}_3(\bar{\mathbf{x}}_3,t)\,\tilde{\mathbf{x}}_2, \tag{3.2.16}$$

and the matrix $\bar{\mathbf{B}}_3$ of dimension $(n-n_1-n_2)\times n_2$ is of full rank, that is,

$$\mathrm{rank}\bar{\mathbf{B}}_3=n-n_1-n_2, \qquad \forall x,t\geq 0, \tag{3.2.17}$$

then system (3.2.15) under conditions (3.2.16), (3.2.17) represents the block-controlled form; otherwise one has to pass to the third step and continue analogous transformations till the block-controlled form is obtained.

Thus, the conditions of existence of the block-controlled form for system (3.2.1) can be summarized in the following theorem.

Theorem 3.1. *Suppose the following conditions hold:*

1. *System (3.2.1) is controllable;*
2. *the Pfaff system is completely integrable;*
3. *In the system*

$$\begin{cases} \dot{\mathbf{x}}'_q = \mathbf{f}'_q\left(\mathbf{x}'_q, \mathbf{x}_{q-1}, t\right), \\ \dot{\mathbf{x}}_i = \mathbf{f}_i\left(\mathbf{x}'_q, \mathbf{x}_{q-1}, \ldots, \mathbf{x}_i, t\right) + \mathbf{B}_i\left(\mathbf{x}'_q, \mathbf{x}_{q-1}, \ldots, \mathbf{x}_i, t\right)\mathbf{x}_{i-1}, \quad i = q-1, \ldots, 2, \\ \dot{\mathbf{x}}_1 = \mathbf{f}_1\left(\mathbf{x}'_q, \mathbf{x}_{q-1}, \ldots, \mathbf{x}_1, t\right) + \mathbf{B}_1\left(\mathbf{x}'_q, \mathbf{x}_{q-1}, \ldots, \mathbf{x}_1, t\right)u, \end{cases} \tag{3.2.18}$$

$\mathbf{x} = col\left(\mathbf{x}'_q, \mathbf{x}_{q-1}, \ldots, \mathbf{x}_1\right)$, $\mathbf{x}'_q \in X'_q \subseteq \mathbb{R}^{n_j}$, $j = 1, \ldots, q-1$, $\dim X_j = rank\mathbf{B}_j = n_j, \forall x, t \geq 0$, $j = 1, \ldots, q-1$, $n'_q = n - \sum_{i=1}^{q-1} n_i$, *which is constructed on the* $(q-1)$*-th step of the transformation procedure, we have*

(a) *the map* $\mathbf{f}'_q$ *is linear with respect to* $\mathbf{x}_{q-1}$*:*

$$\mathbf{f}'_q\left(\mathbf{x}'_q, \mathbf{x}_{q-1}, t\right) = \mathbf{f}'_q\left(\mathbf{x}'_q, t\right) + \mathbf{B}'_q\left(\mathbf{x}'_q, t\right)\mathbf{x}_{q-1}, \qquad q = 2, \ldots, r; \tag{3.2.19}$$

(b) *there exists a minor* $\mathbf{B}_q\left(\mathbf{x}_{q+1}, \mathbf{x}_q, t\right)$ *of dimension* $n_q \times n_{q-1}$ *of matrix* B'_q *such that* $rank\mathbf{B}_q\left(\mathbf{x}_{q+1}, \mathbf{x}_q, t\right) = rank\mathbf{B}'_q\left(\mathbf{x}_{q+1}, \mathbf{x}_q, t\right) = n_q < n'_q$, $\forall x, t \geq 0$; *and the corresponding Pfaff system*

$$d\mathbf{x}_{q+1} + \mathbf{A}_q\left(\mathbf{x}_{q+1}, \mathbf{x}_q, t\right)d\mathbf{x}_q = 0,$$

where $\mathbf{A}_q = -\mathbf{B}_{q+1}\mathbf{B}_q^+$, $\mathbf{B}_q^+ = \mathbf{B}_q^T\left(\mathbf{B}_q\mathbf{B}_q^T\right)^{-1}$ $\mathbf{x}'_q = col(\mathbf{x}_{q+1}, \mathbf{x}_q)$, $\mathbf{x}_q \in X_q \subseteq \mathbb{R}^{n_q}$, $x_{q+1} \in X_{q+1} \subseteq \mathbb{R}^{n_{q+1}}$, $\mathbf{B}_q\left(x_{q+1}, x_q, t\right) = \begin{bmatrix} \mathbf{B}_{q+1}\left(x_{q+1}, x_q, t\right) \\ \mathbf{B}_q\left(x_{q+1}, x_q, t\right) \end{bmatrix}$, $n'_q = n_q + n_{q+1}$, $q = x, \ldots, r-1$, *is completely integrable;*

(c) $rank\mathbf{B}'_q\left(x'_q, t\right) = n'_q, \forall x, t \geq 0$ *for* $q = r$. *Then system (3.2.1) can be represented in the block form.*

Secondly, the sliding mode technique is used to compensate the matched uncertainty.

Finally, a high gain approach is used to obtain hierarchical fast motions on the sliding manifold, the goals being to achieve stabilization of the sliding the mode equation and compensation of the unmatched uncertainty.

Usually, the block indexes are reordered in an increasing way leading to the classical block controllable form.

The block control approach has, in fact, successfully been employed for control of linear systems, [112], including linear systems with delay, [113], [114]; for stabilization and regulation of nonlinear (including mechanical) systems, [115], [116], [117], [118], [119]; for automotive control [120]; for electric motors and power systems control [121], [122], [123] [124], [125], [126] and with real-time application [127]; for finite time unmatched perturbation rejection [128], [129]. Here the possibility of applying the same method for obtaining upper estimations and bounds of uncertain nonlinear system solutions, is investigated.

3.2.1 Block control for linear systems

For a high order linear system, the block control principle can be adopted if the system can be transformed into the so-called *block control form* [103], [104] represented by

$$\begin{aligned} \dot{\mathbf{x}}_1 &= \mathbf{A}_1\mathbf{x}_1 + \mathbf{B}_1\mathbf{x}_2 \\ \dot{\mathbf{x}}_2 &= \mathbf{A}_2 \left[\begin{array}{cc} \mathbf{x}_1^T & \mathbf{x}_2^T \end{array} \right]^T + \mathbf{B}_2\mathbf{x}_3 \\ &\vdots \\ \dot{\mathbf{x}}_{r-1} &= \mathbf{A}_{r-1} \left[\begin{array}{ccc} \mathbf{x}_1^T & \mathbf{x}_2^T & \cdots \quad \mathbf{x}_{r-1}^T \end{array} \right]^T + \mathbf{B}_{r-1}\mathbf{x}_r \\ \dot{\mathbf{x}}_r &= \mathbf{A}_r \left[\begin{array}{cccc} \mathbf{x}_1^T & \mathbf{x}_2^T & \cdots \quad \mathbf{x}_{r-1}^T & \mathbf{x}_r^T \end{array} \right]^T + \mathbf{B}_r\mathbf{u} \end{aligned} \tag{3.2.20}$$

where dimension $d_i = \text{rank}\,(\mathbf{B}_i) = \dim\,(\mathbf{x}_i)$; $i = 1, 2, \ldots, r$ and $\sum_{i=1}^{r} d_i = n$.

It can be seen, each equation (or subsystem) of the control form (3.2.20) is called a *block*. The state of each block can be treated as a virtual control input to the preceding upper block. The state dimension of each block is equal to the dimension of its corresponding control inputs. Any linear controllable system can be reduced to the block control form [107].

A hierarchical design procedure based on the block control form is summarized as follows: Let Λ_i, $i = 1, 2, \ldots, r$; $\Lambda_i = \{\lambda_{ij}\}$, $j = 1, 2, \ldots, d_i$, be the desired spectra.

Step 1: Starting from the top of the block form (3.2.20), the desired dynamical behaviour can be obtained if the virtual control, $\mathbf{x}_2$, can be assigned as

$$\mathbf{x}_2 = \mathbf{B}_1^{+}\left(-\mathbf{A}_1\mathbf{x}_r + \Lambda_1\mathbf{x}_1\right)$$

where $\mathbf{B}_1^+$ is the pseudoinverse of $\mathbf{B}_1$. Then,

$$\dot{\mathbf{x}}_1 = \Lambda_1 \mathbf{x}_1$$

Step 2: Denote the deviation of virtual control from the desired one as

$$\mathbf{s}_2 = \mathbf{x}_2 - \mathbf{B}_1^+ \left(-\mathbf{A}_1 \mathbf{x}_1 + \Lambda_1 \mathbf{x}_1\right) \tag{3.2.21}$$

Differentiating equation (3.2.21) yields

$$\dot{\mathbf{s}}_2 = \tilde{\mathbf{A}}_2 \tilde{\mathbf{S}}_2 + \mathbf{B}_2 \mathbf{x}_3 \tag{3.2.22}$$

where $\tilde{\mathbf{S}}_2^T = \left[\mathbf{s}_1^T, \mathbf{s}_2^T\right]$; $\mathbf{s}_1 = \mathbf{x}_1$, and $\tilde{\mathbf{A}}_2$ can be found after differentiation. The desired dynamical behaviour of the block 2,

$$\dot{\mathbf{s}}_2 = \Lambda_2 \mathbf{s}_2,$$

can be obtained if the virtual control, $\mathbf{x}_{r-2}$, is selected as

$$\mathbf{x}_3 = \mathbf{B}_2^+ \left(-\tilde{\mathbf{A}}_2 \tilde{\mathbf{S}}_2 + \Lambda_2 \mathbf{s}_2\right) \tag{3.2.23}$$

where $\mathbf{B}_2^+$ is the pseudoinverse of $\mathbf{B}_2$.

Step 3, 4, ..., r-1: Consider the succeeding lower blocks. Since the matrices $\mathbf{B}_i\,(i = 3, 4, \ldots, r)$, have pseudoinverse matrices $\mathbf{B}_i^+\,(i = 3, 4, \ldots, r)$, there exists a sequence of desired virtual controls which are obtained in a similar fashion as for the block 2,

$$\mathbf{x}_{i+1} = \mathbf{B}_i^+ \left(-\tilde{\mathbf{A}}_i \tilde{\mathbf{S}}_i + \Lambda_i \mathbf{s}_i\right) \tag{3.2.24}$$

and the deviations,

$$\mathbf{s}_i = \mathbf{x}_i - \mathbf{B}_{i-1}^+ \left(-\tilde{\mathbf{A}}_{i-1} \tilde{\mathbf{S}}_{i-1} + \Lambda_{i-1} \mathbf{s}_{i-1}\right) \tag{3.2.25}$$

where $\tilde{\mathbf{S}}_i^T = \left[\mathbf{s}_1^T, \mathbf{s}_2^T, \ldots, \mathbf{s}_i^T\right]$ for $i = 2, 3, \ldots, r-2$.

Step r: For the lowest block, since

$$\mathbf{s}_r = \mathbf{x}_r - \mathbf{B}_{r-1}^+ \left(-\tilde{\mathbf{A}}_{r-1} \tilde{\mathbf{S}}_{r-1} + \Lambda_{r-1} \mathbf{s}_{r-1}\right),$$

the time derivative of s_r is found as a function of the real control

$$\dot{\mathbf{s}}_r = \tilde{\mathbf{A}}_{r-1} \tilde{\mathbf{S}}_{r-1} + \mathbf{B}_r \mathbf{u}.$$

The whole system is written as

$$\begin{aligned} \dot{\mathbf{s}}_1 &= \Lambda_1 \mathbf{s}_1 + \mathbf{s}_2 \\ \dot{\mathbf{s}}_i &= \Lambda_i \mathbf{s}_i + \mathbf{s}_{i+1} \\ \dot{\mathbf{s}}_r &= \tilde{\mathbf{A}}_{r-1} \tilde{\mathbf{S}}_{r-1} + \mathbf{B}_r \mathbf{u} \end{aligned} \tag{3.2.26}$$

with $i = 2, \ldots, r-1$.

Linear feedback, discontinuous and Super-Twisting controllers

Based on the above hierarchical design approach, it is obvious that $\mathbf{s}_r = 0$ is the desired manifold for stabilization of the control system. As a first alternative, to obtain zero deviation of the function $\mathbf{s}_r = 0$, a linear feedback control

$$\mathbf{u} = \mathbf{B}_r^+ \left(-\tilde{\mathbf{A}}_r \tilde{\mathbf{S}}_r + \Lambda_r \mathbf{s}_r \right)$$

can be applied for stabilizing the linear system (3.2.26), yielding the closed-loop system

$$\begin{aligned} \dot{\mathbf{s}}_1 &= \Lambda_1 \mathbf{s}_1 + \mathbf{s}_2 \\ \dot{\mathbf{s}}_i &= \Lambda_i \mathbf{s}_i + \mathbf{s}_{i+1} \\ \dot{\mathbf{s}}_r &= \Lambda_r \mathbf{s}_r \end{aligned} \tag{3.2.27}$$

with $i = 2, \ldots, r-1$. The stability of (3.2.27) depends on the correct choice of the spectra provided by $\Lambda_1, \ldots, \Lambda_r$.

Another alternative is the use of a sliding mode controller, the most distinguishing features of the SMC methodology are its finite time convergence to the sliding manifold and an inherent insensitivity to parameter variations and external disturbances once in sliding mode.

In order to generate sliding mode motion in the desired manifold, the following control

$$\mathbf{u} = -\bar{\mathbf{B}}_r^+ \bar{u}. \tag{3.2.28}$$

is assigned.

On the one hand, the discontinuous control strategy

$$\bar{u} = M \text{sign}\left(\mathbf{s}_r\right). \tag{3.2.29}$$

can be employed by selecting M based on the design methodology of the SMC, where $\tilde{\mathbf{A}}_r \tilde{\mathbf{S}}_r$ is considered as a bounded external perturbation.

On the other hand, the second order sliding mode algorithm so-called *Super-Twisting Algorithm* [100, Ch. 3] [130] is proposed:

$$\bar{u} = \bar{u}_1 + \bar{u}_2 \tag{3.2.30}$$

with $\bar{u}_1 = \alpha_1 |\mathbf{s}_r|^{1/2} \text{sign}\left(\mathbf{s}_r\right)$ and $\dot{\bar{u}}_2 = \alpha_2 \text{sign}\left(\mathbf{s}_r\right)$, where $\alpha_1 > 0$ and $\alpha_2 > 0$ are the control parameters.

Resulting the following equation

$$\dot{\mathbf{s}}_r = \varphi + \mathbf{u} \tag{3.2.31}$$

where $\varphi = \tilde{\mathbf{A}}_r \tilde{\mathbf{S}}_r$ is considered as a bounded external perturbation. In addition, it is supposed φ is differentiable and $|\dot{\varphi}| < N$, $\forall t > 0$ with N a known constant.

The sliding motion condition for the system (3.2.31) in closed-loop by (3.2.30) can be obtained via the transformation

$$y(t) = \varphi - \alpha_2 \int_0^t \text{sign}(\tau)\, d\tau$$

reducing the system to

$$\begin{aligned} \dot{\mathbf{s}}_r &= y - \alpha_1 |\mathbf{s}_r|^{1/2} \text{sign}(\mathbf{s}_r) \\ \dot{y} &= \dot{\varphi} - \alpha_2 \text{sign}(\mathbf{s}_r). \end{aligned} \tag{3.2.32}$$

In this form, with the Lyapunov function proposed in [131], if the parameters α_1 and α_2 are chosen as $\alpha_2 > 5N$ and $32N < \alpha_1^2 < 8(\alpha_2 - N)$, it is provided finite time convergence of the system (3.2.32) to the origin $(0, 0)$. An alternative approach for the stability is given in [132].

In sliding motion the closed-loop dynamics is given by the so-called sliding mode equation

$$\begin{aligned} \dot{\mathbf{s}}_1 &= \Lambda_1 \mathbf{s}_1 + \mathbf{s}_2 \\ \dot{\mathbf{s}}_i &= \Lambda_i \mathbf{s}_i + \mathbf{s}_{i+1} \end{aligned} \tag{3.2.33}$$

with $i = 2, \ldots, r-1$. The stability of the sliding mode equation (3.2.33) depends on the correct choice of the spectra provided by $\Lambda_1, \ldots, \Lambda_{r-1}$.

3.2.2 Robust block control for a class of nonlinear systems

The essential feature of the proposed method is the conversion of the system (3.2.1) to the BC-form consisting of r blocks:

$$\dot{\mathbf{x}}_1 = \mathbf{f}_1(\mathbf{x}_1, t) + \mathbf{B}_1(\mathbf{x}_1, t)\, \mathbf{x}_2 + \mathbf{g}_1(\mathbf{x}_1, t) \tag{3.2.34}$$

$$\dot{\mathbf{x}}_i = \mathbf{f}_i(\mathbf{x}_i, t) + \mathbf{B}_1(\bar{\mathbf{x}}_i, t)\, \mathbf{x}_{i+1} + \mathbf{g}_i(\bar{\mathbf{x}}_i, t) \tag{3.2.35}$$

$$\dot{\mathbf{x}}_r = \mathbf{f}_r(\mathbf{x}_r, t) + \mathbf{B}_r(\bar{\mathbf{x}}_r, t)\, \mathbf{u} + \mathbf{g}_r(\bar{\mathbf{x}}_r, t) \tag{3.2.36}$$

with $i = 2, \ldots, r-1$, where the vector $\mathbf{x}$ is decomposed as $\mathbf{x} = (\mathbf{x}_1, \mathbf{x}_2, \ldots, \mathbf{x}_r, \mathbf{x}_{r+1})^T$, $\bar{\mathbf{x}}_i = (\mathbf{x}_1, \mathbf{x}_2, \ldots, \mathbf{x}_i)^T$, $i = 2, \ldots, r$, $\mathbf{x}_i$ is a $n_i \times 1$ vector, and the indices $(n_1, n_2, \ldots n_r)$ define the structure of the system and satisfy the following relation:

$$n_1 \leq n_2 \leq \ldots \leq n_r \leq m \quad \text{and} \quad \sum_{i=1}^{r} n_i = n \tag{3.2.37}$$

The matrix $\mathbf{B}_i$, before the fictitious $\mathbf{x}_{i+1}$ in each ith block of (3.2.34)-(3.2.36), has full rank, that is

$$\operatorname{rank}(\mathbf{B}_i) = n_i \quad \forall \mathbf{x} \in \mathbf{X} \subset \mathbb{R}^n \text{ and } t \in [0, \infty), \ i = 1, \ldots, r. \tag{3.2.38}$$

The procedure of reducing the system (3.2.1) to the BC-form (3.2.34)-(3.2.35) based on the integral transformation method [102], as well as conditions of the BC-form existence [133]

The relation (3.2.37) means $n_i = n_{i+1}$ or $n_i < n_{i+1}$ Let us first consider the plant with the structure

$$n_1 < n_2 < \cdots < n_r < m \tag{3.2.39}$$

Block Recursive Transformation

The following assumptions of the bounds on the unknown terms in (3.2.34)-(3.2.36) are stated: (H1) There exist positive constants $\bar{q}_{i,j}$ and $\bar{d}_i$ such that

$$\begin{aligned} \|\mathbf{g}_1(\mathbf{x}_1, t)\| &\leq \bar{q}_{11} \|\mathbf{x}_1\| + \bar{d}_1 \\ \|\mathbf{g}_2(\mathbf{x}_2, t)\| &\leq \bar{q}_{21} \|\mathbf{x}_1\| + \bar{q}_{22} \|\mathbf{x}_2\| + \bar{d}_2 \\ \|\mathbf{g}_i(\mathbf{x}_i, t)\| &\leq \sum_{j=1}^{i} \bar{q}_{ij} \|\mathbf{x}_j\| + \bar{d}_i \end{aligned}$$

with $i = 3, \ldots, r-1$.

Taking into account the structure (3.2.39), the following recursive transformation is introduced

$$\mathbf{z}_1 = \mathbf{x}_1 := \Phi_1(\mathbf{x}_1, t) \tag{3.2.40}$$

$$\mathbf{z}_2 = \tilde{\mathbf{B}}_2(\bar{\mathbf{x}}_1, t)\mathbf{x}_2 + \begin{bmatrix} \mathbf{f}_1(\mathbf{x}_1, t) + k_1 \Phi_1(\mathbf{x}_1, t) \\ 0 \end{bmatrix} := \Phi_2(\bar{\mathbf{x}}_2, t) \tag{3.2.41}$$

$$\mathbf{z}_{i+1} = \tilde{\mathbf{B}}_{i+1}(\bar{\mathbf{x}}_i, t)\mathbf{x}_{i+1} + \begin{bmatrix} \bar{\mathbf{f}}_i(\bar{\mathbf{x}}_i, t) + k_i \Phi_i(\bar{\mathbf{x}}_i, t) \\ 0 \end{bmatrix} := \Phi_{i+1}(\bar{\mathbf{x}}_{i+1}, t) \tag{3.2.42}$$

with $i = 3, \ldots, r-1$, where $\mathbf{z}_i$ is a $n_1 \times 1$ new variables vector, $k_i > 0$, $\tilde{\mathbf{B}}_{i+1} = \begin{bmatrix} \bar{\mathbf{B}}_i \\ \mathbf{E}_{i,2} \end{bmatrix}$, $\mathbf{E}_{i,2} = \begin{bmatrix} 0 & \mathbf{I}_{n_{i+1}-n_i} \end{bmatrix} \in \mathbb{R}^{(n_{i+1}-n_i)\times n_i}$. $\mathbf{I}_{n_{i+1}-n_i}$ is the identity matrix.

The transformation (3.2.40)-(3.2.42) reduces the system (3.2.34)-(3.2.36) to the following

desired form:

$$\dot{\mathbf{z}}_1 = -k_1\mathbf{z}_1 + \mathbf{E}_{11}\mathbf{z}_2 + \bar{\mathbf{g}}_1(\mathbf{z}_1, t) \tag{3.2.43}$$

$$\dot{\mathbf{z}}_i = -k_i\mathbf{z}_i + \mathbf{E}_{i,1}\mathbf{z}_{i+1} + \bar{\mathbf{g}}_i(\bar{\mathbf{z}}_i, t) \tag{3.2.44}$$

$$\dot{\mathbf{z}}_r = \bar{\mathbf{f}}_r(\mathbf{z}, t) + \bar{\mathbf{B}}_r(\mathbf{z}, t)\,\mathbf{u} + \bar{\mathbf{g}}_r(\bar{\mathbf{z}}_r, t) \tag{3.2.45}$$

with $i = 2, \ldots, r-1$, where $\mathbf{z} = (\mathbf{z}_1, \ldots, \mathbf{z}_r)^T$ $\bar{\mathbf{f}}_r(\mathbf{z}, t)$ is a bounded function, $\text{rank}\bar{\mathbf{B}}_r = n_1$, $\bar{\mathbf{B}}_r = \tilde{\mathbf{B}}_{r-1}\mathbf{B}_r$.

Discontinuous and Super-Twisting controllers

In order to generate sliding mode motion in (3.2.43)-(3.2.45), a natural choice of the sliding manifold using transformation (3.2.40)-(3.2.42), is

$$\mathbf{z}_r = 0, \qquad \mathbf{z}_r = \Phi_r(\bar{\mathbf{x}}_r, t)\,. \tag{3.2.46}$$

and the control strategy, is proposed:

$$\mathbf{u} = -\bar{\mathbf{B}}_r^{-1}\bar{u}. \tag{3.2.47}$$

On the one hand, taking into account the bound (3.2.2), the following discontinuous control strategy, is proposed:

$$\bar{u} = M\text{sign}(\mathbf{z}_r)\,. \tag{3.2.48}$$

The control law (3.2.48) guaranties the convergence of the closed-loop system motion to manifold $\mathbf{z}_r = 0$ (3.2.46) in a finite time, [133], defined as

$$t_s < t_0 + \frac{1}{\eta}\left\|\mathbf{z}_r(t_0)\right\|_2, \qquad \eta > 0. \tag{3.2.49}$$

On the other hand, the second order sliding mode algorithm so-called *Super-Twisting Algorithm* [100, Ch. 3] [130] is proposed:

$$\bar{u} = \bar{u}_1 + \bar{u}_2 \tag{3.2.50}$$

with $\bar{u}_1 = \alpha_1|\mathbf{z}_r|^{1/2}\text{sign}(\mathbf{z}_r)$ and $\dot{\bar{u}}_2 = \alpha_2\text{sign}(\mathbf{z}_r)$, where $\alpha_1 > 0$ and $\alpha_2 > 0$ are the control parameters.

From equation (3.2.45) results the following equation

$$\dot{\mathbf{z}}_r = \varphi + \mathbf{u} \tag{3.2.51}$$

where $\varphi = \bar{\mathbf{f}}_r(\mathbf{z}, t) + \bar{\mathbf{g}}_r(\bar{\mathbf{z}}_r, t)$ is considered as a bounded external perturbation. In addition, it is supposed that $\varphi(t)$ is differentiable and $|\dot{\varphi}| < N$, $\forall t > 0$ with N a known constant.

The stability condition for the system (3.2.51) in closed-loop by (3.2.50) can be obtained via the transformation

$$y(t) = \varphi - \alpha_2 \int_0^t \text{sign}(\tau)\, d\tau$$

reducing the system to

$$\begin{aligned} \dot{\mathbf{z}}_r &= y - \alpha_1 |\mathbf{z}_r|^{1/2} \text{sign}(\mathbf{z}_r) \\ \dot{y} &= \dot{\varphi} - \alpha_2 \text{sign}(\mathbf{z}_r). \end{aligned} \tag{3.2.52}$$

In this form, with the Lyapunov function proposed in [131], if the parameters α_1 and α_2 are chosen as $\alpha_2 > 5N$ and $32N < \alpha_1^2 < 8(\alpha_2 - N)$, it is provided finite time convergence of the system (3.2.52) to the origin $(0,0)$. An alternative approach for the stability is given in [132].

Robustness to Unmatched Uncertainty

For the system constrained to the sliding surface $\mathbf{z}_r = 0$ the system (3.2.43)-(3.2.45) reduces to

$$\dot{\mathbf{z}}_1 = -k_1 \mathbf{z}_1 + \mathbf{E}_{11} \mathbf{z}_2 + \bar{\mathbf{g}}_1(\mathbf{z}_1, t) \tag{3.2.53}$$

$$\dot{\mathbf{z}}_i = -k_i \mathbf{z}_i + \mathbf{E}_{i,1} \mathbf{z}_{i+1} + \bar{\mathbf{g}}_i(\bar{\mathbf{z}}_i, t), \quad i = 2, ..., r-1 \tag{3.2.54}$$

$$\dot{\mathbf{z}}_{r-1} = -k_r \mathbf{z}_{r-1} + \bar{\mathbf{g}}_r(\bar{\mathbf{z}}_{r-1}, t) \tag{3.2.55}$$

Thus now, the original stability analysis problem is reduced to the analysis of robustness property of a reduced-order sliding mode dynamics (3.2.53)-(3.2.55) which can be considered as linear system with nonlinear perturbation. Note that this perturbation is unmatched with respect to the control $\mathbf{u}$ in (3.2.34)-(3.2.36). It will be shown that the convergence rate of the linear part of (3.2.53)-(3.2.55) is defined by values of coefficients $k_1, \ldots, k_{r-1}$. For, the bounds from the physical constraints on the original system (3.2.34)-(3.2.36) (see -Assumption H1) can be rewritten by using the change or variables (3.2.40)-(3.2.42) as (H2) There exist positive constants q_{ij} and $\mathbf{d}_i$, such that

$$\|\bar{\mathbf{g}}_1(\mathbf{z}_1, t)\| \leq q_{11} \|\mathbf{z}_1\| + \mathbf{d}_1 \tag{3.2.56}$$

$$\|\bar{\mathbf{g}}_2(\bar{\mathbf{z}}_2, t)\| \leq q_{22} \|\mathbf{z}_2\| + k_1 q_{21} \|\mathbf{z}_1\| + \mathbf{d}_2 \tag{3.2.57}$$

$$\|\bar{\mathbf{g}}_2(\bar{\mathbf{z}}_2, t)\| \leq q_{33} \|\mathbf{z}_3\| + k_2 q_{32} \|\mathbf{z}_2\| + k_1^2 q_{21} \|\mathbf{z}_1\| + \mathbf{d}_3 \tag{3.2.58}$$

$$\|\bar{\mathbf{g}}_i(\bar{\mathbf{z}}_i, t)\| \leq q_{i,i} \|\mathbf{z}_i\| + \sum_{j=1}^{i-1} k_j^{(i-j)} q_{ij} \|\mathbf{z}_j\| + \mathbf{d}_i, \qquad i = 4, \ldots, r-1. \tag{3.2.59}$$

To achieve the robustness property with respect to unknown but bounded uncertainty, the controller gains $k_1, \ldots, k_{r-1}$ have to be chosen hierarchically high. Thus, since $\mathbf{g}_1$ does not depend on k_1, the value of the coefficient k_1 can be chosen so high that the term $k_1\mathbf{z}_1$ in (3.2.53) dominates the term $\mathbf{g}_1$. By block linearization procedure, the term $\mathbf{g}_2$ depends on k_1 but not on $k_2, \ldots, k_{r-1}$ [133]. Then for fixed k_1, the appropriate choice of value of k_2 provides the dominations of term $k_2\mathbf{z}_2$ in the second block of (3.2.54), and so on.

In order to establish property of the sliding mode motion on the surface $\mathbf{z}_r = 0$, the following hierarchy of the control gains $k_1, \ldots, k_{r-1}$ with respect to the given bounds on the unknown terms of (3.2.53)-(3.2.55), is proposed:

$$k_1 > q_{11} \tag{3.2.60}$$

$$k_2 > q_{22} + k_1 q_{21}\alpha_{12}, \quad \alpha_{12} = (k_1 - q_{11})^{-1} \tag{3.2.61}$$

$$k_3 > q_{33} + k_2 q_{32}\alpha_{23} + k_1^2 q_{31}\alpha_{13}, \quad \alpha_{23} = (k_2 - q_{22} - k_1 q_{21}\alpha_{12})^{-1}, \quad \alpha_{13} = \alpha_{12}\alpha_{23} \tag{3.2.62}$$

$$k_i > q_{i,i} + \sum_{j=1}^{i-1} k_j^{(i-j)} q_{i,j}\alpha_{j,i}, \quad \alpha_{i-1,i} = \left(k_{i-1} - q_{i-1,i-1} - \sum_{j=1}^{i-2} k_j^{(i-j)} q_{i-1,j}\alpha_{j,i-1} \right)^{-1},$$

$$\alpha_{j,i} = \alpha_{j,i-1}\alpha_{i-1,i} \qquad i = 4, \ldots, r-1. \tag{3.2.63}$$

Let the Assumption H2 holds, and the values of positive scalars $k_1, \ldots, k_{r-1}$ satisfy the inequalities (3.2.60)-(3.2.63). Then there exist positive scalars γ_{ij} and h_i, $i = 1, \ldots, r-1, j = i, \ldots, r-1$ such that the solutions of system (3.2.53)-(3.2.55) are estimated by

$$\|\mathbf{z}_{r-1}(t)\| \leq \gamma_{r-1,r-1} \exp\left[-\frac{1}{2}\alpha_{r-1}(t - t_0)\right] + h_{r-1} \tag{3.2.64}$$

$$\|\mathbf{z}_{r-2}(t)\| \leq \gamma_{r-2,r-2} \exp\left[-\frac{1}{2}\alpha_{r-2}(t - t_0)\right] + \gamma_{r-2,r-1} \exp\left[-\frac{1}{2}\alpha_{r-1}(t - t_0)\right] + h_{r-2} \tag{3.2.65}$$

$$\|\mathbf{z}_i(t)\| \leq \sum_{j=1}^{r-1} \gamma_{i,j} \exp\left[-\frac{1}{2}\alpha_j(t - t_0)\right] + h_i, \qquad i = 1, \ldots, r-3 \tag{3.2.66}$$

and these solutions are uniformly ultimately bounded, i.e.

$$\lim_{t\to\infty} \sup \|\mathbf{z}_i(t)\| \leq h_i, \qquad i = 1, \ldots, r-1. \tag{3.2.67}$$

This result establishes property of the sliding mode motion on the surface $\mathbf{z}_r = 0$, and provides the required values of the controller gains $k_1, \ldots, k_{r-1}$ is derived in [133]. It is interesting to note that with increasing the values of $k_1, \ldots, k_{r-1}$ the values of bounds h_i becomes arbitrary small. But in this case the domain of sliding mode stability [133], can be decreased since function $\bar{f}_r$ depends as well on gains $k_1, \ldots, k_{r-1}$.

3.3 Integral sliding mode with block control

In this section the Integral Sliding Modes with Block Control (ISM) [134], [135], [136], [137] technique on the basis of integral Sliding Mode (SM) [101] in combination with nested SM [105] is presented. This technique allows to achieve robustness to matched, and unmatched perturbations, and ensure output tracking. Theoretically, this integral nested SM control can guarantee the robustness of the system throughout the entire response starting from the initial time instance and reduce the sliding functions gains in comparison with standard SM. The description of the ISM is presented in generic terms to show the generality of the approach.

3.3.1 Problem statement

The class of nonlinear systems presented in the NBC (nonlinear block controllable) form is studied, this class of system can be seem as an extension of the system presented in equation (3.2.20). The NBC form consist of r blocks [115]

$$\begin{aligned} \dot{\mathbf{x}}_i &= \mathbf{f}_i(\bar{\mathbf{x}}_i) + \mathbf{B}_i(\bar{\mathbf{x}}_i)\mathbf{x}_{i+1} + \mathbf{g}_i(t,\mathbf{x}) \\ \dot{\mathbf{x}}_r &= \mathbf{f}_r(\mathbf{x}) + \mathbf{B}_r(\mathbf{x}) + \mathbf{g}_r(t,\mathbf{x}), \qquad i = 1,\ldots,r-1, \\ \mathbf{y} &= \mathbf{x}_1 \end{aligned} \tag{3.3.1}$$

where, $\mathbf{x} = [\mathbf{x}_1 \cdots \mathbf{x}_r]^T \in \mathbb{R}^n$ is the state vector, $\mathbf{x}_i \in \mathbb{R}^{n_i}$. $\bar{\mathbf{x}}_i = [\mathbf{x}_1 \cdots \mathbf{x}_i]^T$; $\mathbf{u} \in \mathbb{R}^m$ is the control vector. Moreover, $\mathbf{f}(\cdot)$ and the columns of $\mathbf{B}(\cdot)$ are smooth vector fields, $\mathbf{g}_i(\cdot)$is a bounded unknown perturbation term due to parameter variations and external disturbances, and $\operatorname{rank}[\mathbf{B}_i(\mathbf{x}_1,\cdots,\mathbf{x}_i)] = n_i$, $\forall \mathbf{x}$.

The integers $n_1,\ldots,n_r$ define the dimension of the i^{th} block (system structure) and satisfy

$$n_1 \leq n_2 \leq \cdots \leq n_r = m, \qquad \sum_{i=1}^{r} n_i = n.$$

The control objective is to design a controller such that the output $\mathbf{y}$ in (3.3.1) tracks a desired reference $\mathbf{x}_{ref}(t)$ with bounded derivatives, in spite of unknown but bounded perturbations. To induce quasi sliding mode in the i^{th} block of the system (3.3.1), the continuously differentiable sigmoid function $\operatorname{sigm}(\varepsilon; x)$, where we use the result that the sign function can be approximated by the sigmoid function in the form $\lim_{\varepsilon\to\infty} \operatorname{sigm}(\varepsilon; x) = \operatorname{sign}(x)$. The figure 3.1 shows the approximation for various values of the sigmoid function slope. The used sigmoid function in the hyperbolic tangent, $\operatorname{sigm}(\varepsilon; x) = \tanh(\varepsilon x)$

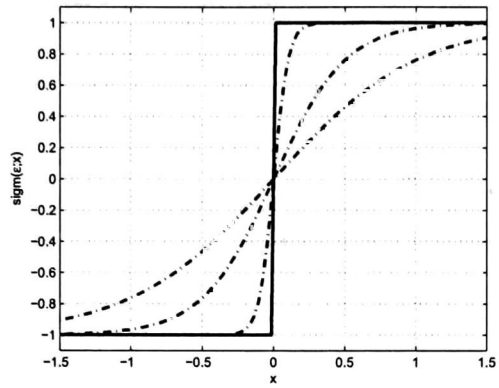

Figure 3.1: Sigmoid function for various values of the parameter ε

3.3.2 Control design

According to the block control technique [115], [133], the state $\mathbf{x}_{i+1}$, $i = 1, \ldots, r-1$ is considered as a virtual control vector in the i^{th} block of the system (3.3.1). The design procedure is described in r steps.

Step 1. The control error in the first block of the system (3.3.1) is defined as

$$\mathbf{z}_1 = \mathbf{x}_1 - \mathbf{x}_{ref} := \Psi_1(\mathbf{x}_1)$$

then

$$\dot{\mathbf{z}}_1 = \mathbf{f}_1(\mathbf{x}_1) + \mathbf{B}_1(\mathbf{x}_1)\mathbf{x}_2 + \bar{\mathbf{g}}_1(t, \mathbf{x}) \tag{3.3.2}$$

with $\bar{\mathbf{g}}_1(t, \mathbf{x}) = \mathbf{g}_1(t, \mathbf{x}) - \dot{\mathbf{x}}_{ref}$.

And the virtual control $\mathbf{x}_2$ in (3.3.2) is redefined of the form

$$\mathbf{x}_2 = \mathbf{x}_{2,0} + \mathbf{x}_{2,1} \tag{3.3.3}$$

where the nominal part, $\mathbf{x}_{2,0}$ is selected to eliminate the old dynamics in (3.3.2) and introduce the new desired ones, $k_1\mathbf{z}_1$, $k_1 > 0$ i. e.

$$\mathbf{x}_{2,0} = -\mathbf{B}_1^+(\mathbf{x}_1)\left(\mathbf{f}_1(\mathbf{x}_1) + k_1\mathbf{z}_1 - \mathbf{E}_1\mathbf{z}_2\right), \quad k_1 > 0 \tag{3.3.4}$$

where $\mathbf{z}_2 \in \mathbb{R}^{n_2}$ is a new variables vector, $\mathbf{E}_1 = \begin{bmatrix} \mathbf{I}_{n_1} & 0 \end{bmatrix} \in \mathbb{R}^{n_1 \times n_2}$ and $\mathbf{B}_1^+$ is the right pseudoinverse of $\mathbf{B}_1$, defined as $\mathbf{B}_1^+ = \mathbf{B}_1^T\left(\mathbf{B}_1\mathbf{B}_1^T\right)^{-1}$

In order to reject the perturbation term $\bar{\mathbf{g}}_1(t,\mathbf{x})$ in (3.3.2), the second part of the virtual control (3.3.3), $\mathbf{x}_{2,1}$ is designed by using the integral sliding mode technique [101]. The pseudo-sliding manifold $\mathbf{s}_1$ is chosen as

$$\mathbf{s}_1 = \mathbf{z}_1 + \sigma_1 = 0 \qquad \mathbf{s}_1, \sigma_1 \in \mathbb{R}^{n1} \tag{3.3.5}$$

Then, from (3.3.2)-(3.3.5) it follows

$$\dot{\mathbf{s}}_1 = -k_1\mathbf{z}_1 + \mathbf{E}_1\mathbf{z}_2 + \mathbf{B}_1(\mathbf{x}_1)\mathbf{x}_{2,1} + \bar{\mathbf{g}}_1(t,\mathbf{x}) + \sigma_1. \tag{3.3.6}$$

Choosing the dynamics for the integral variable σ_1 of the form

$$\dot{\sigma}_1 = k_1\mathbf{z}_1 - \mathbf{E}_1\mathbf{z}_2, \quad \sigma_1(0) = -\mathbf{z}_1(0) \tag{3.3.7}$$

the equation (3.3.6) becomes

$$\dot{\mathbf{s}}_1 = \mathbf{B}_1(\mathbf{x}_1)\mathbf{x}_{2,1} + \bar{\mathbf{g}}_1(t,\mathbf{x}). \tag{3.3.8}$$

The control input $\mathbf{x}_{2,1}$ in (3.3.8) is selected as follows:

$$\mathbf{x}_{2,1} = -\rho_1(\mathbf{x}_1)\mathbf{B}_1^{+}\mathrm{sigm}(\mathbf{s}_1;\varepsilon_1) \tag{3.3.9}$$

where $\mathrm{sigm}(\mathbf{s}_1;\varepsilon_1) = [\mathrm{sigm}(\mathbf{s}_{1,1};\varepsilon_1),\ldots,\mathrm{sigm}(\mathbf{s}_{1,n_1};\varepsilon_1)]^T$ Substituting (3.3.3), (3.3.4) and (3.3.9) in (3.3.2) results in

$$\dot{\mathbf{z}}_1 = -k_1\mathbf{z}_1 + \mathbf{E}_1\mathbf{z}_2 - \rho_1(\mathbf{x}_1)\mathrm{sigm}(\mathbf{s}_1;\varepsilon_1) + \bar{\mathbf{g}}_1(t,\mathbf{x}). \tag{3.3.10}$$

If the matrix $\mathbf{M}_1(\mathbf{x}_1) \in \mathbb{R}^{(n_2-n_1)\times n_2}$ is chosen such that the square matrix $\tilde{\mathbf{B}}_2(\mathbf{x}_1) = \left[\begin{array}{cc}\mathbf{B}_1(\mathbf{x}_1) & \mathbf{M}_1(\mathbf{x}_1)\end{array}\right]^T$ has full rank, the new variables vector $\mathbf{z}_2$ can be obtained from equations (3.3.3), (3.3.4) and (3.3.9) as

$$\mathbf{z}_2 = \tilde{\mathbf{B}}_2\mathbf{x}_2 + \left[\begin{array}{c}\mathbf{f}_1(\mathbf{x}_1) - k_1\boldsymbol{\Psi}_1(\mathbf{x}_1) - \rho_1(\mathbf{x}_1)\mathrm{sigm}(\mathbf{s}_1;\varepsilon_1)\\ 0\end{array}\right] := \boldsymbol{\Psi}_2(\bar{\mathbf{x}}_2) \tag{3.3.11}$$

where $\bar{\mathbf{x}}_2 = \left[\begin{array}{cc}\mathbf{x}_1 & \mathbf{x}_2\end{array}\right]^T$ The procedure described above can be achieved in the i^{th} block of (3.3.1) as follows.

Step i. At this step, the dynamics of the transformed i^{th} block of the system (3.3.1) are given by

$$\dot{\mathbf{z}}_i = \bar{\mathbf{f}}_i(\bar{\mathbf{x}}_i) + \bar{\mathbf{B}}_i(\mathbf{x}_i)\mathbf{x}_{i+1} + \bar{\mathbf{g}}_i(t,\mathbf{x}) \tag{3.3.12}$$

where $\mathbf{z}_i \in \mathbb{R}^{n_i}$ is a new variables vector, $\bar{\mathbf{g}}_i(t,\mathbf{x}) = \bar{\mathbf{g}}_{i-1}(t,\mathbf{x}) - \frac{d}{dt}[\rho_{i-1}(\bar{\mathbf{x}}_{i-1})\mathrm{sigm}(\mathbf{s}_{i-1};\varepsilon_{i-1})]$, $\mathbf{z}_i = \boldsymbol{\Psi}_i(\bar{\mathbf{x}}_i)$ and $\bar{\mathbf{B}}_i = \tilde{\mathbf{B}}_i\mathbf{B}_i$. The virtual control $\mathbf{x}_{i+1}$ in (3.3.12) is redefined as

$$\mathbf{x}_{i+1} = \mathbf{x}_{i+1,0} + \mathbf{x}_{i+1,1}. \tag{3.3.13}$$

Taking into account the procedure achieved in *step 1*, $\mathbf{x}_{i+1,0}$ and $\mathbf{x}_{i+1,1}$ are selected, respectively, of the form

$$\mathbf{x}_{i+1,0} = -\bar{\mathbf{B}}_i^{+}(\bar{\mathbf{x}}_i)\left(\bar{\mathbf{f}}_i(\bar{\mathbf{x}}_i) + k_i\mathbf{z}_i - \mathbf{E}_i\mathbf{z}_{i+1}\right), \quad k_i > 0 \tag{3.3.14}$$

$$\mathbf{x}_{i+1,1} = -\rho_i(\bar{\mathbf{x}}_i)\,\mathbf{B}_i^{+}\mathrm{sigm}(\mathbf{s}_i;\varepsilon_i), \quad \rho_i > 0 \tag{3.3.15}$$

where $\mathbf{z}_{i+1} \in \mathbb{R}^{n_{i+1}}$ is a new variables vector, $\mathbf{E}_i = \left[\begin{array}{cc} \mathbf{I}_{n_i} & 0 \end{array}\right] \in \mathbb{R}^{n_i \times n_{i+1}}$ and $\bar{\mathbf{B}}_i^{+} = \bar{\mathbf{B}}_i^T\left(\bar{\mathbf{B}}_i\bar{\mathbf{B}}_i^T\right)^{-1}$ The proposed pseudo-sliding manifold and its derived dynamics, respectively, are:

$$\mathbf{s}_i = \mathbf{z}_i + \sigma_i = 0, \quad \mathbf{s}_i, \sigma_i \in \mathbb{R}^{n_i}$$

$$\dot{\mathbf{s}}_i = -k_i\mathbf{z}_i + \mathbf{E}_i\mathbf{z}_{i+1} + \mathbf{B}_i(\mathbf{x}_i)\,\mathbf{x}_{i+1,1} + \bar{\mathbf{g}}_i(t,\mathbf{x}) + \sigma_i. \tag{3.3.16}$$

If σ_i satisfies

$$\dot{\sigma}_i = k_i\mathbf{z}_i - \mathbf{E}_i\mathbf{z}_{i+1}, \quad \sigma_i(0) = -\mathbf{z}_i(0) \tag{3.3.17}$$

the equation (3.3.16) can be rewritten as

$$\dot{\mathbf{s}}_i = -\rho_i(\bar{\mathbf{x}}_i)\,\mathrm{sigm}(\mathbf{s}_i;\varepsilon_i) + \bar{\mathbf{g}}_i(t,\mathbf{x}), \quad \rho_i(\bar{\mathbf{x}}_i) > 0.$$

The substitution of (3.3.14) and (3.3.15) in the block (3.3.12) yields

$$\dot{\mathbf{z}}_i = -k_i\mathbf{z}_i + \mathbf{E}_i\mathbf{z}_{i+1} - \rho_i(\bar{\mathbf{x}}_i)\,\mathrm{sigm}(\mathbf{s}_i;\varepsilon_i) + \bar{\mathbf{g}}_i(t,\mathbf{x}).$$

Again, choosing a $(n_{i+1} - n_i) \times n_{i+1}$ matrix $\mathbf{M}_i(\bar{\mathbf{z}}_i)$ such that the square matrix $\tilde{\mathbf{B}}_{i+1}(\bar{\mathbf{x}}_i) = \left[\begin{array}{cc} \bar{\mathbf{B}}_i(\bar{\mathbf{x}}_i) & \mathbf{M}_i(\bar{\mathbf{x}}_i) \end{array}\right]^T$ has full rank, the new variables vector $\mathbf{z}_{i+1}$ can be obtained from equations (3.3.12)-(3.3.15) as

$$\begin{aligned} \mathbf{z}_{i+1} &= \tilde{\mathbf{B}}_{i+1}\mathbf{x}_{i+1} + \left[\begin{array}{c} \bar{\mathbf{f}}_i(\bar{\mathbf{x}}_i) - k_i\boldsymbol{\Psi}_i(\bar{\mathbf{x}}_i) - \rho_i(\mathbf{x}_i)\,\mathrm{sigm}(\mathbf{s}_i;\varepsilon_i) \\ 0 \end{array}\right] \quad i = 2,\ldots,r-1, \\ &:= \boldsymbol{\Psi}_{i+1}(\bar{\mathbf{x}}_{i+1}). \end{aligned}$$

Step r. At the last step, the transformed complete system can be presented in the new variables $\mathbf{z}_1,\ldots,\mathbf{z}_t$ as

$$\begin{aligned} \dot{\mathbf{z}}_i &= -k_i\mathbf{z}_i + \mathbf{E}_i\mathbf{z}_{i+1} - \rho_i(\bar{\mathbf{x}}_i)\,\mathrm{sigm}(\mathbf{s}_i;\varepsilon_i) + \bar{\mathbf{g}}_i(t,\mathbf{x}) \\ \dot{\mathbf{s}}_i &= -\rho_i(\bar{\mathbf{x}}_i)\,\mathrm{sigm}(\mathbf{s}_i;\varepsilon_i) + \bar{\mathbf{g}}_i(t,\mathbf{x}) \\ \dot{\mathbf{z}}_r &= \bar{\mathbf{f}}_r(\mathbf{x}) + \bar{\mathbf{B}}_r(\mathbf{x})\,\mathbf{u} + \bar{\mathbf{g}}_r(t,\mathbf{x}), \quad i = 1,\ldots,r-1 \end{aligned} \tag{3.3.18}$$

where $\bar{\mathbf{B}}_r(\cdot) = \tilde{\mathbf{B}}_{r-1}(\cdot)\,\mathbf{B}_r(\cdot)$ has full rank since $n_r = m$. Design the control input $\mathbf{u}$ in (3.3.18) as

$$\mathbf{u} = \mathbf{u}_0 + \mathbf{u}_1 \tag{3.3.19}$$

and define a sliding variable $\mathbf{s}_r \in \mathbb{R}^{n_r}$ of the form

$$\mathbf{s}_r = \mathbf{z}_r + \sigma_r, \quad \sigma_r \in \mathbb{R}^{n_r} \tag{3.3.20}$$

Then

$$\dot{\mathbf{s}}_r = \bar{\mathbf{f}}_r(\mathbf{x}) + \bar{\mathbf{B}}_r(\mathbf{x})\mathbf{u}_0 + \bar{\mathbf{B}}_r(\mathbf{x})\mathbf{u}_1 + \bar{\mathbf{g}}_r(t,\mathbf{x}) + \dot{\sigma}_r \tag{3.3.21}$$

Choosing

$$\dot{\sigma}_r = -\bar{\mathbf{f}}_r(\mathbf{x}) - \bar{\mathbf{B}}_r(\mathbf{x})\mathbf{u}_0, \qquad \sigma_r(0) = -\mathbf{z}_r(0)$$

simplifies the equation (3.3.21) to

$$\dot{\mathbf{s}}_r = \bar{\mathbf{B}}_r(\mathbf{x})\mathbf{u}_1 + \bar{\mathbf{g}}_r(t,\mathbf{x}) \tag{3.3.22}$$

The second part of the control input (3.3.19) is selected as

$$\mathbf{u}_1 = -\rho_r(\mathbf{x})\bar{\mathbf{B}}_r^{-1}\mathrm{sign}(\mathbf{s}_r), \quad \rho_r(\mathbf{x}) > 0. \tag{3.3.23}$$

Under the condition $\rho_r(\mathbf{x}) > \left\|\bar{\mathbf{B}}_r^{-1}(\mathbf{x})\bar{\mathbf{g}}_r(t,\mathbf{x})\right\|$ sliding mode occurs on the manifold $\mathbf{s}_r = 0$ (3.3.20) in a finite time. Solving (3.3.22) for $\mathbf{u}_{r-1}$, formally setting $\dot{\mathbf{s}}_r = 0$, shows

$$\mathbf{u}_{1eq} = \bar{\mathbf{B}}_r^{-1}(\mathbf{x})\bar{\mathbf{g}}_r(t,\mathbf{x})$$

where $\mathbf{u}_{1eq}(t,\mathbf{x})$ is the equivalent control [101]. Therefore, the integral control (3.3.23) rejects the perturbation term $\bar{\mathbf{g}}_r(t,\mathbf{x})$ in the last block of (3.3.18):

$$\dot{\mathbf{z}}_r = \bar{\mathbf{f}}_r(\mathbf{x}) + \bar{\mathbf{B}}_r(\mathbf{x})\mathbf{u}_0 + \bar{\mathbf{B}}_r(\mathbf{x})\mathbf{u}_{1eq} + \bar{\mathbf{g}}_r(t,\mathbf{x})$$

and we have

$$\dot{\mathbf{z}}_r = \bar{\mathbf{f}}_r(\mathbf{x}) + \bar{\mathbf{B}}_r(\mathbf{x})\mathbf{u}_0.$$

Now, choosing

$$\mathbf{u}_0 = -\bar{\mathbf{B}}_r^{-1}(\mathbf{x})\left[\bar{\mathbf{f}}_r(\mathbf{x}) + k_r\mathbf{z}_r\right] \qquad k_r > 0$$

the sliding mode dynamics are described by

$$\begin{aligned}
\dot{\mathbf{z}}_i &= -k_i\mathbf{z}_i + \mathbf{E}_i\mathbf{z}_{i+1} - \rho_i(\bar{\mathbf{x}}_i)\,\mathrm{sigm}(\mathbf{s}_i;\varepsilon_i) + \bar{\mathbf{g}}_i(t,\mathbf{x}) \\
\dot{\mathbf{s}}_i &= -\rho_i(\bar{\mathbf{x}}_i)\,\mathrm{sigm}(\mathbf{s}_i;\varepsilon_i) + \bar{\mathbf{g}}_i(t,\mathbf{x}) \\
\dot{\mathbf{z}}_r &= -k_r\mathbf{z}_r, \quad i = 1,\ldots,r-1.
\end{aligned} \tag{3.3.24}$$

Now, it is possible to establish the following result:

Theorem 3.2. *If*

H1) the unmatched $\bar{\mathbf{g}}_1(\cdot), \ldots, \bar{\mathbf{g}}_{r-1}(\cdot)$ *and matched* $\bar{\mathbf{g}}_r(\cdot)$ *perturbations are bounded, i.e., there exists a known scalar function* $\beta_i(\mathbf{x})$ *such that*

$$\|\bar{\mathbf{g}}_i(t,\mathbf{x})\| \leq \beta_i(\mathbf{x}), \quad i = 1, \ldots, r$$

then, there exist constants $h_1, \ldots, h_{r-1}$ *such that the states of the system (3.3.24), are uniformly bounded, i. e.*

$$\|\mathbf{z}_i(t)\| \leq h_i, \quad i = 1, \ldots, r-1.$$

Moreover the perturbed system (3.3.24) reaches to a neighbourhood of the output $\mathbf{y} = \mathbf{x}_1$ *in finite time and remains in this neighbourhood.*

Proof. The proof is constructive and consists of r steps, begin with the step r.

Step r. First, the stability of the sliding variable $\mathbf{s}_r$ is analyzed. Considering the Lyapunov function $\mathbf{V}_r = \mathbf{s}_r^T \mathbf{s}_r$, it follows:

$$\dot{\mathbf{V}}_r = \mathbf{s}_r^T \left[-\rho_r(\mathbf{x}) \operatorname{sign}(\mathbf{s}_r) + \bar{\mathbf{g}}_r(t,\mathbf{x})\right]. \tag{3.3.25}$$

Under the assumption *H1*, the equation (3.3.25) can be written as

$$\begin{aligned} \dot{\mathbf{V}}_r &= \mathbf{s}_r^T \left[-\rho_r(\mathbf{x}) \operatorname{sign}(\mathbf{s}_r) + \beta_r(\mathbf{X})\right] \\ &\leq \|\mathbf{s}_r\| \left[-\rho_r(\mathbf{x}) + \|\beta_r(\mathbf{X})\|\right] \end{aligned} \tag{3.3.26}$$

From (3.3.26) it is easy to see that under the condition

$$\rho_r(\mathbf{x}) > \|\beta_r(\mathbf{X})\|$$

the derivative $\dot{\mathbf{V}}_r$ is definite negative and the equivalent control $\mathbf{u}_{r,1eq}(t,\mathbf{x})$ satisfies

$$\mathbf{u}_{r,1eq} = -\bar{\mathbf{g}}_r(t,\mathbf{x})$$

rejecting the perturbation term $\bar{\mathbf{g}}_r(t,\mathbf{x})$ in the last block of (3.3.24). Now, it is necessary to analyze the stability of the last block. Using the Lyapunov function $\mathbf{V}_r = \frac{1}{2}\mathbf{z}_r^T \mathbf{z}_r$, leads to

$$\dot{\mathbf{V}}_r \leq -k_r \|\mathbf{z}_r\|^2 \quad k_r > 0.$$

Thus, the trajectories of the last variables vector $\mathbf{z}_r$ are asymptotically stable.

Step r-1. Proceeding in a similar way as in previous step, the Lyapunov function $\mathbf{V}_{r-1} = \mathbf{s}_{r-1}^T \mathbf{s}_{r-1}$ is proposed, then

$$\dot{\mathbf{V}}_{r-1} = \mathbf{s}_{r-1}^T \left[-\rho_{r-1}(\bar{\mathbf{x}}_{r-1}) \operatorname{sigm}(\mathbf{s}_{r-1}) + \bar{\mathbf{g}}_{r-1}(t,\mathbf{x})\right] \tag{3.3.27}$$

In the region $\|\mathbf{s}_{r-1}\| > \varepsilon_{r-1}$ the equation (3.3.27) becomes

$$\begin{aligned} \dot{\mathbf{V}}_{r-1} &= \mathbf{s}_{r-1}^T \left[-\rho_{r-1}\left(\bar{\mathbf{x}}_{r-1}\right) \operatorname{sign}\left(\mathbf{s}_{r-1}\right) + \bar{\mathbf{g}}_{r-1}\left(t, \mathbf{x}\right)\right] \\ &\leq \|\mathbf{s}_{r-1}\| \left[-\rho_{r-1}\left(\bar{\mathbf{x}}_{r-1}\right) + \|\bar{\mathbf{g}}_{r-1}\left(t, \mathbf{x}\right)\|\right] \end{aligned} \tag{3.3.28}$$

Moreover, under the condition $\rho_{r-1}\left(\bar{\mathbf{x}}_{r-1}\right) > \|\bar{\mathbf{g}}_{r-1}\left(t, \mathbf{x}\right)\|$, $\|\mathbf{s}_{r-1}\|$ will be decreasing until it reaches the set $\{\|\mathbf{s}_{r-1}\| \leq \varepsilon_{r-1}\}$ in a finite time and it remains inside. The upper bound of this reaching time can be calculated by using the comparison lemma [138] as follows:

$$t_{r-1} \leq \|\mathbf{s}_{r-1}\left(0\right)\| - \varepsilon_{r-1}.$$

Furthermore the equivalent control $\mathbf{x}_{r-1,1eq}$ fulfills

$$\dot{\mathbf{s}}_{r-1} = \mathbf{x}_{r-1,1eq} + \bar{\mathbf{g}}_{r-1}\left(t, \mathbf{x}\right) = \varepsilon_{r-1}\gamma_{r-1} \tag{3.3.29}$$

where $\varepsilon_{r-1}\gamma_{r-1}$ is the error introduced by using the control law (3.3.15). To analyze the stability of the $r-1$ block of the system (3.3.24), the Lyapunov function $\mathbf{V}_{r-1} = \frac{1}{2}\mathbf{z}_{r-1}^T\mathbf{z}_{r-1}$ is considered and its time derivative is given by

$$\begin{aligned} \dot{\mathbf{V}}_{r-1} &= \mathbf{z}_{r-1}^T \left[-k_{r-1}\mathbf{z}_{r-1} + \mathbf{E}_{r-1}\mathbf{z}_r - \rho_{r-1}\left(\bar{\mathbf{x}}_{r-1}\right) \operatorname{sigm}\left(\mathbf{s}_{r-1}; \varepsilon_{r-1}\right) + \bar{\mathbf{g}}_{r-1}\left(t, \mathbf{z}\right)\right] \\ &\leq -k_{r-1}\|\mathbf{z}_{r-1}\|^2 + \|\mathbf{z}_{r-1}\| \left[\|\mathbf{z}_r\| - \rho_{r-1}\left(\bar{\mathbf{x}}_{r-1}\right) \operatorname{sigm}\left(\mathbf{s}_{r-1}; \varepsilon_{r-1}\right) + \bar{\mathbf{g}}_{r-1}\left(t, \mathbf{z}\right)\right]. \end{aligned}$$

In the region $\|\mathbf{s}_{r-1}\| > \varepsilon_{r-1}$, the derivative $\dot{\mathbf{V}}_{r-1}$ becomes

$$\begin{aligned} \dot{\mathbf{V}}_{r-1} &\leq -k_{r-1}\|\mathbf{z}_{r-1}\|^2 + \|\mathbf{z}_{r-1}\| \left[\|\mathbf{z}_r\| - \rho_{r-1}\left(\bar{\mathbf{x}}_{r-1}\right) \operatorname{sigm}\left(\mathbf{s}_{r-1}; \varepsilon_{r-1}\right) + \bar{\mathbf{g}}_{r-1}\left(t, \mathbf{z}\right)\right] \\ &\leq k_{r-1}\|\mathbf{z}_{r-1}\|^2 + \|\mathbf{z}_{r-1}\| \left[\|\mathbf{z}_r\| + \dot{\mathbf{s}}_{r-1}\right] \end{aligned}$$

and considering (3.3.29), it can be rewritten as

$$\dot{\mathbf{V}}_{r-1} \leq -k_{r-1}\|\mathbf{z}_{r-1}\|^2 + \|\mathbf{z}_{r-1}\| \left[\|\mathbf{z}_r\| + \varepsilon_{r-1}\gamma_{r-1}\right]. \tag{3.3.30}$$

Suppose that $\varepsilon_{r-1}\gamma_{r-1}$ satisfies the following bound:

$$\varepsilon_{r-1}\gamma_{r-1} \leq \alpha_{r-1}\|\mathbf{z}_{r-1}\| + \beta_{r-1}, \quad \alpha_{r-1}, \quad \beta_{r-1} \in \mathbb{R}.$$

Then it is possible to present the equation (3.3.30) of the form

$$\begin{aligned} \dot{\mathbf{V}}_{r-1} &\leq k_{r-1}\|\mathbf{z}_{r-1}\|^2 + \|\mathbf{z}_{r-1}\| \left[\|\mathbf{z}_r\| + \alpha_{r-1}\|\mathbf{z}_{r-1}\| + \beta_{r-1}\right] \\ &\leq -\|\mathbf{z}_{r-1}\| \left[\left(k_{r-1} - \alpha_{r-1}\right)\|\mathbf{z}_{r-1}\| - \|\mathbf{z}_r\| - \beta_{r-1}\right] \end{aligned}$$

which is negative in the region

$$\|\mathbf{z}_{r-1}\| > \delta_{r-1}\|\mathbf{z}_r\| + \lambda_{r-1} \tag{3.3.31}$$

where $\delta_{r-1} = \frac{1}{k_{r-1}-\alpha_{r-1}}$ and $\lambda_{r-1} = \frac{\beta_{r-1}}{k_{r-1}-\alpha_{r-1}}$. Moreover δ_{r-1} and λ_{r-1} are positive for $k_{r-1} > \alpha_{r-1}$. Thus the trajectories of the vector state enter ultimately in the region defined by

$$\|\mathbf{z}_{r-1}\| \leq \delta_{r-1} \|\mathbf{z}_r\| + \lambda_{r-1}.$$

Step i. The step $r-1$ can be generalized for the block i, with $i = r-1, r-2, \ldots, 1$.

In the region $\|\mathbf{s}_i\| > \varepsilon_i$ the derivative of the Lyapunov function $\mathbf{V}_i = \mathbf{s}_i^T \mathbf{s}_i$ is calculated as

$$\begin{aligned} \dot{\mathbf{V}}_i &= \mathbf{s}_i^T \left[-\rho_i(\bar{\mathbf{x}}_i) \operatorname{sign}(\mathbf{s}_i) + \bar{\mathbf{g}}_i(t, \mathbf{x})\right] \\ &\leq \|\mathbf{s}_i\| \left[-\rho_i(\bar{\mathbf{x}}_i) + \|\bar{\mathbf{g}}_i(t, \mathbf{x})\|\right]. \end{aligned} \tag{3.3.32}$$

Again, under the condition $-\rho_i(\bar{\mathbf{x}}_i) > \|\bar{\mathbf{g}}_i(t, \mathbf{x})\|$, $\mathbf{s}_i$ enter in the region $\{\|\mathbf{s}_i\| \leq \varepsilon_i\}$ in a finite time given by

$$t_i \leq \|\mathbf{s}_i(0)\| - \varepsilon_i.$$

The equivalent control $\mathbf{x}_{i,1eq}$ satisfies

$$\dot{\mathbf{s}}_i = \mathbf{x}_{i,1eq} + \bar{\mathbf{g}}_i(t, \mathbf{x}) = \varepsilon_i \gamma_i. \tag{3.3.33}$$

Considering the function $\mathbf{V}_i = \frac{1}{2}\mathbf{z}_i^T \mathbf{z}_i$ inside the subspace $\|\mathbf{s}_i\| \leq \varepsilon_i$, it follows

$$\begin{aligned} \dot{\mathbf{V}}_i &\leq -k_i \|\mathbf{z}_i\|^2 + \|\mathbf{z}_i\| \left[\|\mathbf{z}_{i+1}\| - \rho_i(\bar{\mathbf{x}}_i) \operatorname{sigm}(\mathbf{s}_i; \varepsilon_i) + \bar{\mathbf{g}}_i(t, \mathbf{z})\right] \\ &\leq -k_i \|\mathbf{z}_i\|^2 + \|\mathbf{z}_i\| \left[\|\mathbf{z}_{i+1}\| + \dot{\mathbf{s}}_i\right] \end{aligned}$$

and with (3.3.33), $\dot{\mathbf{V}}_i$ becomes

$$\dot{\mathbf{V}}_i \leq -k_i \|\mathbf{z}_i\|^2 + \|\mathbf{z}_i\| \left[\|\mathbf{z}_{i+1}\| + \varepsilon_i \gamma_i\right]$$

Supposing that $\varepsilon_i \gamma_i$ fulfills

$$\varepsilon_i \gamma_i \leq \alpha_i \|\mathbf{z}_i\| + \beta_i, \quad \alpha_i, \beta_i \epsilon \mathbb{R}$$

then

$$\dot{\mathbf{V}}_i \leq -\|\mathbf{z}_i\| \left[(k_i - \alpha_i) \|\mathbf{z}_i\| - \|\mathbf{z}_{i+1}\| - \beta_i\right]$$

which is negative in the region

$$\|\mathbf{z}_i\| > \delta_i \|\mathbf{z}_{i+1}\| + \lambda_i$$

where $\delta_i = \frac{1}{k_i - \alpha_i}$ and $\lambda_i = \frac{\beta_i}{k_i - \alpha_i}$, which are positive for $k_i > \alpha_i$. Therefore a solution for $\mathbf{z}_i$ is ultimately bounded by

$$\|\mathbf{z}_i\| \leq \delta_i \|\mathbf{z}_{i+1}\| + \lambda_i.$$

Then with the bound

$$\varepsilon_i \gamma_i \leq \alpha_i \|\mathbf{z}_i\| + \beta_i, \quad i = 1, 2, \ldots, r-1$$

the convergence region is defined by:

$$\begin{aligned} \|\mathbf{z}_{r-1}\| &> \delta_{r-1} \|\mathbf{z}_r\| + \lambda_{r-1} := h_{r-1} \\ \|\mathbf{z}_{r-2}\| &> \delta_{r-2} \|\mathbf{z}_{r-1}\| + \lambda_{r-2} := h_{r-2} \\ &\vdots \\ \|\mathbf{z}_1\| &> \delta_1 \|\mathbf{z}_2\| + \lambda_1 := h_1 \end{aligned}$$

□

3.4 Conclusions

In this chapter control methods are introduced; the Regular Form is presented, giving convenient interpretation of the reduced order dynamics provided by sliding mode control; the Block Control Principle, as a generalization of the Regular form, and the Integral Sliding Modes with Block Control are presented in detail for the design of sliding surfaces for robust sliding mode controllers.

Chapter 4

Brake system control

In this chapter we propose controllers based on the block control principle and sliding mode for the brake system. These controllers maximize the friction force in the wheel and avoids brake locking. Different cases are presented; it includes problems as tire deformation and the addition of an active suspension. This work considers the real situation: the control input can take only two values "0" or "1", depending on the corresponding valve being open or closed.

In section 4.1 the joint application of sliding mode control and block control principle is proposed, [115], [133]. The block control principle is used to design the sliding surface and provide linear dynamics in the sliding manifold. In this case tire deformation is not considered.

Subsequently, the use of integral nested sliding mode [135], [134] for the cases of no tire deformation and tire deformation are considered in sections 4.2 and 4.3, respectively. Theoretically, the integral nested sliding mode control can guarantee the robustness of the system throughout the entire response starting from the initial time and reduce the sliding functions gains in comparison with standard sliding mode. In addition, as example, the use of a continuous pneumatic valve is studied and a Super Twisting control is used [100, Ch. 2].

The section 4.4 presents a sliding mode block control regulator for the asymptotically tracking of the relative slip to a desired trajectory. To solve this problem we propose to use the block control technique combined with the SM control algorithm to achieve robustness to perturbations, and to ensure asymptotic output tracking along with the stabilization of the residual dynamic consisting of the vehicle velocity.

Finally in section 4.5 the control of a brake with active suspension is presented. An ABS control based on integral nested sliding mode is designed in order to impose a desired vehicle motion and as a consequence, to provide adequate vehicle stability. On the other hand, active suspension are designed with the objective to guarantee the improvement of the ride quality and comfort for the passengers. For the active suspension, another new controller

based on the regular form [102], sliding mode control and geometric linear control methods [139] for the sliding surface design is proposed in order to achieve robustness to matched, and unmatched perturbations and ensure output tracking. In both subsystems a Super-Twisting control is used [100, Ch. 2].

Throughout the development of the controller, we will assume that all the state variables are available for measurement.

4.1 Sliding mode block control for brake with no tire deformation

In this section, the joint application of sliding mode control and block control principle is proposed. The block control principle is used to design the sliding surface and provide linear dynamics in the sliding manifold. In this case the deformation on the tire is not considered. Based on system (2.1.11) the problem is to design an Sliding Mode Block controller that obtains reference tracking in despite of the perturbations in the system. Define s^* as the desired trajectory of the relative slip, which must maximize the friction function $\phi(s)$. The system model is presented again

$$\begin{aligned} \dot{x}_1 &= -a_0 x_1 + a_1 f(s) - a_2 x_2 \\ \dot{x}_2 &= -a_3 x_2 + bu \\ \dot{x}_3 &= -a_4 F(s) - f_w(x_3) \end{aligned} \tag{4.1.1}$$

with output $y = s = h(x) = 1 - r\frac{x_1}{x_3}$, where $a_0 = B_b/J$, $a_1 = r/J$, $a_2 = k_b/J$, $a_3 = 1/\tau$, $a_4 = 1/M$, $b = P_c/\tau$ and $f_w(x_3) = \frac{1}{2M}(\rho C_d A_f)(x_3 + v_w)^2$

4.1.1 Control design

Let $s^*(t)$ be a twice differentiable function, but with unknown derivatives, now we define the output tracking error as $e_1 \triangleq s - s^*$ then its derivative is

$$\dot{e}_1 = c_1(x) + c_2(x)x_2 + f_y(x) - \dot{s}^* \tag{4.1.2}$$

where

$$\begin{aligned} c_1(x) \triangleq c_1 &= r\left(-a_0\frac{x_1}{x_3} + \frac{a_1}{x_3}f(s) + a_4\frac{x_1}{x_3^2}F(s)\right) \\ c_2(x) \triangleq c_2 &= -\frac{a_2}{x_3}r \\ f_y(x) \triangleq f_y &= -r\frac{x_1}{x_3}f_w(x_3) + \Delta(\mu) \end{aligned}$$

$f_y(x)$ will be considered as an unmatched and bounded perturbation term

$$|f_y(x,t)| < \beta < \infty$$

and the term $\Delta(\mu)$ contains the variations of the friction parameter μ.

Considering the variable x_2 as virtual control in (4.1.2) we propose the desired dynamics $\dot{e}_1 = -k_0 e_0 - k_1 e_1$ by means of

$$x_{2ref} = -\frac{1}{c_2}\left[c_1 + k_0 e_0 + k_1 e_1\right] \tag{4.1.3}$$

where $k_0 > 0$, $k_1 > 0$ and e_0 is the integral of the tracking error e_1 that is

$$\dot{e}_0 = e_1. \tag{4.1.4}$$

The variable x_{2ref} is used to put the desired dynamic for e_1 and obtain the control aim. Now we define a new error variable $e_2 \triangleq \alpha_2(x,t)$ in the form

$$e_2 = x_{2ref} - x_2. \tag{4.1.5}$$

Using (4.1.1) and (4.1.3), straightforward calculations reveal

$$\dot{e}_2 = -a_3 e_2 - bu + f_{2e}(x) \tag{4.1.6}$$

where

$$f_{2e}(x) = a_3 x_{2ref} + \frac{\partial \alpha_2(x,t)}{\partial x_1}\dot{x}_1 + \frac{\partial \alpha_2(x,t)}{\partial x_3}\dot{x}_3.$$

To induce sliding mode on the sliding manifold $e_2 = 0$ we choose the control signal as

$$u = \frac{1}{2}\text{sign}(e_2) + \frac{1}{2}. \tag{4.1.7}$$

4.1.2 Stability analysis

Using the new variables e_0, e_1 and e_2 the extended closed loop system (4.1.2), (4.1.4), (4.1.6) and (4.1.7) is presented as:

$$\dot{e}_0 = e_1 \tag{4.1.8}$$

$$\dot{e}_1 = -k_0 e_0 - k_1 e_1 + c_2 e_2 + g_1(x,t) \tag{4.1.9}$$

$$\dot{e}_2 = -a_3 e_2 + f_{2e}(x) - \frac{1}{2}\text{sign}(e_2)\, b - \frac{1}{2}b \tag{4.1.10}$$

with $g_1(x,t) = f_y(x) - \dot{s}^*$

The stability of (4.1.8) (4.1.10) can be is studied step by step:

A) SM stability of the projection motion (4.1.10);

B) SM stability of the projection motion (4.1.8)-(4.1.9);

We use the following assumptions:

$$|g_1(x,t)| \leqslant \alpha_1 |e_1| + \beta_1 \tag{4.1.11}$$

and

$$|f_{2e}(x)| \leqslant \alpha_2 |e_2| + \beta_2 \tag{4.1.12}$$

with $\alpha_1 > 0$, $\alpha_2 > 0$, $\beta_1 > 0$, $\beta_2 > 0$, $a_3 > \alpha_2$ and $b > |f_{2e}(x)|$.

A) The system (4.1.10) can be presented as follows:

CASE 1, $e_2 < 0$, then

$$\dot{e}_2 = -a_3 e_2 + f_{2e}(x) \tag{4.1.13}$$

CASE 2, $e_2 > 0$, then

$$\dot{e}_2 = -a_3 e_2 + f_{2e}(x) - b \tag{4.1.14}$$

we use the Lyapunov candidate function $V_2 = \frac{1}{2} e_2^2$ to analyze the stability conditions. The derivative of V_2 with respect to time in CASE 1 is

$$\dot{V}_2 = e_2 (-a_3 e_2 + f_{2e}(x)) \tag{4.1.15}$$

under condition (4.1.12) we have

$$\dot{V}_2 \leq |e_2| (-a_3 |e_2| + \alpha_2 |e_2| + \beta_2)$$

In this case, the solution of (4.1.10) is ultimately bounded [138] by

$$|e_2(t)| \leqslant \delta_0, \quad \delta_0 = \frac{\beta_2}{a_3 - \alpha_2} \tag{4.1.16}$$

that is similar in CASE 2.

B) To analyze stability of the sliding mode equations (4.1.8)-(4.1.9) in a vecinity of $e_2 = 0$, that system can be regarded as a linear system with non-vanishing perturbation in the form:

$$\dot{\xi} = A\xi + D(\xi) \tag{4.1.17}$$

where

$$\xi = \begin{bmatrix} e_1 & e_2 \end{bmatrix}^T ; A = \begin{bmatrix} 0 & 1 \\ -k_0 & -k_1 \end{bmatrix} ; D = \begin{bmatrix} 0 \\ g_1(t) \end{bmatrix}$$

Now we use the following Lyapunov candidate function:

$$V_1 = \frac{1}{2}\xi^T P \xi \tag{4.1.18}$$

with P positive definite. With the correct selection of the elements k_0 and k_1 the matrix A is Hurwitz, there exists one unique solution ($P > 0$) to the Lyapunov equation

$$A^T P + PA = -Q$$

where $Q = Q^T \quad Q > 0$.

Lyapunov equation satisfies:

$$\begin{aligned} \lambda_{\min}(P)\,|\xi|_2^2 \le \xi^T P \xi \le \lambda_{\max}(P)\,|\xi|_2^2 \\ \frac{\partial V_1}{\partial \xi} A\xi = -\xi^T Q \xi \le -\lambda_{\min}(Q)\,|\xi|_2^2 \end{aligned} \tag{4.1.19}$$

and the perturbation term is bounded by $|D(\xi)| \le \alpha_1 |\xi|_2 + \beta_1$.

Taking derivative of (4.1.18) we obtain

$$\dot{V}_1 = -\xi^T Q \xi - 2\xi^T P D(\xi) \tag{4.1.20}$$

substituting the bounds (4.1.19) in (4.1.20), we have

$$\begin{aligned} \dot{V}_1 &= -\xi^T Q \xi - 2\xi^T P D(\xi) \\ &\le -\lambda_{\min}(Q)\,|\xi|_2^2 + 2\lambda_{\max}(P)\,|\xi|_2\,(\alpha_1 |\xi|_2 + \beta_1) \\ &\le (-\lambda_{\min}(Q) + 2\alpha_1 \lambda_{\max}(P))\,|\xi|_2^2 + 2\beta_1 \lambda_{\max}(P)\,|\xi|_2 \\ &= -\alpha\,(1-\theta)\,|\xi|_2^2 - \alpha\theta\,|\xi|_2^2 + \beta\,|\xi|_2 \end{aligned}$$

where $\alpha = \lambda_{\min}(Q) - 2\alpha_1 \lambda_{\max}(P)$ and $\beta = 2\beta_1 \lambda_{\max}(P)$, then

$$\dot{V}_1 \le -\alpha\,(1-\theta)\,|\xi|_2^2 \tag{4.1.21}$$

for $\forall\, |\xi|_2 > \frac{\beta}{\alpha\theta} = \delta$.

Thus, the nominal system $\dot{\xi} = A\xi$ has an exponentially stable equilibrium point $\xi = 0$, the solution $\xi(t)$ of (4.1.17) is ultimately bounded and the ultimate bound is given by

$$|\xi|_2 \le \delta \frac{\sqrt{\lambda_{\max}(P)}}{\sqrt{\lambda_{\min}(P)}}. \tag{4.1.22}$$

Finally, considering the absolute value of the wind speed in (4.1.1), the remaining dynamics x_3 is locally stable.

4.2 Integral nested sliding mode control for brake in absence of tire deformation

This section presents the use of integral nested sliding mode for the cases of no deformation. Theoretically, the integral nested sliding mode control can guarantee the robustness of the system throughout the entire response starting from the initial time instance and reduce the sliding functions gains in comparison with standard sliding mode presented in the above section. In addition, as example, the use of a continuous pneumatic valve is studied and a Super Twisting control is shown. Given $s^*(t)$ as the desired trajectory of the relative slip s, which must be close to maximize the function $\phi(s)$, the considered problem is to design a controller that obtains reference tracking in despite of the perturbations in the system. As a solution, we propose an Integral Nested Sliding Mode Control [136] based on Sliding Mode Block controller [115], [133], Nested Sliding Mode Control [105] and Integral Sliding Mode Control [101], for system (2.1.11). The system equations are presented again:

$$\begin{aligned} \dot{x}_1 &= -a_0 x_1 + a_1 f(s) - a_2 x_2 \\ \dot{x}_2 &= -a_3 x_2 + bu \\ \dot{x}_3 &= -a_4 F(s) - f_w(x_3) \end{aligned} \tag{4.2.1}$$

with output $y = s = h(x) = 1 - r\frac{x_1}{x_3}$, where $a_0 = B_b/J$, $a_1 = r/J$, $a_2 = k_b/J$, $a_3 = 1/\tau$, $a_4 = 1/M$, $b = P_c/\tau$ and $f_w(x_3) = \frac{1}{2M}(\rho C_d A_f)(x_3 + v_w)^2$

4.2.1 Integral sliding manifold design

Let $s^*(t)$ be a twice differentiable function. We define the output tracking error as

$$e_1 \triangleq s - s^* \tag{4.2.2}$$

then, from (4.2.1) and (4.2.2) the derivative of e_1 is

$$\dot{e}_1 = f_1(x_1, x_3) + b_1(x_1, x_3)\, x_2 + \Delta_1 \tag{4.2.3}$$

where $f_1(x_1, x_3) = -r\left[\frac{a_1 f(s) - a_0 x_1}{x_3} + \frac{x_1}{x_3^2}(a_4 F(s) + f_w(x_3))\right]$ and $b_1(x_1, x_3) = r\frac{a_2}{x_3}$.

The term Δ_1 contains the reference derivative $\dot{s}^*$ the variations of the friction parameter μ, the wind speed v_w and it will be considered as an unmatched and bounded perturbation term.

Considering the variable x_2 as virtual control in (4.2.3) we determinate its desired value $x_{2\delta}$ as

$$x_{2\delta} = x_{2\delta,0} + x_{2\delta,1} \tag{4.2.4}$$

where $x_{2\delta,0}$ is the nominal part of the nominal control and $x_{2\delta,1}$ will be designed using the SM technique to reject the perturbation in (4.2.3) [101].

In this way, we propose the desired dynamics $\dot{e}_1 = -k_0 e_0 - k_1 e_1$, which are introduced by means of

$$x_{2\delta,0} = -\frac{1}{b_1(x_1, x_3)} \left[f_1(x_1, x_3) + k_0 e_0 + k_1 e_1 \right] \tag{4.2.5}$$

where $k_0 > 0$, $k_1 > 0$ and e_0 is defined by

$$\dot{e}_0 = e_1, \qquad e_0(0) = 0. \tag{4.2.6}$$

Now, in order to attenuate the perturbation term Δ_1 in (4.2.3), we define the surface

$$\sigma_1 = e_1 + z \tag{4.2.7}$$

where z is an SM integral variable and will be defined later.

From (4.2.3)-(4.2.7) the derivative of σ_1 is given by

$$\dot{\sigma}_1 = -k_0 e_0 - k_1 e_1 + x_{2\delta,1} + \Delta_1 + \dot{z}. \tag{4.2.8}$$

Selecting

$$\dot{z} = k_0 e_0 + k_1 e_1 \tag{4.2.9}$$

with $z(0) = -e_1(0)$, the equation (4.2.8) reduces to

$$\dot{\sigma}_1 = x_{2\delta,1} + \Delta_1. \tag{4.2.10}$$

To enforce sliding motion in (4.2.10) the term $x_{2\delta,1}$ in (4.2.8) is chosen as

$$x_{2\delta,1} = -k_{\sigma_1} \mathrm{sigm}(\varepsilon, \sigma_1)$$

where we use the result that the sign function can be approximated by the sigmoid function in the form

$$\lim_{\varepsilon \to \infty} \mathrm{sigm}(\varepsilon; x) = \mathrm{sign}(x).$$

The used sigmoid function in the hyperbolic tangent, $\mathrm{sigm}(\varepsilon; x) = \tanh(\varepsilon x)$

Now, we define a new error variable e_2 as

$$e_2 = x_{2\delta} - x_2. \tag{4.2.11}$$

Using (4.2.1) and (4.2.11), straightforward calculations reveal

$$\dot{e}_2 = -a_3 e_2 - bu + \Delta_2 \tag{4.2.12}$$

where the term $\Delta_2 = a_3 x_{2\delta} + \frac{\partial x_{2\delta}}{\partial x_1}\dot{x}_1 + \frac{\partial x_{2\delta}}{\partial x_3}\dot{x}_3$ is considered as a perturbation.

Using the new variables e_0, e_1, e_2 and σ_1 the extended closed loop system (4.2.3), (4.2.6), (4.2.12) and (4.2.10) is presented as

$$\dot{e}_0 = e_1 \tag{4.2.13}$$

$$\dot{e}_1 = -k_0 e_0 - k_1 e_1 + e_2 - k_{\sigma_1} \mathrm{sigm}\,(\varepsilon, \sigma_1) + \Delta_1 \tag{4.2.14}$$

$$\dot{\sigma}_1 = -k_{\sigma_1} \mathrm{sigm}\,(\varepsilon, \sigma_1) + \Delta_1 \tag{4.2.15}$$

$$\dot{e}_2 = -a_3 e_2 - bu + \Delta_2 \tag{4.2.16}$$

$$\dot{x}_3 = -a_4 F(s) - f_w(x_3) \tag{4.2.17}$$

4.2.2 Sliding mode control for two position valves

Taking into account the case of a two position valve, open or closed, to induce sliding mode on the sliding manifold $e_2 = 0$ we choose the control signal as

$$u = \frac{1}{2}\mathrm{sign}\,(e_2) + \frac{1}{2}. \tag{4.2.18}$$

Now, the stability of (4.2.13) (4.2.17) closed-loop by (4.2.18) is outlined in a step by step procedure:

Step A) Reaching phase of the projection motion (4.2.16);

Step B) SM stability of the projection motion (4.2.15);

Step C) SM stability of (4.2.13)-(4.2.14) in the vicinity of the manifold $e_2 = 0$ and $\sigma_1 = 0$.

We use the assumptions $|\Delta_1| \leq \alpha_1 |\sigma_1| + \beta_1$,

$$|\Delta_2| \leq \alpha_2 |e_2| + \beta_2 \tag{4.2.19}$$

and

$$\left|\dot{\Delta}_1\right| \leq \alpha_0 |\dot{\sigma}_1| \tag{4.2.20}$$

with $\alpha_0 > 0$, $\alpha_1 > 0$, $\alpha_2 > 0$, $\beta_1 > 0$, $\beta_2 > 0$, $a_3 > \alpha_2$, and $b > |\Delta_2|$.

Step A) The system (4.2.16) can be presented as follows:

CASE 1, $e_2 < 0$, then $u = 0$ and

$$\dot{e}_2 = -a_3 e_2 + \Delta_2 \tag{4.2.21}$$

CASE 2, $e_2 > 0$, then $u = 1$ and

$$\dot{e}_2 = -a_3 e_2 + \Delta_2 - b \tag{4.2.22}$$

We use the Lyapunov function candidate $V_2 = \frac{1}{2}e_2^2$ to analyse the stability conditions. The derivative of V_2 with respect to time in CASE 1 is

$$\dot{V}_2 = e_2\left(-a_3 e_2 + \Delta_2\right)$$

under condition (4.2.19) we have

$$\dot{V}_2 \leq |e_2|\left(-a_3|e_2| + \alpha_2|e_2| + \beta_2\right)$$

In this case, the solution of (4.2.16) is ultimately bounded by [138]

$$|e_2(t)| \leqslant \delta_0, \quad \delta_0 = \frac{\beta_2}{a_3 - \alpha_2} \tag{4.2.23}$$

that is similar in CASE 2.

Step B) To analyse the stability of the projection motion (4.2.15) we assume that the sign function can be approximated by the sigmoid function in the form $\text{sigm}(\varepsilon; x) \to \text{sign}(x)$ when $\varepsilon \to \infty$, then we can establish the equality $\text{sign}(x) - \text{sigm}(\varepsilon; x) = \Delta_s(\varepsilon; x)$. It is evident that $\Delta_s(x)$ is bounded, that is, for a given ε there is a positive constant $0 < \gamma < 1$ such that $\|\Delta_s(\varepsilon; x)\| = \gamma$.

Taking the Lyapunov candidate $V_1 = \frac{1}{2}\sigma_1^2$ and taking its derivative

$$\begin{aligned}\dot{V}_1 &= \sigma_1\left[-k_{\sigma_1}\text{sigm}(\varepsilon, \sigma_1) + \Delta_1\right] \\ &\leq -|\sigma_1|\left[k_{\sigma_1}(1-\gamma) - \alpha_1|\sigma_1| - \beta_1\right]\end{aligned}$$

when $k_{\sigma_1} > \frac{\beta_1}{1-\gamma}$ then σ_1 converges to a vicinity of zero, $|\sigma_1| < \vartheta$, with $\vartheta = \frac{\ln\left(\frac{2-\gamma}{\gamma}\right)}{2\varepsilon}$ and, with (4.2.20), $\dot{\sigma}_1$ converges to zero in finite time [134].

Step C) To analyse the SM stability of (4.2.13)-(4.2.14) in the vicinity of the manifold $e_2 = 0$ and $\sigma_1 = 0$, we define the Lyapunov function $V_2 = \frac{1}{2}\left(e_0^2 + e_1^2\right)$ and taking its derivative

$$\begin{aligned}\dot{V}_2 &= e_1\left[(1-k_0)|e_0| - k_1 e_1 + e_2\right] \\ &\leq -|e_1|\left[(k_0 - 1)|e_0| + k_1|e_1| - \delta_0\right]\end{aligned}$$

therefore, if $k_0 > 1$ then, e_1 converges to an arbitrary small vicinity of zero, $|e_1| < \delta_0/k_1$.

4.2.3 Sliding mode control for continuous position valves

We now consider the types of valve that can vary its position in a continuous range. To induce sliding mode on the sliding manifold $e_2 = 0$, the super-twisting control algorithm is

applied [100, Ch. 2]

$$\begin{aligned} u &= \frac{\lambda_1}{b}|e_2|^{\frac{1}{2}}\,\mathrm{sign}\,(e_2) - u_1 \\ \dot{u}_1 &= -\lambda_2 \mathrm{sign}\,(e_2)\,. \end{aligned} \tag{4.2.24}$$

Equation (4.2.16) closed-loop by control (4.2.24) results in the following dynamic system:

$$\begin{aligned} \dot{e}_2 &= -\lambda_1 |e_2|^{\frac{1}{2}}\,\mathrm{sign}\,(e_2) + u_1 + \psi_2 \\ \dot{u}_1 &= -\lambda_2 \mathrm{sign}\,(e_2) \end{aligned} \tag{4.2.25}$$

where $\psi_2 = -a_3 e_2 + \Delta_2$. By using (4.2.16) and (4.2.19) one can write

$$\psi_2 = a_3 x_2 + \frac{\partial x_{2\delta}}{\partial x_1}\dot{x}_1 + \frac{\partial x_{2\delta}}{\partial x_3}\dot{x}_3 \leq \bar{\beta}_2.$$

Proposing the following candidate Lyapunov function [132]:

$$\begin{aligned} \mathcal{V} &= 2\lambda_2|e_2| + \frac{1}{2}u_1^2 + \frac{1}{2}(\lambda_1|e_2|^{1/2}\mathrm{sign}(e_2) - u_1)^2 \\ &= \xi^T P \xi \end{aligned}$$

where $\xi^T = \begin{bmatrix} |e_2|^{1/2}\mathrm{sign}(e_2) & u_1 \end{bmatrix}$ and $P = \frac{1}{2}\begin{pmatrix} 4\lambda_2 + \lambda_1^2 & -\lambda_1 \\ -\lambda_1 & 2 \end{pmatrix}$

Its time derivative along the solution of (4.2.25) results as follows:

$$\dot{\mathcal{V}} = -\frac{1}{|e_2|^{1/2}}\xi^T Q \xi + \frac{\psi_2}{|e_2|^{1/2}} q_1^T \xi$$

where

$$Q = \frac{\lambda_1}{2}\begin{pmatrix} 2\lambda_2 + \lambda_1^2 & -\lambda_1 \\ -\lambda_1 & 1 \end{pmatrix} \quad q_1^T = \left(2\lambda_2 + \tfrac{1}{2}\lambda_1^2, \quad -\tfrac{1}{2}\lambda_1\right).$$

Moreover, one can easily see that

$$\frac{\psi_2}{|e_2|^{1/2}} q_1^T \xi \leq \frac{\bar{\beta}_2}{|e_2|^{1/2}} \xi^T Q_1 \xi$$

with

$$Q_1 = \begin{pmatrix} 2\lambda_2 + \frac{1}{2}\lambda_1^2 & 0 \\ 0 & -\frac{1}{2}\lambda_1 \end{pmatrix}$$

then, the derivative of the Lyapunov function can be simplified to the following form:

$$\dot{\mathcal{V}} = -\frac{k_1}{2|e_2|^{1/2}}\xi^T \tilde{Q}\xi$$

where

$$\tilde{Q} = \begin{pmatrix} \lambda_1\lambda_2 + \frac{1}{2}\lambda_1^3 + (2\lambda_2 + \frac{1}{2}\lambda_1^2)\bar{\beta}_2 & -\lambda_1 \\ -\lambda_1 & 1 - \frac{1}{2}\lambda_1\bar{\beta}_2 \end{pmatrix}$$

In this case the controller gains can easily be chosen such that $\tilde{Q} > 0$, implying that the derivative of the Lyapunov function is negative definite. Finally the analysis can be continued as in **Step B** of the above subsection.

4.3 Integral nested sliding mode control for brake in presence of tire deformation

In a similar way to the last section, in this section the use of integral nested sliding mode for the brake with deformation on the tire is considered. The introduction of the deformation increases the complexity of the system and represents a more realistic case. However, the design of the controller is almost the same to the no deformation case. Given $s^*(t)$ as the desired trajectory of the relative slip s, which must be close to maximize the function $\phi(s)$, the considered problem is to design a controller that obtains reference tracking in despite of the perturbations in the system. As a solution, we propose an Integral Nested Sliding Mode Control [136] based on Sliding Mode Block controller [115], [133], Nested Sliding Mode Control [105] and Integral Sliding Mode Control [101], for system (2.2.4). The system equations are presented again:

$$\begin{aligned} \dot{x}_1 &= c_1\left(rf(s) - B_b x_1 - k_b x_2\right) \\ \dot{x}_2 &= -c_2 x_2 + bu \\ \dot{x}_3 &= x_4 \\ \dot{x}_4 &= -a_{41}x_1 - a_{42}x_2 - a_{43}x_3 - a_{44}x_4 + f_4(x_1, x_4) \\ \dot{x}_5 &= -c_3 F(s) - f_w(x_5) \end{aligned} \tag{4.3.1}$$

with output

$$y = s = h(x) = 1 - r\frac{x_1}{x_5} - \frac{x_4}{x_5}$$

where $b = c_2 k_b P_c$, $c_1 = 1/J$, $c_2 = 1/\tau$, $c_3 = 1/M$, $a_{41} = (B_b r)/J$, $a_{42} = (rk_b)/J$, $a_{43} = k_x/M_c$, $a_{44} = c_x/M_c$, $f_4(x_1, x_4) = \left(\frac{r^2}{J} + \frac{1}{M_c}\right) f(s) + \frac{1}{M}F(s) + \frac{1}{MM_c}F_a$ and $f_w(x_5) = \frac{1}{2M}\left(x_5 + v_{wind}\right)^2$

4.3.1 Control formulation

To calculate the control law, we obtain the output dynamics

$$\dot{y} = a_1(x_1, x_5) + a_2(x_5)x_2 + f_1(x_4, x_5)$$

where $a_1(x_1, x_5) \triangleq a_1 = -\frac{r}{x_5^2}\left[x_1\left(c_3F\left(s\right) + f_w\left(x_5\right)\right) + c_1x_5\left(rf\left(s\right) - B_bx_1\right)\right]$, $a_2(x_5) \triangleq a_2 = \frac{rc_1k_b}{x_5}$ and $f_1(x_4, x_5) = -\frac{d}{dt}\left(\frac{x_4}{x_5}\right) + \Delta(\mu)$. The term $\Delta(\mu)$ contains variations of the friction parameter μ.

The control objective is to design an Integral Nested Sliding Mode controller to obtain output trajectory tracking in despite of the system perturbations. Define $y_{ref}\left(t\right)$ as the desired trajectory of the relative slip. Let $y_{ref}\left(t\right)$ be a twice differentiable function, but with unknown derivatives, now define the output tracking error as $e_1 = y\left(t\right) - y_{ref}\left(t\right) \triangleq \alpha_1(x, t)$ then its derivative is

$$\dot{e}_1 = a_1 + a_2x_2 + g_1(x, t) \tag{4.3.2}$$

where $g_1\left(x, t\right)$ is the unmatched perturbation term defined by

$$g_1(x, t) = f_1(x) - \dot{y}_{ref}. \tag{4.3.3}$$

Considering x_2 as virtual control in (4.3.2), we propose

$$x_{2ref} = x_{2,0} + x_{2,1} \tag{4.3.4}$$

where $x_{2,0}$ is the nominal part of the virtual control and $x_{2,1}$ is the part which will be designed to reject the perturbation in (4.3.2) [101].

Now, we define a new error variable e_2 as

$$e_2 = x_2 - x_{2ref} \triangleq \alpha_2(x, t) \tag{4.3.5}$$

and two auxiliary variables σ_1 and σ_2 of the form

$$\sigma_1 = e_1 + w_1 \tag{4.3.6}$$

$$\sigma_2 = e_2 + w_2 \tag{4.3.7}$$

where x_{2ref} is the desired value of x_2 to obtain the control aim, w_1 and w_2 are integral variables used to reduce the control gain, σ_1 and σ_2 are pseudo-sliding functions proposed to attenuate the perturbation terms. All the variables will be designed later. Using equations (4.3.1)-(4.3.7) we obtain

$$x_2 = \sigma_2 + x_{2,0} + x_{2,1} - w_2. \tag{4.3.8}$$

Taking the derivative of σ_1 results in

$$\dot{\sigma}_1 = a_1 + a_2 x_2 + \dot{w}_1 + g_1(t). \tag{4.3.9}$$

Substituting (4.3.8) in (4.3.9) yields

$$\dot{\sigma}_1 = a_1 + a_2 (\sigma_2 + x_{2,0} + x_{2,1} - w_2) + \dot{w}_1 + g_1(t)$$

or

$$\dot{\sigma}_1 = a_1 + a_2 (e_2 + x_{2,0} + x_{2,1}) + \dot{w}_1 + g_1(t). \tag{4.3.10}$$

Choosing the dynamics of the integral variable w_1 as

$$\dot{w}_1 = -a_1 - a_2 (e_2 + x_{2,0}) \tag{4.3.11}$$

with $w_1(0) = -e_1(0)$, the nominal part $x_{2,0}$ is designed to eliminate the old known dynamics in (4.3.2) and assign the desired dynamics $\dot{e}_1 = -k_{10} e_1$, $k_{10} > 0$

$$x_{2,0} = -\frac{1}{a_2} (a_1 + k_{10} e_1). \tag{4.3.12}$$

Substituting (4.3.11) and (4.3.12) in (4.3.10) yields

$$\dot{\sigma}_1 = a_2 x_{2,1} + g_1(t). \tag{4.3.13}$$

To attenuate the perturbation term $g_1(x,t)$ in (4.3.13) using the integral SM technique and to enforce a sliding motion on $\sigma_1 = 0$ the virtual control $x_{2,1}$ is chosen as

$$x_{2,1} = -k_{11} \text{sigm} (\varepsilon_1 \sigma_1)$$

with $k_{11} > 0$.

Using (4.3.1) and (4.3.5), straightforward calculations reveal

$$\dot{e}_2 = -c_2 e_2 + bu + f_{2e}(x) \tag{4.3.14}$$

where $f_{2e}(x) = -c_2 x_{2ref} + \frac{\partial \alpha_2(x,t)}{\partial x_1} \dot{x}_1 + \frac{\partial \alpha_2(x,t)}{\partial x_3} \dot{x}_3 + \frac{\partial \alpha_2(x,t)}{\partial \sigma_1} \dot{\sigma}_1 + \frac{\partial \alpha_2(x,t)}{\partial x_5} \dot{x}_5$.

To induce sliding mode in (4.3.14) we choose the control signal as

$$u = \frac{1}{2} - \frac{1}{2} \text{sign} (e_2). \tag{4.3.15}$$

4.3.2 Stability analysis

Using the new variables e_1, e_2 and σ_1 the extended closed loop system (4.3.2), (4.3.10) and (4.3.15) is presented as

$$\dot{e}_1 = -k_{10}e_1 - a_2k_{11}\text{sigm}(\varepsilon_1\sigma_1) + g_1(x,t) \tag{4.3.16}$$

$$\dot{\sigma}_1 = -k_{11}\text{sigm}(\varepsilon_1\sigma_1) + g_1(x,t) \tag{4.3.17}$$

$$\dot{e}_2 = -c_2e_2 + f_{2e}(x) - \frac{1}{2}b\text{sign}\,(e_2) + \frac{1}{2}b \tag{4.3.18}$$

$$\begin{aligned} \dot{x}_3 &= x_4 \\ \dot{x}_4 &= -a_{41}x_3 - a_{42}x_4 - a_{43}x_2 - f_4(x_1,x_4) \\ \dot{x}_5 &= -c_3\left(F + f_5(x_5)\right). \end{aligned} \tag{4.3.19}$$

The stability of (4.3.16) (4.3.19) can be studied step by step:

A) SM stability of the projection motion (4.3.18);

B) SM stability of the projection motion (4.3.17);

C) SM dynamics (4.3.16) stability in the neighbourhood of SM manifold $e_2 = 0$ and $\sigma_1 = 0$.

We use the following assumptions:

$$|f_{2e}(x)| \leqslant \alpha_2\,|e_2| + \beta_2 \tag{4.3.20}$$

$$|g_1(x,t)| \leqslant \alpha_1\,|\sigma_1| + \beta_1 \tag{4.3.21}$$

$$\begin{aligned} &|\dot{g}_1(x,t)| \leqslant \alpha_0\,|\sigma_2| + \beta_0 \\ &\varsigma = \dot{\sigma}_1 \end{aligned} \tag{4.3.22}$$

with $\alpha_0 > 0$, $\alpha_1 > 0$, $\alpha_2 > 0$, $\beta_0 > 0$, $\beta_1 > 0$, $\beta_2 > 0$, $c_2 > \alpha_2$ and $b > |f_{2e}(x)|$

A) The system (4.3.18) can be presented as follows:

Case 1, $e_2 > 0$, then

$$\dot{e}_2 = -c_2e_2 + f_{2e}(x). \tag{4.3.23}$$

In this case, under condition (4.3.20) the solution of (4.3.18) is ultimately bounded by ([138])

$$|e_2(t)| \leqslant \delta_0, \quad \delta_0 = \frac{\beta_2}{c_2 - \alpha_2} \tag{4.3.24}$$

Case 2, $e_2 < 0$, then

$$\dot{e}_2 = -c_2 e_2 + f_{2e}(x) + b. \tag{4.3.25}$$

In this case $\dot{e}_2 > 0$, therefore, there is a time t_1 such that

$$e_2(t_1) = 0.$$

B) To analyze stability of (4.3.17) we use $V_1 = (1/2)\sigma_1^2$. Using (4.3.17) we have

$$\dot{V}_1 = \sigma_1 \left(-k_{11}\text{sigm}(\varepsilon_1\sigma_1) + g_1(x,t)\right). \tag{4.3.26}$$

Now we establish the following equality:

$$\text{sigm}(\varepsilon_1\sigma_1) = \text{sign}\,(\sigma_1) - \Delta\,(\varepsilon_1, \sigma_1) \tag{4.3.27}$$

where $\Delta\,(\varepsilon_1, \sigma_1)$ is the difference between the sign and sigmoid functions. It is evident that $\Delta\,(\varepsilon_1, \sigma_1)$ is bounded. That is, there is a constant $0 < \gamma_1 < 1$ such that $|\Delta\,(\varepsilon_1, \sigma_1)| < \gamma_1$. Then using (4.3.27) the derivative (4.3.26) becomes

$$\begin{aligned} \dot{V}_1 &\leqslant -|\sigma_1| \left(k_{11}\left(1 - |\Delta\,(\varepsilon_1 \quad, \sigma_1)|\right) - |g_1(x,t)|\right) \\ &\leqslant -|\sigma_1| \left(k_{11}\left(1 - \gamma_1\right) - \beta_1\right) - \alpha_1 |\sigma_1|). \end{aligned} \tag{4.3.28}$$

Under the condition $k_1\left(1 - \gamma_1\right) > \beta_1$ we have $\dot{V}_1 < 0$, and hence $\sigma_1\,(t)$ converges to the region given by

$$\|\sigma_1(t)\| \leqslant \delta_1, \quad \delta_1 = \frac{k_{11}\left(1 - \gamma_1\right) - \beta_1)}{\alpha_1} \tag{4.3.29}$$

Now, consider the derivative $\varsigma = \dot{\sigma}_1$ (4.3.17) described by

$$\dot{\varsigma} = -k_2\varsigma + \dot{g}_1(x,t), \;\; k_2 = k_{11}\varepsilon_1(1 - \tanh^2(\varepsilon_1\sigma_1(1)) \tag{4.3.30}$$

and $V_2 = (1/2)\varsigma^2$ Then using (4.3.30) and (4.3.22) the straightforward calculations give

$$\dot{V}_2 = \varsigma\left(-k_2\varsigma + \dot{g}_1(x,t)\right) \leqslant -|\varsigma| \left(\left(k_2 - \alpha_0\right)|\varsigma| - \beta_1\right) \tag{4.3.31}$$

Under the condition $k_2 > \alpha_0$, the derivative $\varsigma = \dot{\sigma}_1$ is ultimately bounded by

$$|\varsigma(t)| \leqslant \delta_2, \quad \delta_2 = \frac{\beta_1}{k_2 - \alpha_0}. \tag{4.3.32}$$

C) Stability of the equation (4.3.16) in the neighbourhood of the sliding manifold $e_2 = 0$ and $\sigma_1 = 0$ is studied by $V_0 = (1/2)e_1^2$. Using (4.3.24) and (4.3.31) we have

$$\begin{aligned} \dot{V}_1 &= e_1[-k_{10}e_1 - a_2k_{11}\text{sigm}(\varepsilon_1\sigma_1) + g_1(x,t)] \\ &\leqslant -|e_1|\left(k_{10}|e_1| - \delta_0 - \delta_2\right) \end{aligned} \tag{4.3.33}$$

If $k_{10} > 0$, then the control error $e_1(t)$ converges to an arbitrary small neighbourhood of the equilibrium point, defined by $|e_1(t)| < \delta$, $\delta = (\delta_0 + \delta_2)/k_{10}$. Moreover it is possible to show that an equilibrium point of the residual dynamics (4.3.19) is exponentially stable, therefore the control objectives are fulfilled, and the desired performance of the closed-loop system is obtained.

4.4 Sliding mode regulator

In the above approaches, the stability of the residual dynamics is assumed. This section deals with the problem of the asymptotically tracking of the relative slip to a desired trajectory. To solve this problem we propose to use the block control technique combined with the SM control algorithm to achieve robustness to perturbations, and ensure asymptotically output tracking along with the stabilization of the residual dynamic consisting of the vehicle velocity. Given $s^*(t)$ as the desired trajectory of the relative slip s, which must be close to maximize the friction function $\phi(s)$, the considered problem is to design a controller that obtains reference tracking in despite of the perturbations in the system. As a solution, we propose a Sliding Mode Block Control regulator based in [115] for system. In addition, we introduce an estimation term for the steady state vehicle velocity in order to stabilize these dynamics. The system model is presented again

$$\begin{aligned} \dot{x}_1 &= -a_0x_1 + a_1f(s) - a_2x_2 \\ \dot{x}_2 &= -a_3x_2 + bu \\ \dot{x}_3 &= -a_4F(s) - f_w(x_3) \end{aligned} \tag{4.4.1}$$

with output $y = s = h(x) = 1 - r\frac{x_1}{x_3}$, where $a_0 = B_b/J$, $a_1 = r/J$, $a_2 = k_b/J$, $a_3 = 1/\tau$, $a_4 = 1/M$, $b = P_c/\tau$ and $f_w(x_3) = \frac{1}{2M}(\rho C_d A_f)(x_3 + v_w)^2$

4.4.1 Control design

Let z be an estimate of the steady state of vehicle velocity residual dynamics x_3 and $s^*(t)$ be a twice differentiable function. Taking into account the direct action of the pressure P_b in

the brake cylinder over the wheels motion, we define the output tracking error as

$$e_1 \triangleq x_1 - \frac{1-s^*}{r} x_3, \tag{4.4.2}$$

the estimation error

$$e_3 \triangleq x_3 - z \tag{4.4.3}$$

and the manifold

$$s_1 \triangleq e_1 + k_3 e_3. \tag{4.4.4}$$

Hence, from (4.4.1) and (4.4.4) the derivative of s_1 is

$$\dot{s}_1 = f_1(x_1, x_3) + b_1(x_1, x_3)\, x_2 - k_3 \dot{z} + \Delta_1 \tag{4.4.5}$$

where $f_1(x_1, x_3) = \frac{k_3 r + 1 - s^*}{r} [a_4 F(s) - f_w(x_3)] - a_0 x_1 + a_1 f(s)$ and $b_1(x_1, x_3) = -a_2$. The term Δ_1 contains the reference derivative $\dot{s}^*$, the variations of the friction parameter μ, the wind speed v_{wind} and will be considered as an unmatched and bounded perturbation term.

Considering the variable x_2 as virtual control in (4.4.5) we determinate its desired value $x_{2\delta}$ as

$$x_{2\delta} = x_{2\delta,0} + x_{2\delta,1} \tag{4.4.6}$$

where $x_{2\delta,0}$ is the nominal part of the nominal control and $x_{2\delta,1}$ will be designed using the SM technique to attenuate the perturbation Δ_1 in (4.4.5)

In this way, we propose the desired dynamics $\dot{s}_1 = -k_0 s_0 - k_1 s_1$, which are introduced by means of

$$x_{2\delta,0} = -\frac{1}{b_1(x_1, x_3)} [f_1(x_1, x_3) + k_0 s_0 + k_1 s_1 + k_3 \dot{z}] \tag{4.4.7}$$

where $k_0 > 0$, $k_1 > 0$ and s_0 is defined by

$$\dot{s}_0 = s_1,\ s_0(0) = 0 \tag{4.4.8}$$

Now, in order to attenuate the perturbation term Δ_1 in (4.4.5), we define the surface

$$\sigma_1 = s_1 + \zeta \tag{4.4.9}$$

where ζ is an SM integral variable and will be defined later. From (4.4.5), (4.4.7), (4.4.6) and (4.4.9) the derivative of σ_1 is given by

$$\dot{\sigma}_1 = -k_0 s_0 - k_1 s_1 + x_{2\delta,1} + \Delta_1 + \dot{\zeta} \tag{4.4.10}$$

Selecting $\dot{\zeta} = k_0 s_0 + k_1 s_1$ with $\zeta(0) = -s_1(0)$, the equation (4.4.10) reduces to

$$\dot{\sigma}_1 = x_{2\delta,1} + \Delta_1 \tag{4.4.11}$$

To enforce quasi-sliding motion in (4.4.11) the term $x_{2\delta,1}$ in (4.4.10) is chosen as

$$x_{2\delta,1} = -k_{\sigma_1}\text{sigm}\,(\varepsilon, \sigma_1)$$

where we use the result that the sign function can be approximated by the sigmoid function in the form $\text{sigm}\,(\varepsilon; x) \to \text{sign}\,(x)$ as $\varepsilon \to \infty$.

Now we define a new error variable e_2 in the form

$$e_2 = x_{2\delta} - x_2 \tag{4.4.12}$$

Using (4.4.1) and (4.4.12), straightforward calculations reveal

$$\dot{e}_2 = \Delta_2 + bu \tag{4.4.13}$$

where the term $\Delta_2 = a_3 x_2 + \frac{\partial x_{2\delta}}{\partial x_1}\dot{x}_1 + \frac{\partial x_{2\delta}}{\partial x_3}\dot{x}_3$ is considered as a matched perturbation.

Defining $s_2 \triangleq e_2$, to induce sliding mode on the manifold $s_2 = 0$ we choose the control signal as

$$u = -\frac{1}{2}\text{sign}\,(s_2) - \frac{1}{2} \tag{4.4.14}$$

4.4.2 Stability analysis

Using the new variables s_0, s_1, s_2 and σ_1 the extended closed loop system (4.4.5), (4.4.8), (4.4.11) and (4.4.13) is presented as

$$\dot{s}_0 = s_1 \tag{4.4.15}$$
$$\dot{s}_1 = -k_0 s_0 - k_1 s_1 + s_2 - k_{\sigma_1}\text{sigm}\,(\varepsilon, \sigma_1) + \Delta_1 \tag{4.4.16}$$
$$\dot{\sigma}_1 = -k_{\sigma_1}\text{sigm}\,(\varepsilon, \sigma_1) + \Delta_1 \tag{4.4.17}$$
$$\dot{s}_2 = \Delta_2 + bu \tag{4.4.18}$$
$$\dot{x}_3 = -a_4 F\,(s) - f_w\,(x_3) \tag{4.4.19}$$

The stability of (4.4.15) (4.4.19) closed loop by (4.4.14) is outlined in a step by step procedure:

Step A) Reaching phase of the projection motion (4.4.18);

Step B) SM stability of the projection motion (4.4.17)

Step C) SM Stability of (4.4.15)-(4.4.16);.

Step D) Stability of residual dynamics (4.4.19).

We use the following assumptions:

$$|\Delta_1| \leq \alpha_1 |s_1| + \beta_1 \tag{4.4.20}$$

$$\left|\dot{\Delta}_1\right| \leq \alpha_0 |\dot{\sigma}_1| \tag{4.4.21}$$

$$|\Delta_2| \leq \beta_2 \tag{4.4.22}$$

and

$$\alpha_0 > 0,\ \alpha_1 > 0,\ \beta_1 > 0,\ \beta_2 > 0,\ a_3 > \alpha_2,\ b > \beta_2. \tag{4.4.23}$$

With $i = 1, 2$, the terms $\alpha_i |s_i|$ and $\alpha_0 |\dot{\sigma}_1|$ are used to represent the parametric variations and uncertain, and the terms β_i represent external disturbances.

Step A) For the system (4.5.25) we use the Lyapunov function candidate $V_2 = \frac{1}{2}e_2^2$ to analyze the stability conditions. The derivative of V_2 with respect to time is

$$\dot{V}_2 = e_2 \left(\Delta_2 - b \left(\frac{1}{2} \text{sign}\,(s_2) - \frac{1}{2} \right) \right)$$

under condition (4.4.22) we have

$$\dot{V}_2 \leq -|e_2| (b - \beta_2)$$

Using (4.4.23), the system (4.4.18) is finite time stable.

Step B) To analyze the stability of the projection motion (4.4.17) we assume that the signum function can be approximated by the sigmoid function in the form $\text{sigm}\,(\varepsilon_1; x) \to \text{sign}\,(x)$ as $\varepsilon_1 \to \infty$, then, we can establish the following equality

$$\text{sign}\,(x) - \text{sigm}\,(\varepsilon_1; x) = \Delta_s\,(\varepsilon_1; x) \tag{4.4.24}$$

It is evident that $\Delta_s\,(x)$ is bounded, that is, for a given ε_1 there is a positive constant $0 < \gamma < 1$ such that $\|\Delta_s\,(\varepsilon_1; x)\| = \gamma$. Now, taking the Lyapunov candidate $V_1 = \frac{1}{2}\sigma_1^2$ and taking its derivative, with (4.4.21) results

$$\begin{aligned} \dot{V}_1 &= \sigma_1 \left[-k_{\sigma_1} \text{sigm}\,(\varepsilon_1; \sigma_1) + \Delta_1 \right] \\ &\leq -|\sigma_1| \left[k_{\sigma_1} (1 - \gamma) - \alpha_1 |\sigma_1| - \beta_1 \right] \end{aligned}$$

therefore, if $k_{\sigma_1} > \frac{\beta_1}{1-\gamma}$ then σ_1 converges to a vicinity of zero, $|\sigma_1| < \vartheta_1$, with

$$\vartheta_1 = \frac{\ln\left(\frac{2-\gamma}{\gamma}\right)}{2\varepsilon_1}$$

and, with (4.4.21), $\dot{\sigma}_1$ converges to zero in finite time [134].

Step C) To analyze the SM motion on the manifold $s_2 = 0$, and in the vecinity of $\sigma_1 = 0$ described by (4.4.15)-(4.4.16) , that system can be regarded as a linear system with nonvanishing perturbation in the form:

$$\dot{\eta} = A\eta + D(\eta) \tag{4.4.25}$$

where

$$\eta = \begin{bmatrix} s_0 & s_1 \end{bmatrix}^T ; A = \begin{bmatrix} 0 & 1 \\ -k_0 & -k_1 \end{bmatrix} ; D(\eta) = \begin{bmatrix} 0 \\ \Delta_1 \end{bmatrix}$$

and the perturbation term is bounded by $\|D(\eta)\| \leq \alpha_1 |s_1| + \beta_1$. Now we use the following Lyapunov candidate function:

$$V_\eta = \frac{1}{2}\eta^T P \eta \tag{4.4.26}$$

with P positive definite. With the correct selection of the elements k_0 and k_1 the matrix A is Hurwitz, there exists one unique solution ($P > 0$) to the Lyapunov equation

$$A^T P + PA = -Q$$

where $Q = Q^T \;\; Q > 0$. Taking derivative of (4.4.26) we obtain

$$\dot{V}_\eta = -\eta^T Q \eta - 2\eta^T P D(\eta) \tag{4.4.27}$$

which is bounded by

$$\begin{aligned} \dot{V}_\eta &= -\eta^T Q \eta - 2\eta^T P D(\eta) \\ &\leq -\lambda_{\min}(Q) \|\eta\|_2^2 + 2\lambda_{\max}(P) \|\eta\|_2 (\alpha_1 \|\eta\|_2 + \beta_1) \\ &\leq (-\lambda_{\min}(Q) + 2\alpha_1 \lambda_{\max}(P)) \|\eta\|_2^2 + 2\beta_1 \lambda_{\max}(P) \|\eta\|_2 \\ &= -\alpha(1-\theta) \|\eta\|_2^2 - \alpha\theta \|\eta\|_2^2 + \beta \|\eta\|_2 \end{aligned}$$

where $\alpha = \lambda_{\min}(Q) - 2\alpha_1 \lambda_{\max}(P)$ and $\beta = 2\beta_1 \lambda_{\max}(P)$, then

$$\dot{V}_1 \leq -\alpha(1-\theta) \|\eta\|_2^2 \tag{4.4.28}$$

for $\forall \eta$: $\|\eta\|_2 > \frac{\beta}{\alpha\theta} = \delta_\eta$.

Thus, the solution $\eta(t)$ of (4.4.25) is ultimately bounded and the ultimate bound is given by

$$\|\eta\|_2 \leq \delta_\eta \frac{\sqrt{\lambda_{\max}(P)}}{\sqrt{\lambda_{\min}(P)}} \tag{4.4.29}$$

Step D) For the residual dynamics x_3 we have

$$\dot{x}_3 = -a_4 F(s) - f_w(x_3) \tag{4.4.30}$$

then, defining

$$\begin{aligned} g &= -a_4 F(s) - f_w(x_3) \\ a &= \left.\frac{\partial g}{\partial x_3}\right|_{x_3=0, s=s^*} \\ \lambda &= \left.\frac{\partial g}{\partial s}\right|_{x_3=0, s=s^*} \end{aligned} \tag{4.4.31}$$

yields

$$\dot{x}_3 = a x_3^i + \lambda s + \varphi \tag{4.4.32}$$

where φ contains the nonlinear terms. Hence, the dynamics for e_3 result in

$$\dot{e}_3 = a e_3 + a z + \lambda s + \varphi - \dot{z} \tag{4.4.33}$$

Finally, defining the sigmoid function $\text{sigm}(\varepsilon_2; x) \triangleq \tanh(\varepsilon_2 x)$, and taking

$$\dot{z} = a z + \lambda s - e_1 + k_4 \text{sigm}(\varepsilon_2; e_3) \tag{4.4.34}$$

results

$$\dot{e}_3 = a e_3 + e_1 - k_4 \text{sigm}(\varepsilon_2; e_3) + \Delta_3 \tag{4.4.35}$$

where $\Delta_3 \triangleq \varphi$ will be considered as a nonvanishing perturbation term

$$|\Delta_3| \leq \alpha_3 |e_3| + \beta_3$$

In sliding motion we have $s_1 = 0$, that gives

$$\dot{e}_3 = (a - k_3) e_3 - k_4 \text{sigm}(e_3; \varepsilon_2) + \Delta_3 \tag{4.4.36}$$

Now, assuming that the sign function can be approximated by the sigmoid function in the form

$$\lim_{\varepsilon_2 \to \infty} \text{sigm}(\varepsilon_2; x) = \text{sign}(x)$$

we can establish the following equality

$$\text{sign}(x) - \text{sigm}(\varepsilon_2; x) = \Delta_s(\varepsilon_2; x) \tag{4.4.37}$$

It is evident that $\Delta_s(x)$ is bounded, that is, for a given ε_2 there is a positive constant $0 < \delta < 1$ such that

$$\|\Delta_s(\varepsilon_2; x)\| = \delta$$

Taking the Lyapunov candidate $V_3 = \frac{1}{2} e_3^2$ and taking its derivative

$$\begin{aligned} \dot{V}_3 &= e_3 [(a - k_3) e_3 - k_4 \text{sigm}(\varepsilon_2; e_3) + \Delta_3] \\ &\leq -e_3^2 (k_3 - a - \alpha_3) - |e_3| [k_4 (1 - \delta) - \beta_3] \end{aligned}$$

if $k_3 > a + \alpha_3$ and $k_4 > \beta_3 / (1 - \delta)$ then e_3 converges to a vicinity of zero, $|e_3| < \vartheta_2$, with $\vartheta_2 = \frac{\ln\left(\frac{2-\delta}{\delta}\right)}{2\varepsilon_2}$ and from (4.4.4), e_1 converges to a vicinity of zero, $|e_1| < \vartheta_2 / k_3$.

4.5 Sliding mode control of a ABS with active suspension

Alternatively to the presented controllers, this section presents the control of a brake with active suspension. The brake control is designed using integral nested sliding mode. For the active suspension, a controller based on the regular form, sliding mode control and geometric linear control methods for the sliding surface design is proposed. In both subsystems a Super-Twisting control is used. The structure of the whole system permits to design both controllers in independent way. The system model is presented again

$$\begin{aligned}
\dot{x}_1 &= x_2 \\
\dot{x}_2 &= -a_1(x_1 - x_3) - a_2(x_2 - x_4) + b_1 u_s \\
\dot{x}_3 &= x_4 \\
\dot{x}_4 &= a_3(x_1 - x_3) + a_4(x_2 - x_4) - a_5(x_3 - z_r) - a_6(x_4 - \dot{z}_r) - b_2 u_s \\
\dot{x}_5 &= -a_7 x_5 + a_8 f(s) - a_9 x_6 \\
\dot{x}_6 &= -a_{10} x_6 + b_3 u_b \\
\dot{x}_7 &= -a_{11} F(s) - f_w(x_7)
\end{aligned} \tag{4.5.1}$$

with the outputs

$$y_1 = x_1 \text{ and } y_2 = x_5$$

where $a_1 = K_{cw}/m_c$, $a_2 = C_{cw}/m_c$, $a_3 = K_{cw}/m_w$, $a_4 = C_{cw}/m_w$, $a_5 = K_{wr}/m_w$, $a_6 = C_{wr}/m_w$, $a_7 = b_b/J$, $a_8 = r/J$, $a_9 = k_b/J$, $a_{10} = 1/\tau$, $a_{11} = 1/M$, $b_1 = 1/m_c$, $b_2 = 1/m_w$, $b_3 = 1/\tau$, $u_s = f_{ha}$, $u_b = P_c$ and $f_w(x_7) = \frac{1}{2M}(\rho C_d A_f)(x_7 + v_w)^2$

4.5.1 Suspension control

Define $\mathbf{x}_s = [x_1, x_2, x_3, x_4]$ and $\mathbf{p} = \begin{bmatrix} z_r & \dot{z}_r \end{bmatrix}^T$ then the subsystem is represented of the form

$$\dot{\mathbf{x}}_s = \mathbf{A}_s \mathbf{x}_s + \mathbf{b}_s u_s + \mathbf{D}\mathbf{p} \tag{4.5.2}$$

where

$$\mathbf{A}_s = \begin{bmatrix} 0 & 1 & 0 & 0 \\ -a_1 & -a_2 & a_1 & a_2 \\ 0 & 0 & 0 & 1 \\ a_3 & a_4 & -a_3 - a_5 & -a_4 - a_6 \end{bmatrix}$$

$$\mathbf{b}_s = \begin{bmatrix} 0 \\ b_1 \\ 0 \\ -b_2 \end{bmatrix}; \quad \mathbf{D} = \begin{bmatrix} 0 & 0 \\ 0 & 0 \\ 0 & 0 \\ a_5 & a_6 \end{bmatrix}$$

with the output $y_1 = x_1$. Now, defining the new variables $x_{r1} = x_1$, $x_{r2} = x_2 + \frac{b_1}{b_2}x_4$, $x_{r3} = x_3$ and $x_{r4} = x_4$ the system (4.5.2) is transformed into regular form [102]

$$\dot{\mathbf{x}}_{r1} = \mathbf{A}_{11}\mathbf{x}_{r1} + \mathbf{A}_{12}\mathbf{x}_{r2} + \mathbf{D}_1\mathbf{p} \tag{4.5.3}$$

$$\dot{\mathbf{x}}_{r2} = \mathbf{A}_{21}\mathbf{x}_{r1} + \mathbf{A}_{22}\mathbf{x}_{r2} + \mathbf{D}_2\mathbf{p} + \mathbf{b}_2 u_s \tag{4.5.4}$$

which consists of the two blocks: (4.5.3) with $\mathbf{x}_{r1} = \begin{bmatrix} x_{r1} & x_{r2} & x_{r3} \end{bmatrix}^T$ and (4.5.4) with $\mathbf{x}_{r2} = [x_4]$, where $\mathbf{A}_{11} = \begin{bmatrix} 0 & 1 & 0 \\ a_3\frac{b_1}{b_2} - a_1 & a_4\frac{b_1}{b_2} - a_2 & a_1 - \frac{b_1}{b_2}(a_3 + a_5) \\ 0 & 0 & 0 \end{bmatrix}$, $\mathbf{A}_{12} = \begin{bmatrix} -\frac{b_1}{b_2} \\ a_2 - \frac{b_1}{b_2}(a_4 + a_6 - a_2) - a_4\left(\frac{b_1}{b_2}\right)^2 \\ 1 \end{bmatrix}$, $\mathbf{A}_{21} = \begin{bmatrix} a_3 & a_4 & -a_3 - a_5 \end{bmatrix}$, $\mathbf{A}_{22} = \begin{bmatrix} -a_4\left(\frac{b_1}{b_2} + 1\right) - a_6 \end{bmatrix}$, $\mathbf{b}_2 = [-b_2]$, $\mathbf{D}_1 = \begin{bmatrix} 0 & 0 \\ \frac{b_1}{b_2}a_5 & \frac{b_1}{b_2}a_6 \\ 0 & 0 \end{bmatrix}$ and $\mathbf{D}_2 = \begin{bmatrix} a_5 & a_6 \end{bmatrix}$. Then for the first block (4.5.3), the output can be regarded as $y_1 = \mathbf{c}\mathbf{x}_{r1}$, with $\mathbf{c} = \begin{bmatrix} 1 & 0 & 0 \end{bmatrix}$ The vector $\mathbf{x}_{r2}$ is handled as a control in the first block and it is designed as a linear function of $\mathbf{x}_{r1}$

$$\mathbf{x}_{r2} = -\mathbf{C}_1\mathbf{x}_{r1} + \xi \tag{4.5.5}$$

where $\mathbf{C}_1$ are the feedback gains. Under the assumption that the matrix $(\mathbf{A}_{11} - \mathbf{A}_{12}\mathbf{C}_1)$ is Hurwitz, the term ξ is chosen as $\xi = H_k^{-1} y_{1d}$ with $H_k = \mathbf{c}\left(\mathbf{A}_{12}\mathbf{C}_1 - \mathbf{A}_{11}\right)^{-1}\mathbf{A}_{12}$, yielding a constant stable response y_{1d}. Using (4.5.5), a sliding variable ψ is formulated as

$$\psi = \mathbf{x}_{r2} + \mathbf{C}_1\mathbf{x}_{r1} - \xi \tag{4.5.6}$$

and the dynamics of (4.5.6) are governed by

$$\begin{aligned} \dot{\psi} = {} & \left(\mathbf{C}_1\mathbf{A}_{11} + \mathbf{A}_{21}\right)\mathbf{x}_{r1} + \left(\mathbf{C}_1\mathbf{A}_{12} + \mathbf{A}_{22}\right)\mathbf{x}_{r2} \\ & + \left(\mathbf{C}_1\mathbf{D}_1 + \mathbf{D}_2\right)\mathbf{p} + \mathbf{b}_2 u_s. \end{aligned} \tag{4.5.7}$$

To induce sliding mode on $\psi = 0$, the super-twisting control algorithm [100, Ch. 2] is applied

$$\begin{aligned} u_s = {} & -\mathbf{b}_2^{-1}\left[-\lambda_{s1}\left|\psi\right|^{\frac{1}{2}}\operatorname{sign}(\psi) + u_{s2}\right. \\ & \left. - \left(\mathbf{C}_1\mathbf{A}_{11} + \mathbf{A}_{21}\right)\mathbf{x}_{r1} - \left(\mathbf{C}_1\mathbf{A}_{12} + \mathbf{A}_{22}\right)\mathbf{x}_{r2}\right] \end{aligned} \tag{4.5.8}$$

$$\dot{u}_{s2} = -\lambda_{s2}\operatorname{sign}(\psi) \tag{4.5.9}$$

where $\lambda_{s1} > 0$, $\lambda_{s2} > 0$ are control parameters. The stability condition for the closed-loop system (4.5.7) and (4.5.8) can be obtained via the transformation $q_s = \left(\mathbf{C}_1\mathbf{D}_1 + \mathbf{D}_2\right)\mathbf{p} -$

$\lambda_{s2}\int_0^t \text{sign}(\psi)\,dt$ to

$$\begin{aligned}\dot{\psi} &= -\lambda_{s1}\,|\psi|^{\frac{1}{2}}\,\text{sign}\,(\psi) - q_s \\ \dot{q}_s &= -\lambda_{s2}\text{sign}\,(\psi) + (\mathbf{C}_1\mathbf{D}_1 + \mathbf{D}_2)\,\dot{\mathbf{p}}.\end{aligned} \tag{4.5.10}$$

If $|(\mathbf{C}_1\mathbf{D}_1 + \mathbf{D}_2)\,\dot{\mathbf{p}}| < L < \infty$ and choosing $\lambda_{s2} > 5L$ and $32L \leq \lambda_{s1}^2 \leq 8\,(\lambda_{s2} - L)$ then the system (4.5.10) is finite time globally stable [131], i.e, its solution converges in finite time to the origin $(\psi, q_s) = (0,0)$. The sliding motion on $\psi = 0$ is given by (4.5.3) and (4.5.5), in this way the SM equation is

$$\dot{\mathbf{x}}_{r1} = (\mathbf{A}_{11} - \mathbf{A}_{12}\mathbf{C}_1)\,\mathbf{x}_{r1} + \mathbf{A}_{12}\xi + \mathbf{D}_1\mathbf{p}. \tag{4.5.11}$$

At this point, to reject the unmatched unknown perturbation $\mathbf{p}$ in the SM equation (4.5.11), we apply the well known geometrical approach [139]. The disturbance $\mathbf{p}$ can be rejected preserving SM equation stability if and only if the image of the matrix associated to the disturbance, $\text{Im}\mathbf{D}_1$, belongs to $\mathbf{V}_g^*$, the so-called maximal $(\mathbf{A}_{11}, \mathbf{A}_{12})$-invariant subspace contained in the kernel of the output $y_1 = x_{r1} = \begin{bmatrix} 1 & 0 & 0 \end{bmatrix}\mathbf{x}_{r1}$ It can be seen that this problem is solvable, since clearly $\text{Im}\mathbf{D}_1 = \text{span}\left\{\tilde{\mathbf{D}}_1\right\}$ belongs to $\mathbf{V}_g^* = \text{span}\left\{\mathbf{V}_g^{*(1)}, \mathbf{V}_g^{*(2)}\right\}$ with $\tilde{\mathbf{D}}_1 = \begin{bmatrix} 0 & 1 & 0 \end{bmatrix}^T$, $\mathbf{V}_g^{*(1)} = \begin{bmatrix} 0 & 1 & 0 \end{bmatrix}^T$ and $\mathbf{V}_g^{*(2)} = \begin{bmatrix} 0 & 0 & 1 \end{bmatrix}^T$ Then, using the virtual control $\mathbf{x}_{r2}$ (4.5.5), which produces $\mathbf{V}_g^*$ to be SM equation (4.5.11) invariant, the output $y_1 = x_{r1}$ is not affected at all by the signal $\mathbf{p}$, i.e, this control rejects the disturbance $\mathbf{p}$ in the SM equation. Notice that this control renders the system (4.5.11) maximally non-observable by cancelling out the zeros associated to the transfer function between $\mathbf{p}$ and $y_1 = x_{r1}$ with closed-loop poles. The closed-loop system (4.5.11) is stable, because these zeros are stable, and the remaining pole is located in a suitable stable position.

4.5.2 Brake control

Let $\mathbf{x}_b = [x_5, x_6, x_7]$ and taking into account the direct action of the pressure P_b in the brake cylinder over the wheels motion, we define the output tracking error as

$$e_1 \triangleq x_5 - \frac{1 - s^*}{r}x_7, \tag{4.5.12}$$

Then, from (2.3.2), (2.3.3) and (4.5.12) the derivative of e_1 is

$$\dot{e}_1 = f_1\,(x_5, x_7) + b_1\,(x_5, x_7)\,x_6 + \Delta_1 \tag{4.5.13}$$

where $f_1\,(x_5, x_7) = \frac{1-s^*}{r}\,[a_{11}\mu N_M\psi\,(s) - f_w(x_7)] - a_7x_5 + a_8\mu N_m\psi\,(s)$ and $b_1\,(x_5, x_7) = -a_9$. The term Δ_1 contains the reference derivative $\dot{s}^*$, the variations of the friction parameter μ,

the wind speed v_w, the influence of z_r, $\dot{z}_r$ on $F(s)$ and will be considered as an unmatched and bounded perturbation term.

Considering the variable x_6 as virtual control in (4.5.13) we determinate its desired value $x_{6\delta}$ as

$$x_{6\delta} = x_{6\delta,0} + x_{6\delta,1} \tag{4.5.14}$$

where $x_{2\delta,0}$ is the nominal part of the nominal control and $x_{6\delta,1}$ will be designed using the SM technique to reject the perturbation in (4.5.13). In this way, we propose the desired dynamics $\dot{e}_1 = -k_0 e_0 - k_1 e_1$, which are introduced by means of

$$x_{6\delta,0} = -\frac{1}{b_1(x_5, x_7)}\left[f_1(x_5, x_7) + k_0 e_0 + k_1 e_1\right] \tag{4.5.15}$$

where $k_0 > 0$, $k_1 > 0$ and e_0 is defined by

$$\dot{e}_0 = e_1, \qquad e_0(0) = 0 \tag{4.5.16}$$

Now, in order to attenuate the perturbation term Δ_1 in (4.5.13), we define the surface

$$\sigma_1 = e_1 + z \tag{4.5.17}$$

where z is an SM integral variable and will be defined later. From (4.5.13), (4.5.15), (4.5.14) and (4.5.17) the derivative of σ_1 is given by

$$\dot{\sigma}_1 = -k_0 e_0 - k_1 e_1 + x_{6\delta,1} + \Delta_1 + \dot{z} \tag{4.5.18}$$

Selecting $\dot{z} = k_0 e_0 + k_1 e_1$ with $z(0) = -e_1(0)$, the equation (4.5.18) reduces to

$$\dot{\sigma}_1 = x_{6\delta,1} + \Delta_1 \tag{4.5.19}$$

To enforce quasi-sliding motion in (4.5.19) the term $x_{6\delta,1}$ in (4.5.18) is chosen as

$$x_{6\delta,1} = -k_{\sigma_1} \text{sigm}(\varepsilon, \sigma_1)$$

where we use the result that the sign function can be approximated by the sigmoid function in the form $\text{sigm}(\varepsilon; x) \to \text{sign}(x)$ as $\varepsilon \to \infty$. Now, we define a new error variable e_2 as

$$e_2 = x_{6\delta} - x_6. \tag{4.5.20}$$

Using (4.5.1) and (4.5.20), straightforward calculations reveal

$$\dot{e}_2 = \Delta_2 - b_3 u_b \tag{4.5.21}$$

where the term $\Delta_2 = a_3 x_6 + \frac{\partial x_{6\delta}}{\partial x_5}\dot{x}_5 + \frac{\partial x_{6\delta}}{\partial x_7}\dot{x}_7$ is considered as a perturbation.

Using the new variables e_0, e_1, e_2 and σ_1 the extended closed loop system (4.5.13), (4.5.16), (4.5.21) and (4.5.19) is presented as

$$\dot{e}_0 = e_1 \tag{4.5.22}$$
$$\dot{e}_1 = -k_0 e_0 - k_1 e_1 + e_2 - k_{\sigma_1} \text{sigm}\,(\varepsilon, \sigma_1) + \Delta_1 \tag{4.5.23}$$
$$\dot{\sigma}_1 = -k_{\sigma_1} \text{sigm}\,(\varepsilon, \sigma_1) + \Delta_1 \tag{4.5.24}$$
$$\dot{e}_2 = \Delta_2 - b_3 u_b \tag{4.5.25}$$
$$\dot{x}_7 = -a_{11} F - f_w\,(x_7) \tag{4.5.26}$$

We now consider the types of valve that can vary its position in a continuous range. To induce sliding mode on the sliding manifold $e_2 = 0$, the super-twisting control algorithm is applied [100, Ch. 2] to (4.5.25)

$$u_b = \frac{1}{b_3}\left[u_{b1} + u_{b2}\right] \tag{4.5.27}$$

with $u_{b1} = -\lambda_{b1}\left|e_2\right|^{\frac{1}{2}} \text{sign}(e_2)$, $\dot{u}_{b2} = -\lambda_{b2} \text{sign}(e_2)$, where $\lambda_{b1} > 0$, $\lambda_{b2} > 0$ are control parameters. Now, the stability of (4.5.22) (4.5.25) closed loop by (4.5.27) is outlined in a step by step procedure:

Step A) Reaching phase of the projection motion (4.5.25);

Step B) SM stability of the projection motion (4.5.24);

Step C) SM stability of (4.5.22)-(4.5.23) on the manifold $e_2 = 0$ and in the vicinity of $\sigma_1 = 0$.

We use the assumptions

$$\left|\Delta_1\right| \leq \alpha_1 \left|\sigma_1\right| + \beta_1 \tag{4.5.28}$$
$$\left|\dot{\Delta}_1\right| \leq \alpha_0 \left|\dot{\sigma}_1\right| \tag{4.5.29}$$
$$\left|\dot{\Delta}_2\right| \leq \beta_2 \tag{4.5.30}$$

with $\alpha_0 > 0$, $\alpha_1 > 0$, $\alpha_2 > 0$, $\beta_1 > 0$, $\beta_2 > 0$.

Step A) For (4.5.25) in closed loop with (4.5.27) we use the transformation $q_b = \Delta_2 - \lambda_{b2}\int_0^t \text{sign}(e_2)\,dt$, then, we have

$$\begin{aligned} \dot{e}_2 &= -\lambda_{b1}\left|e_2\right|^{\frac{1}{2}} \text{sign}\,(e_2) - q_b \\ \dot{q}_b &= -\lambda_{b2} \text{sign}\,(e_2) + \dot{\Delta}_2 \end{aligned} \tag{4.5.31}$$

and under the assumption (4.5.30), then choosing $\lambda_{b2} > 5\beta_2$ and $32\beta_2 \leq \lambda_{b1}^2 \leq 8\,(\lambda_{b2} - \beta_2)$, the system (4.5.31) is finite time globally stable [131], i.e, its solution converges in finite time to the origin $(e_2, q_b) = (0, 0)$.

Step B) To analyze the stability of the projection motion (4.5.24) we assume that the signum function can be approximated by the sigmoid function in the form $\text{sigm}(\varepsilon; x) \to \text{sign}(x)$ as $\varepsilon \to \infty$, then, we can establish the following equality

$$\text{sign}(x) - \text{sigm}(\varepsilon; x) = \Delta_s(\varepsilon; x) \tag{4.5.32}$$

It is evident that $\Delta_s(x)$ is bounded, that is, for a given ε there is a positive constant $0 < \gamma < 1$ such that $\|\Delta_s(\varepsilon; x)\| = \gamma$. Now, taking the Lyapunov candidate $V_1 = \frac{1}{2}\sigma_1^2$ and taking its derivative, with (4.5.28) results

$$\begin{aligned} \dot{V}_1 &= \sigma_1 \left[-k_{\sigma_1} \text{sigm}(\varepsilon, \sigma_1) + \Delta_1\right] \\ &\leq -|\sigma_1| \left[k_{\sigma_1}(1-\gamma) - \alpha_1 |\sigma_1| - \beta_1\right] \end{aligned}$$

therefore, if $k_{\sigma_1} > \frac{\beta_1}{1-\gamma}$ then σ_1 converges to a vicinity of zero, $|\sigma_1| < \vartheta$, with

$$\vartheta = \frac{\ln\left(\frac{2-\gamma}{\gamma}\right)}{2\varepsilon}$$

and, with (4.5.29), $\dot{\sigma}_1$ converges to zero in finite time [134].

Step C) To analyse the SM stability of (4.5.22)-(4.5.23) on the manifold $e_2 = 0$ and in the vicinity of $\sigma_1 = 0$ we define the Lyapunov function $V_2 = \frac{1}{2}(e_0^2 + e_1^2)$ and taking its derivative,

$$\begin{aligned} \dot{V}_2 &= e_1 \left[(1-k_0)|e_0| - k_1 e_1\right] \\ &\leq -|e_1| \left[(k_0 - 1)|e_0| + k_1 |e_1|\right] \end{aligned}$$

therefore, when $k_0 > 1$ and $k_1 > 0$ then, e_1 converges asymptotically to zero.

4.6 Conclusions

In this chapter different controllers are presented, for their design problems as tire deformation and the addition of an active suspension are considered. For each case, stability and robustness analysis, in presence of both the matched and unmatched perturbations, are presented in detail. Therefore, the ABS can cope very well with the sliding mode control, as can be applied in a straight fashion without concerning the nature of the actuator (continuous or discontinuous), showing in that way a clear advantage over another control techniques, where the presence of discontinuous elements can not be treated in a natural way.

Chapter 5

Simulation results

In this chapter, simulation result are presented. In the section 5.1, the simulation results of a sliding mode block control for the plant in absence or tire deformation are presented. In the sections 5.2 and 5.2, the integral nested sliding mode control simulations in absence and in presence of tire deformation are respectively shown. The section 5.4 presents the simulations results of a sliding mode block control regulator for ABS. Finally, in section 5.5, the simulation for a controller of a brake with active suspension is presented.

5.1 Sliding mode block control for the plant in absence or tire deformation

To show the effectiveness of the proposed control law, simulations have been carried out on one wheel model design example, the system (4.1.1) parameters used are listed in Table 1.

TABLE 1
Values of Parameters

Parameter	Value	Parameter	Value
A_f	6.6	v_w	-6
P_c	8	v	0.5
M	1800	B	10
J	18.9	C	1.9
r	0.535	D	1
m	450	E	0.97
ρ	1.225	g	9.81
C_d	0.65	P_a	0

In order to maximize the friction force, we suppose that slip tracks a constant signal during the simulations

$$y_{ref} = 0.203$$

which produces a value close to the maximum of the function $\phi(s)$. The parameters used in the control law are $k_0 = 700$ and $k_1 = 120$.

On the other hand, to show robustness property of the control algorithm in presence of parametric variations we introduce a change of the friction coefficient μ which produces different contact forces, namely $\hat{F}$ and $\hat{f}$. Then, $\mu = 0.5$ for $t < 1$ s, $\mu = 0.52$ for $t \in [1, 2.5)$ s, and $\mu = 0.5$ for $t \geq 2.5$ s. It is worth mentioning that just the nominal values were considered in the control design.

In Figure 5.1 the slip performance trough the simulation is shown,

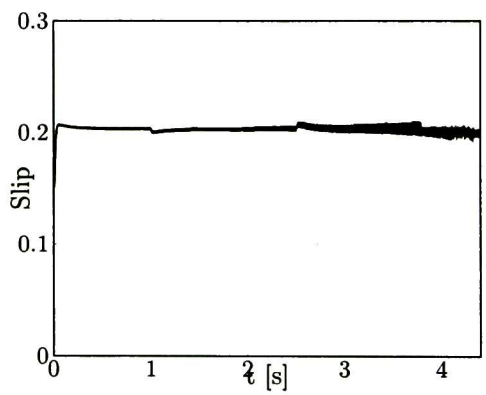

Figure 5.1: Slip, s, performance in the braking process

Figure 5.2 shows the friction function behaviour $\phi(s)$ during the braking process,

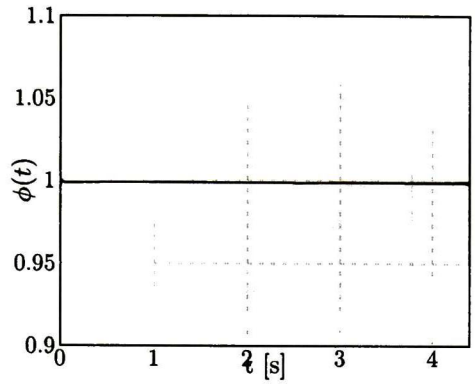

Figure 5.2: Performance of ϕ in the braking process

while Figure 5.3 and Figure 5.4 summarize the behaviour of the error variables e_1 and e_2 respectively.

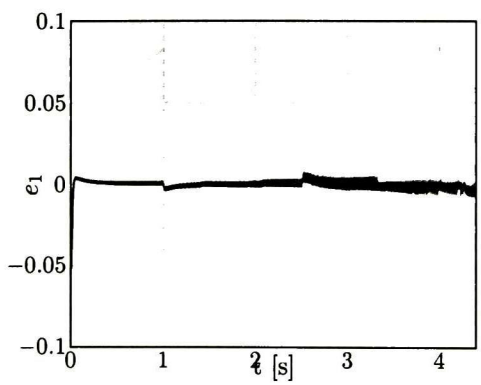

Figure 5.3: Tracking error e_1

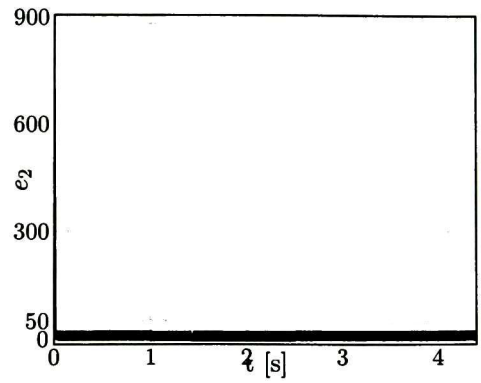

Figure 5.4: Sliding surface error e_2

In Figure 5.5 the longitudinal speed v and the linear wheel speed $r\omega$ are shown; it is worth noting that the slip controller should be turn off when the longitudinal speed v is close to zero.

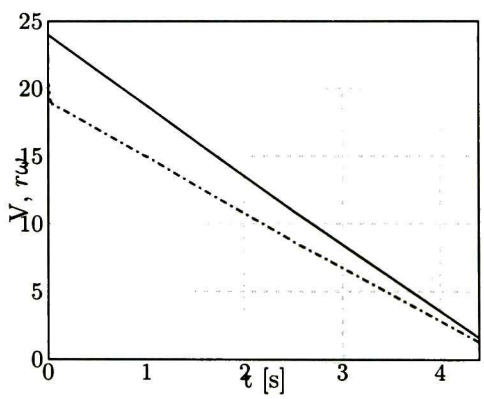

Figure 5.5: Longitudinal speed v (solid) and linear wheel speed $r\omega$ (dashed)

In Figure 5.6 the nominal F, and the $\hat{F}$ contact force are shown.

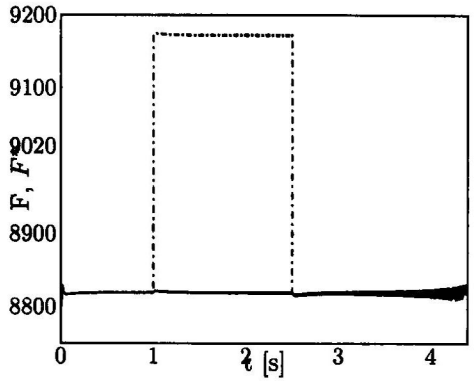

Figure 5.6: Nominal F (solid) and $\hat{F}$ (dashed) contact forces

Finally, in Figure 5.7 the control action is shown.

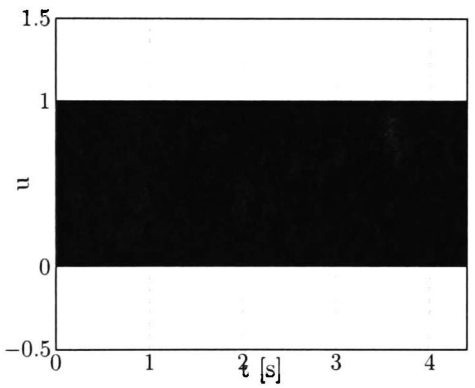

Figure 5.7: Control input u

The simulation results show good performance and robustness of the closed-loop system in presence of both the matched and unmatched perturbations, namely, parametric variations and neglected dynamics.

5.2 Integral nested sliding mode control for the plant in absence of tire deformation

To show the effectiveness of the proposed control law, simulations have been carried out on the wheel model design example, the system (4.2.1) parameters used are listed in Table 2.

TABLE 2
Values of Parameters (MKS Units)

Parameter	Value	Parameter	Value
A_f	6.6	V_w	-6
P_c	8	v	0.5
M	1800	B	10
J	18.9	C	1.9
R	0.535	D	1
m	450	E	0.97
ρ	1.225	g	9.81
C_d	0.65	P_a	0

In order to maximize the friction force, we suppose that slip tracks a constant signal during the simulations

$$s^* = 0.203$$

which produces a value close to the maximum of the function $\phi(s)$. The parameters used in the control law are $k_0 = 700$, $k_1 = 120$, $k_3 = 2$, $k_4 = 100$, $k_{\sigma_1} = 10$, $\lambda_1 = 1$, $\lambda_2 = 2$ and $\varepsilon = 100$.

On the other hand, to show robustness property of the control algorithm in presence of parametric variations we introduce a change of the friction coefficient μ which produces different contact forces, namely F and $\hat{F}$. Then, $\mu = 0.5$ for $t < 1$ s, $\mu = 0.52$ for $t \in [1, 2.5)$ s, and $\mu = 0.5$ for $t \geq 2.5$ s. It is worth mentioning that just the nominal values were considered in the control design.

5.2.1 Sliding mode control for two position valves

In the Figure 5.8 and Figure 5.9 are shown, respectively, the slip and the friction function ϕ in the braking process

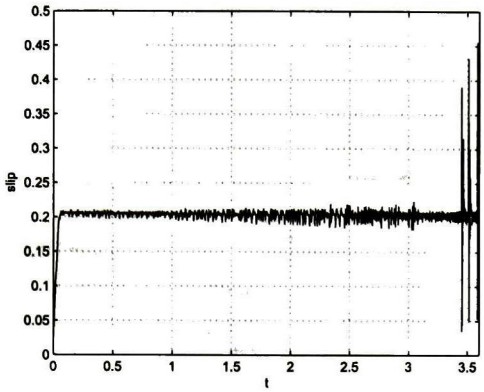

Figure 5.8: Slip, s, performance in the braking process

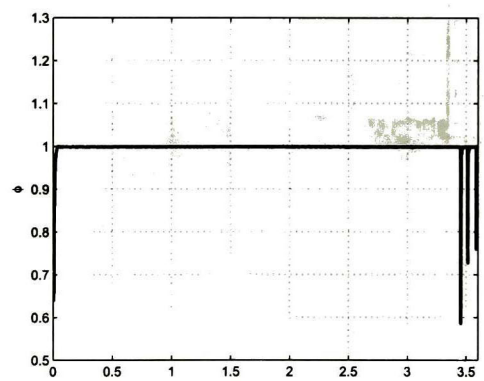

Figure 5.9: Performance of ϕ in the braking process

while Figure 5.10 and Figure 5.11 summarize the behaviour of the error variables e_1 and e_2 respectively.

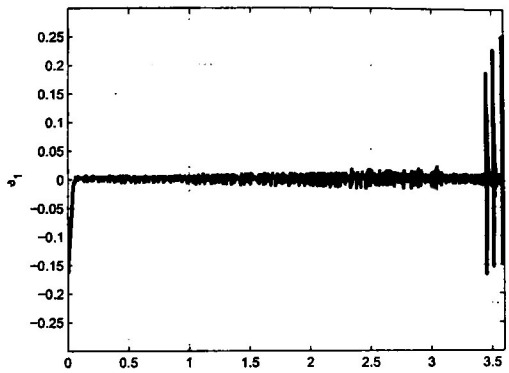

Figure 5.10: Tracking error e_1

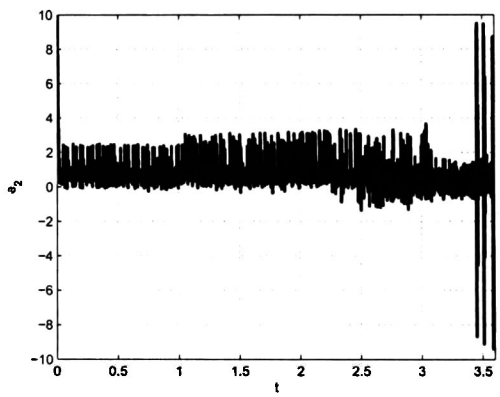

Figure 5.11: Sliding surface error e_2

In Figure 5.12 the longitudinal speed v and the linear wheel speed $r\omega$ are shown; it is worth noting that the slip controller should be turn off when the longitudinal speed v is close to zero.

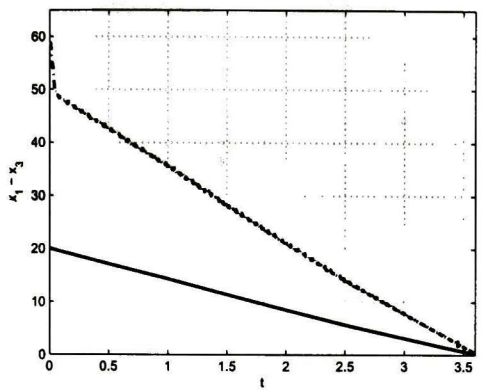

Figure 5.12: Longitudinal speed v (solid) and linear wheel speed $r\omega$ (dashed)

In Figure 5.13 the nominal F, and the $\hat{F}$ contact force are shown

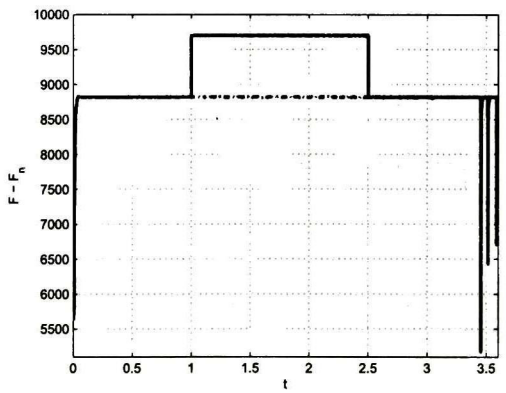

Figure 5.13: Nominal F (solid) and $\hat{F}$ (dashed) contact forces

Finally, in Figure 5.14 the control action is shown.

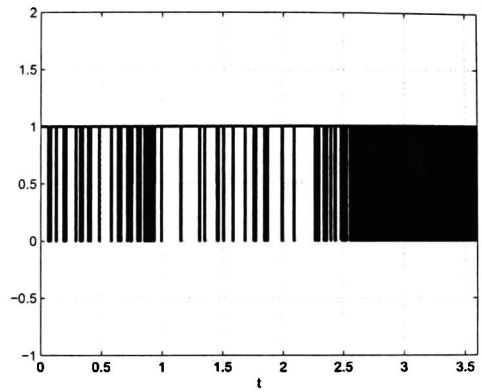

Figure 5.14: Control input u

5.2.2 Sliding mode control for continuous position valves

In Figure 5.15 and Figure 5.16 are shown, respectively, the slip and the friction function ϕ in the braking process

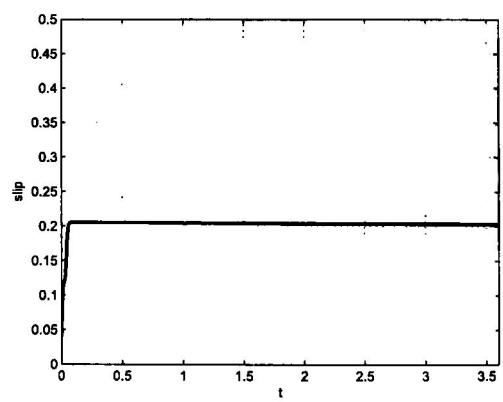

Figure 5.15: Slip, s, performance in the braking process

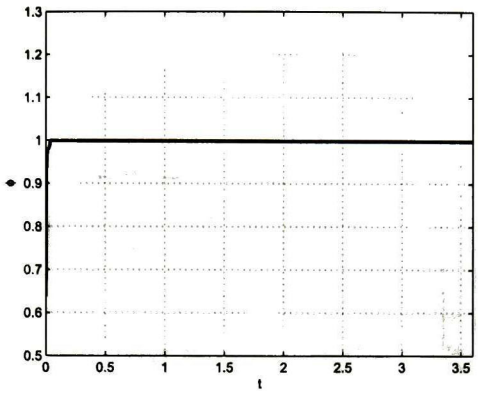

Figure 5.16: Performance of ϕ in the braking process

while Figure 5.17 and Figure 5.18 summarize the behaviour of the error variables e_1 and e_2 respectively.

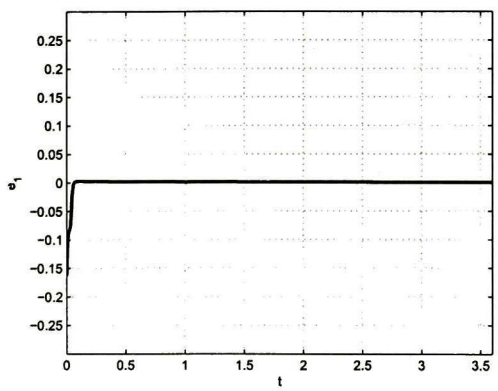

Figure 5.17: Tracking error e_1

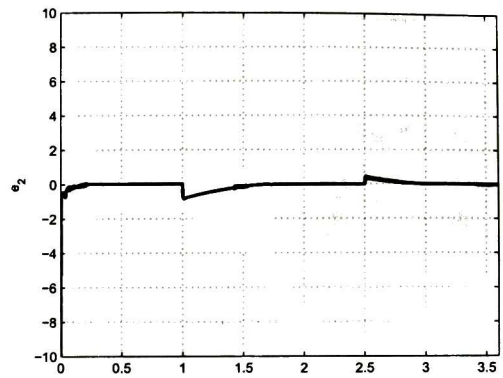

Figure 5.18: Sliding surface error e_2

In Figure 5.19 the longitudinal speed v and the linear wheel speed $r\omega$ are shown; it is worth noting that the slip controller should be turn off when the longitudinal speed v is close to zero.

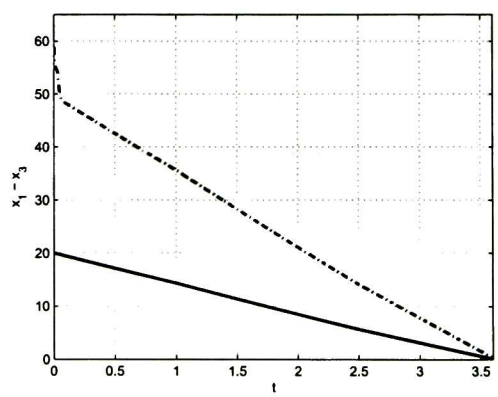

Figure 5.19: Longitudinal speed v (solid) and linear wheel speed $r\omega$ (dashed)

In Figure 5.20 the nominal F, and the $\hat{F}$ contact force are shown

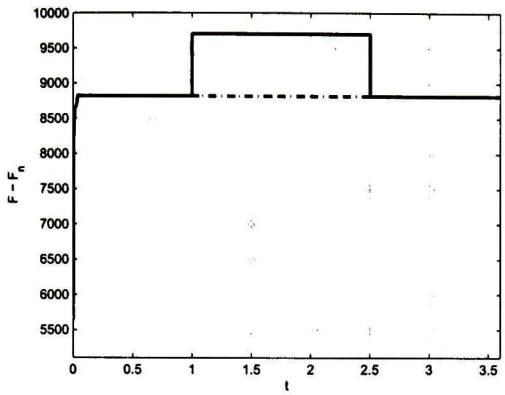

Figure 5.20: Nominal F (solid) and $\hat{F}$ (dashed) contact forces

Finally, in Figure 5.21 the control action is shown.

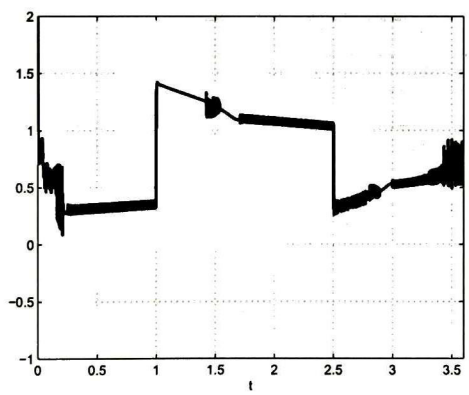

Figure 5.21: Control input u

The simulation results show good performance and robustness of the closed-loop system in presence of both the matched and unmatched perturbations, namely, parametric variations and neglected dynamics.

5.3 Integral nested sliding mode control for the plant in presence or tire deformation

To show the effectiveness of the proposed control law, simulations have been carried out on one wheel model design example, the system (4.3.1) parameters used are listed in Table 3.

In order to maximize the friction force, in the simulations we suppose that slip tracks a constant signal.

$$y_{ref} = 0.205$$

which produces a value close to the maximum of the function $\phi(s)$. The parameters used in the control law are $k_{10} = 8700$, $k_{11} = 1000$ and $\varepsilon_1 = 100$.

TABLE 3
Values of Parameters (MKS)

Parameter	Value	Parameter	Value
C_x	10	v_w	-5
K_x	9000	μ	0.8
M	2396	B	10
J	18.9	C	1.9
r	0.535	D	1
K_b	1000	E	0.97
ρ	1.225	N	23504.76
C_d	0.65	P_a	0
A_f	6.6	P_c	8

On other hand, to show robustness property of the control algorithm in presence of parametric variations we introduce a change of the friction coefficient μ which produces a different contact force, namely $\hat{F}$ Then, $\mu = 0.5$ for $t < 1$ s, $\mu = 0.52$ for $t \in [1, 2)$ s, and $\mu = 0.5$ for $t > 2$ s. It is worth mentioning that just the nominal values were considered in the control design.

In Figure 5.22 and Figure 5.23 are shown, respectively, the slip and the friction function ϕ in the braking process

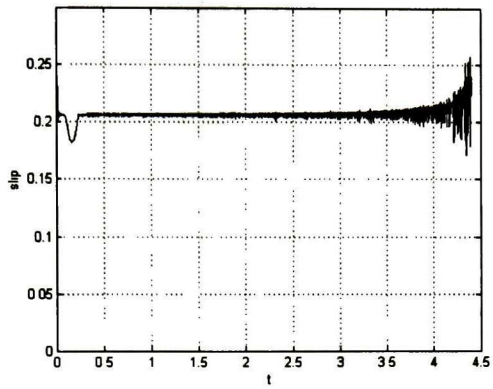

Figure 5.22: Slip, s, performance in the braking process

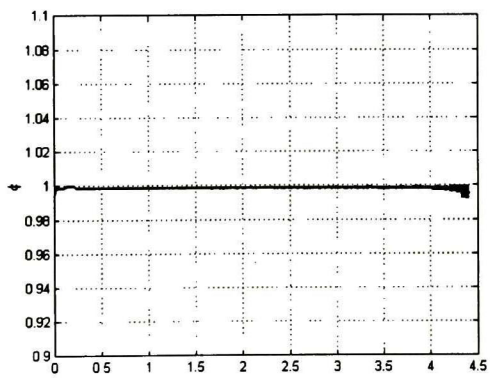

Figure 5.23: Performance of ϕ in the braking process

while Figure 5.24 and Figure 5.25 summarize the behaviour of the error variables e_1 and e_2 respectively.

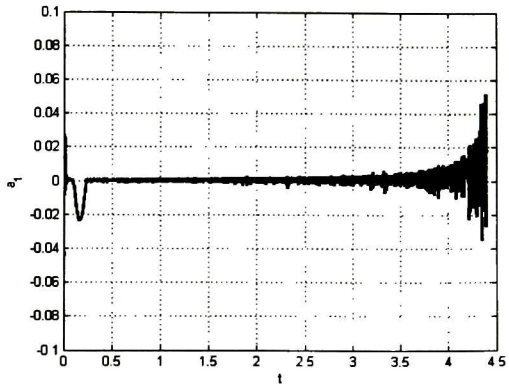

Figure 5.24: Tracking error e_1

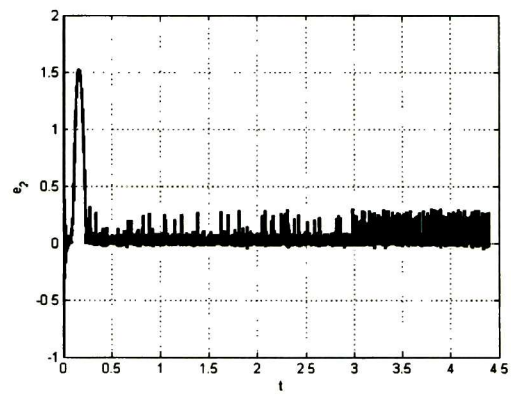

Figure 5.25: Sliding surface error e_2

In Figure 5.26 the longitudinal speed v and the linear wheel speed $r\omega$ are shown; it is worth noting that the slip controller should be turn off when the longitudinal speed v is close to zero.

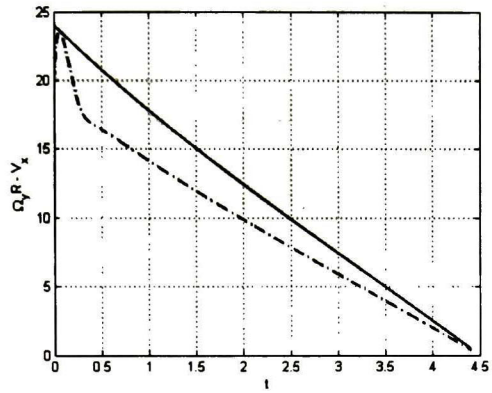

Figure 5.26: Longitudinal speed v (solid) and linear wheel speed $r\omega$ (dashed)

In Figure 5.27 the nominal F, and the $\hat{F}$ contact force are shown.

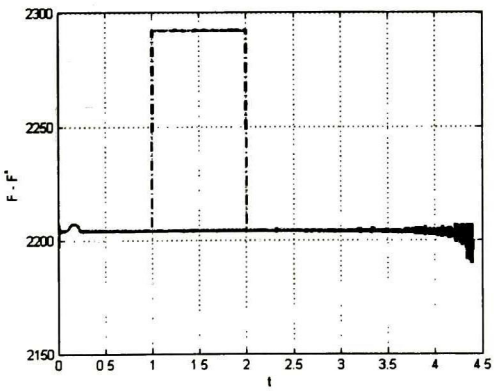

Figure 5.27: Nominal F (solid) and $\hat{F}$ (dashed) contact forces

Finally, in Figure 5.28 the control action is shown.

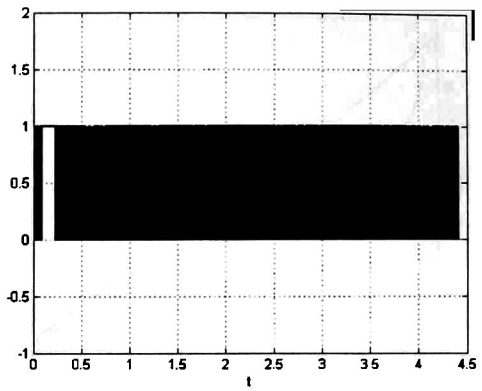

Figure 5.28: Control input u

The simulation results show good performance and robustness of the closed-loop system in presence of both the matched and unmatched perturbations, namely, parametric variations and neglected dynamics.

5.4 Sliding mode regulator

To show the effectiveness of the proposed control law, simulations have been carried out on one wheel model design example, the system (4.4.1) parameters used are listed in Table 4.

TABLE 4
Values of Parameters (MKS Units)

Parameter	Value	Parameter	Value
A_f	6.6	v_w	-6
P_c	8	v	0.5
M	1800	B	10
J	18.9	C	1.9
R	0.535	D	1
m	450	E	0.97
ρ	1.225	g	9.81
C_d	0.65	B_b	0.08

In order to maximize the friction force, we suppose that slip tracks a constant signal during the simulations

$$y_{ref} = 0.203$$

which produces a value close to the maximum of the function $\phi(s)$. The parameters used in the control law are $k_0 = 700$, $k_1 = 120$, $k_3 = 2$, $k_4 = 100$ and $\varepsilon_1 = \varepsilon_2 = 100$.

On the other hand, to show robustness property of the control algorithm in presence of parametric variations we introduce a change of the friction coefficient μ which produces different contact forces, namely F and $\hat{F}$. Then, $\mu = 0.5$ for $t < 1$ s, $\mu = 0.52$ for $t \in [1, 2.5)$ s, and $\mu = 0.5$ for $t \geq 2.5$ s. It is worth mentioning that just the nominal values were considered in the control design.

In Figure 5.29 the slip performance trough the simulation is shown, Figure 5.30 shows the friction function behaviour $\phi(s)$ during the braking process

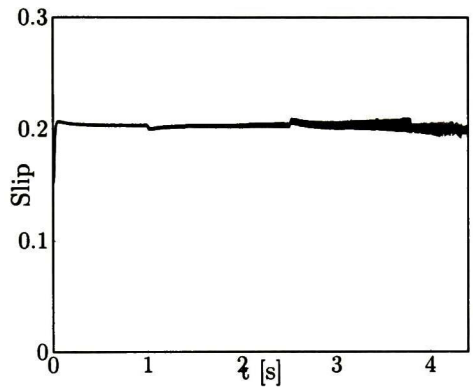

Figure 5.29: Slip, s, performance in the braking process

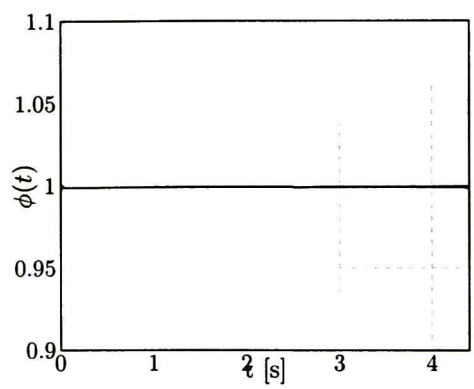

Figure 5.30: Performance of ϕ in the braking process

while Figure 5.31 and Figure 5.32 summarize the behaviour of the error variables e_1 and e_2 respectively.

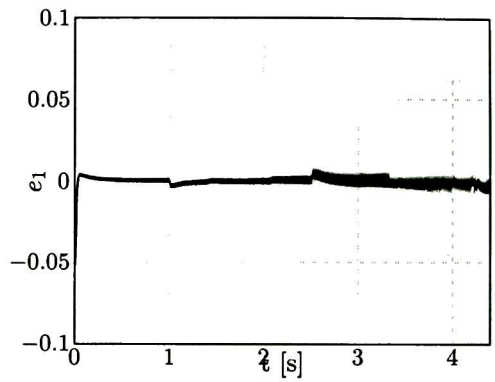

Figure 5.31: Tracking error e_1

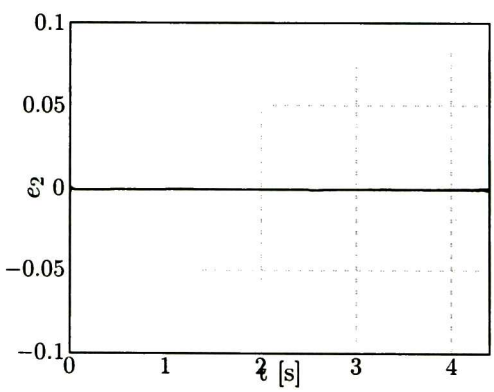

Figure 5.32: Sliding surface error e_2

In Figure 5.33 the longitudinal speed v and the linear wheel speed $r\omega$ are shown; it is worth noting that the slip controller should be turn off when the longitudinal speed v is close to zero.

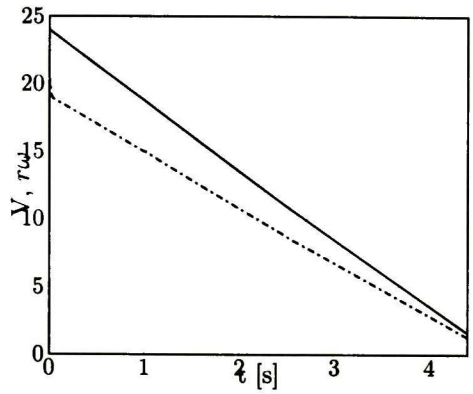

Figure 5.33: Longitudinal speed v (solid) and linear wheel speed $r\omega$ (dashed)

In Figure 5.34 the nominal F, and the $\hat{F}$ contact force are shown.

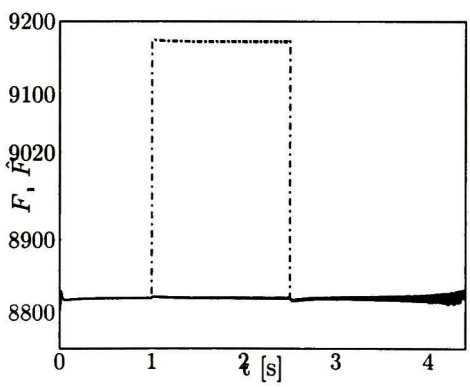

Figure 5.34: Nominal F (solid) and $\hat{F}$ (dashed) contact forces

Finally, in Figure 5.35 the control action is shown.

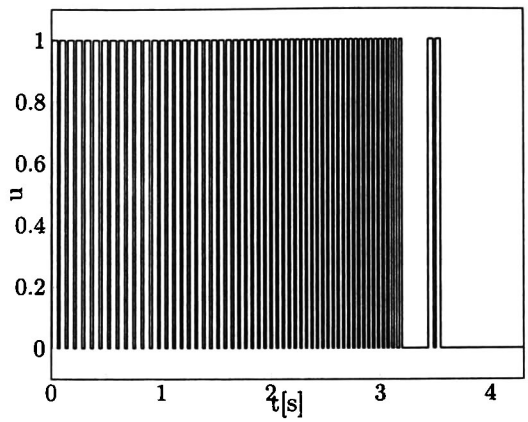

Figure 5.35: Control input u

The simulation results show good performance and robustness of the closed-loop system in presence of both the matched and unmatched perturbations, namely, parametric variations and neglected dynamics.

5.5 Sliding mode control of a ABS with active suspension

To show the effectiveness of the proposed control law, simulations have been carried out on the wheel model design example, the system (4.5.1) parameters used are listed in Table 5.

TABLE 5
Values of Parameters (MKS Units)

Parameter	Value	Parameter	Value	Parameter	Value
m_c	1800	J	18.9	E	0.97
m_w	50	k_b	100	A_f	6.6
K_{cw}	1050	b_b	0.08	C_d	0.65
K_{wr}	175500	r	0.535	ρ	1.225
C_{cw}	19960	B	10	v_w	-6
C_{wr}	1500	C	1.9	g	9.81
τ	0.0043	D	1	v	0.5

During the breaking process we want to maximize the friction force, for that reason throughout simulations we suppose that slip tracks a constant signal $s^* = 0.203$, which in

this case produces a value close to the maximum of the function $\phi(s)$. The reference for suspension is $y_{1d} = -0.2$. The road perturbation is considered as $z_r = 0.1\cos(10t)$. The parameters used in the control law are $\lambda_{s1} = 10$, $\lambda_{s2} = 15$, $\mathbf{C}_1 = \begin{bmatrix} -175 & -35 & 0 \end{bmatrix}^T$ $k_0 = 700$, $k_1 = 120$, $k_{\sigma_1} = 10$, $\lambda_{b2} = 1$, $\lambda_{b2} = 2$ and $\varepsilon = 10$.

On the other hand, to show robustness property of the control algorithm in presence of parametric variations we introduce a change of the friction coefficient μ which produces different contact forces, namely F and $\hat{F}$. Then, $\mu = 0.5$ for $t < 1$ s, $\mu = 0.52$ for $t \in [1, 2.5)$ s, and $\mu = 0.5$ for $t \geq 2.5$ s. It is worth mentioning that just the nominal values were considered in the control design.

Longitudinal speed v and the linear wheel speed $r\omega$ are shown in Fig. 5.36, the ABS controller should be turned off when the longitudinal speed is close to zero.

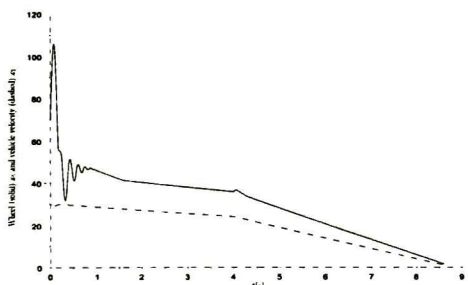

Figure 5.36: Longitudinal speed v (dashed) and the linear wheel speed $r\omega$ (solid)

Figure 5.37 shows the slip ratio during the breaking process, we can see the fast convergence to the reference value s^*

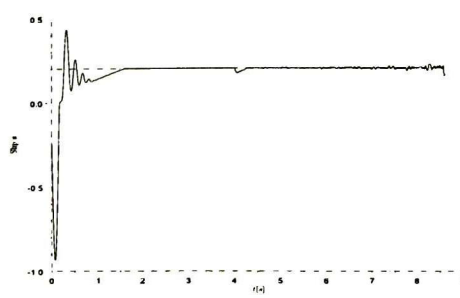

Figure 5.37: Slip performance in the braking process

and Figure 5.38 presents the friction/slip characteristic relation $\phi(s)$ obtained during the breaking process under control actions.

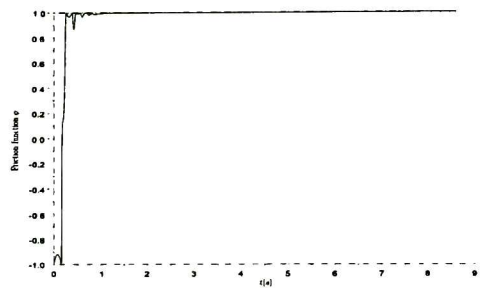

Figure 5.38: Performance of $\phi(s)$ in the braking process

Figure 5.39 shows the vertical vehicle position during the breaking process. We could see the position is lowered 0.2 m under zero position and that is kept constant until the car is almost stopped,

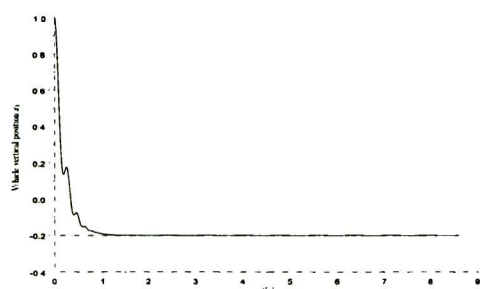

Figure 5.39: Vehicle position x_1

until Figure 5.40 presents the suspension position of the vehicle, we note that moves constantly trying to counteract the changes on the road and wheel.

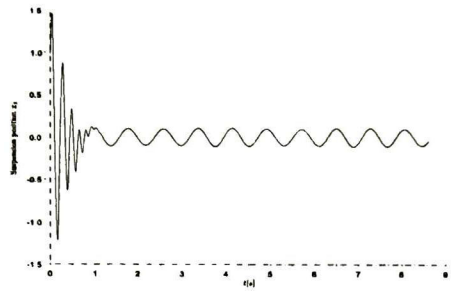

Figure 5.40: Suspension position x_3

The control action u_s for the suspension is shown in Figure 5.41. Note that the valve can put or extract fluid into the reservoir to obtain the necessary forces.

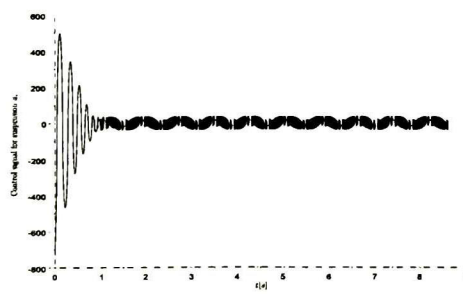

Figure 5.41: Control signal for suspension u_s

The sliding variable ψ is presented in Figure 5.42.

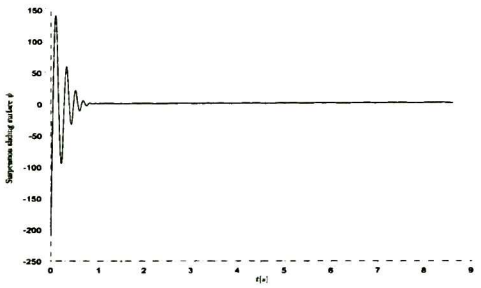

Figure 5.42: Sliding surface for suspension control ψ

The control signal u_b for the ABS system is presented in Figure 5.43.

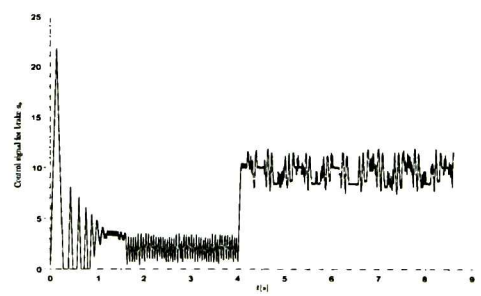

Figure 5.43: Control signal for ABS u_b

The sliding variable σ is presented in Figure 5.44,

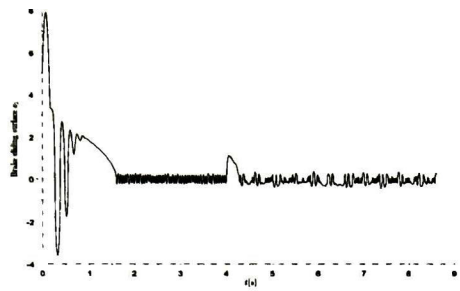

Figure 5.44: Sliding surface for ABS control e_2

while Figure 5.45 summarize the behaviour of the tracking error variable e_1

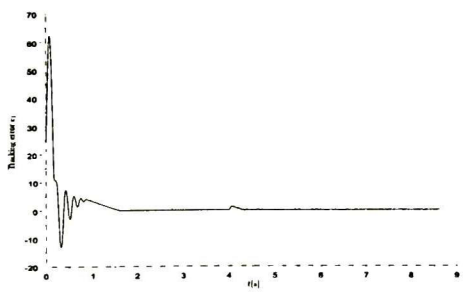

Figure 5.45: Tracking error e_1

Finally, in Figure 5.46 the nominal F, and the $\hat{F}$ contact forces are shown

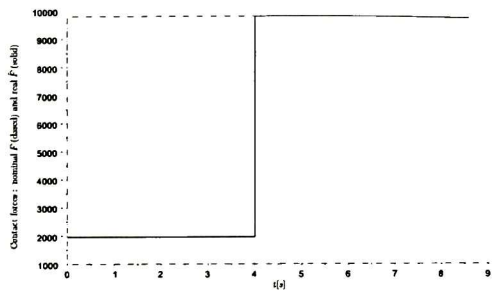

Figure 5.46: Nominal contact force F (dashed) and real force $\hat{F}$ (solid)

The simulation results show good performance and robustness of the closed-loop system in presence of both the matched and unmatched perturbations, namely, parametric variations and neglected dynamics.

Chapter 6

Conclusions and future work

General conclusions

In this work, different controllers for the ABS on the basis the block control principle and sliding mode, the related technique of integral nested sliding mode and a sliding mode block control regulator are presented as follows:

- A controller designed on the basis of the block control principle and sliding mode to ensure asymptotically output tracking consisting of the relative slip.
- A controller designed on the basis of the technique of integral nested sliding mode to ensure asymptotically output tracking consisting of the relative slip.
- A sliding mode block control regulator to ensure asymptotically output tracking along with the stabilization of the residual dynamic consisting of the vehicle velocity for the brake system.
- In addition, controllers for active suspension coupled with the brake with objective to guarantee the improvement of the ride quality and comfort for the passengers. For the active suspension, a controller based on the regular form, sliding mode control and geometric linear control methods for the sliding surface design is proposed in order to achieve and ensure output tracking.

Each one of these controllers ensures asymptotically output tracking, in addition the sliding mode block control regulator also guarantees the stabilization of the residual dynamic consisting of the vehicle velocity for the brake system. These controllers maximize the friction force in the wheel and avoid brake locking and provide robustness to matched, and unmatched perturbations. The cases of no deformation on the tire and with deformation are considered.

Detailed stability and robustness analysis is presented, for the cases of discontinuous and continuous valve action; simulation results show good performance and robustness of the closed-loop system in presence of both, matched and unmatched perturbations, namely, parametric variations and neglected dynamics.

Therefore, the ABS can cope very well with the SM mode control, as it can be applied in a straight fashion without concerning the nature of the actuator (continuous or discontinuous), showing in that way a clear advantage over another control techniques, where the presence of discontinuous elements can not be treated in a natural way giving an important application of the sliding modes control theory in the automotive problems. Therefore, the ABS and active suspensions can cope very well with the sliding mode control.

Future work

Almost all the results presented in this thesis can be improved. It means that the results here presented can be extended to a more realistic mathematical model and can be implemented jointly with additional control methods.

Suggestions for future work are:

- The used models are taken from the references and we can not guarantee their validation trough experimental test. Therefore, a first step in order to improve the current work is the use of more realistic and detailed models.
- Secondly, it is proposed the use of another control techniques as quasi-continuous high order sliding modes, $\mathcal{H}_\infty$ methods for sliding surface design, finite time disturbance rejection methods, zero average dynamics (ZAD) controllers, etc.
- The optimal slip value and the state variable were assumed to be known. Therefore, the design of the extremun seeking controllers to find the optimal slip value is proposed. In addition, the development of fixed parameters and adaptive state observers and parameter estimators based on sliding mode is suggested.

Bibliography

[1] M. Petrov, V. Balankin, and O. Naruzhnyi, "Study of automobiles brakes and pneumatic tires work. model of the work process of antiblock brake system," Novosibirsk, NISI, Tech. Rep., 1977, (In Russian).

[2] N. Rittmannsberger, "Antilock braking system and traction control," in *Proc. Int. Congress Transportation Electronics Convergence 88*, 1988, pp. 195–202.

[3] R. Emig, H. Goebels, and H. J. Schramm, "Antilock braking systems (abs) for commercial vehicles - status 1990 and future prospects," in *Proc. Int Transportation Electronics Congress Vehicle Electronics in the 90's:*, 1990, pp. 515–523.

[4] U. Kiencke and L. Nielsen, *Automotive Control Systems: For Engine, Driveline, and Vehicle*, softcover reprint of hardcover 2nd ed. 2005 ed. Springer, 11 2010.

[5] R. Rajamani, *Vehicle Dynamics and Control (Mechanical Engineering Series)*, softcover reprint of hardcover 1st ed. 2006 ed. Springer, 2 2011.

[6] G. Celentano, R. Iervolino, S. Porreca, and V. Fontana, "Car brake system modeling for longitudinal control design," in *Proc. IEEE Conf. Control Applications CCA 2003*, vol. 1, 2003, pp. 25–30.

[7] D. Margolis and T. Shim, "A bond graph model incorporating sensors, actuators, and vehicle dynamics for developing controllers for vehicle safety," *Journal of the Franklin Institute*, vol. 338, no. 1, pp. 21 – 34, 2001.

[8] R. Merzouki, B. Ould Bouamama, M. A. Djeziri, and M. Bouteldja, "Modelling and estimation for tire-road system using bond graph approach," in *Proc. IEEE/RSJ Int Intelligent Robots and Systems Conf*, 2006, pp. 3785–3790.

[9] W. Li, X. Wang, X. Leng, and M. Wang, "Modeling and simulation of automobile braking system based on kinetic energy conversion," in *Proc. IEEE Vehicle Power and Propulsion Conf. VPPC '08*, 2008, pp. 1–3.

[10] F. Grossi, W. Lhomme, R. Zanasi, and A. Bouscayrol, "Modelling and control of a vehicle with tire-road interaction using energy-based techniques," in *Proc. IEEE Vehicle Power and Propulsion Conf. VPPC '09*, 2009, pp. 1842–1848.

[11] H. B. Pacejka, *Tire and Vehicle Dynamics, 2nd edition*, 2nd ed. SAE International, 2005.

[12] H. Zhang, J. Wu, W. Chen, Y. Zhang, and L. Chen, "Object oriented modeling and simulation of a pneumatic brake system with abs," in *Proc. IEEE Intelligent Vehicles Symp*, 2009, pp. 780–785.

[13] M. Branciforte, A. Meli, G. Muscato, and D. Porto, "Ann and non-integer order modeling of abs solenoid valves," *IEEE Transactions on Control Systems Technology*, vol. PP, no. 99, pp. 1–8, 2010, early Access.

[14] S. Zhen-Jun, Z. Tian-Jun, and Z. Hong-Yan, "Research on road friction coefficient estimation algorithm based on extended kalman filter," in *Proc. Int Intelligent Computation Technology and Automation (ICICTA) Conf*, vol. 2, 2008, pp. 418–422.

[15] C. Canudas-de Wit and R. Horowitz, "Observers for tire/road contact friction using only wheel angular velocity information," in *Proc. 38th IEEE Conf. Decision and Control*, vol. 4, 1999, pp. 3932–3937.

[16] M. Tanelli, L. Piroddi, and S. M. Savaresi, "Real-time identification of tire-road friction conditions," *IET Control Theory & Applications*, vol. 3, no. 7, pp. 891–906, 2009.

[17] C. Lee, K. Hedrick, and K. Yi, "Real-time slip-based estimation of maximum tire-road friction coefficient," *IEEE/ASME Transactions on Mechatronics*, vol. 9, no. 2, pp. 454–458, 2004.

[18] L. Li, F.-Y. Wang, and Q. Zhou, "Integrated longitudinal and lateral tire/road friction modeling and monitoring for vehicle motion control," *IEEE Transactions on Intelligent Transportation Systems*, vol. 7, no. 1, pp. 1–19, 2006.

[19] H. Imine and Y. Delanne, "Triangular observers for road profiles inputs estimation and vehicle dynamics analysis," in *Proc. IEEE Int. Conf. Robotics and Automation ICRA 2005*, 2005, pp. 4751–4756.

[20] W. Zhang, N. Ding, G. Yu, and W. Zhou, "Virtual sensors design in vehicle sideslip angle and velocity of the centre of gravity estimation," in *Proc. 9th Int. Conf. Electronic Measurement & Instruments ICEMI '09*, 2009, pp. 3–652.

[21] C. R. Carlson and J. C. Gerdes, "Consistent nonlinear estimation of longitudinal tire stiffness and effective radius," *IEEE Transactions on Control Systems Technology*, vol. 13, no. 6, pp. 1010–1020, 2005.

[22] J. Yi, L. Alvarez, and R. Horowitz, "Adaptive emergency braking control with underestimation of friction coefficient," *IEEE Transactions on Control Systems Technology*, vol. 10, no. 3, pp. 381–392, 2002.

[23] M.-B. Radac, R.-E. Precup, S. Preitl, J. K. Tar, J. Fodor, and E. M. Petriu, "Gain-scheduling and iterative feedback tuning of pi controllers for longitudinal slip control," in *Proc. IEEE Int. Conf. Computational Cybernetics ICCC 2008*, 2008, pp. 183–188.

[24] G. Burgio, B. Castillo-Toledo, and S. Di Gennaro, "Nonlinear adaptive tracking for ground vehicles," in *Proc. 48th IEEE Conf. held jointly with the 2009 28th Chinese Control Conf Decision and Control CDC/CCC 2009*, 2009, pp. 7645–7650.

[25] P. E. Wellstead and N. B. O. L. Pettit, "Analysis and redesign of an antilock brake system controller," *IEE Proceedings -Control Theory and Applications*, vol. 144, no. 5, pp. 413–426, 1997.

[26] P. Tsiotras and C. C. De Wit, "On the optimal braking of wheeled vehicles," in *Proc. American Control Conf the 2000*, vol. 1, no. 6, 2000, pp. 569–573.

[27] F. Jiang and Z. Gao, "An application of nonlinear pid control to a class of truck abs problems," in *Proc. 40th IEEE Conf. Decision and Control*, vol. 1, 2001, pp. 516–521.

[28] J. S. Yu, "A robust adaptive wheel-slip controller for antilock brake system," in *Proc. 36th IEEE Conf. Decision and Control*, vol. 3, 1997, pp. 2545–2546.

[29] J.-H. Choi, J.-K. Lee, S.-Y. Yang, and S.-T. Park, "A robust controller for maximizing braking force despite of the parameter variation," in *Proc. 4th Korea-Russia Int. Symp. Science and Technology KORUS 2000*, vol. 3, 2000, pp. 61–65.

[30] T.-T. Lee, C.-F. Hsu, and S. Lee, "Robust hybrid control for antilock braking systems," in *Proc. IEEE Int Systems, Man and Cybernetics Conf*, vol. 1, 2003, pp. 84–89.

[31] Y.-E. Mao, Y. Zheng, Y. Jing, G. M. Dimirovski, and S. Hang, "An lmi approach to slip ratio control of vehicle antilock braking systems," in *Proc. ACC '09. American Control Conf*, 2009, pp. 3350–3354.

[32] R. Chikhi, A. El Hadri, and J. C. Cadiou, "Optimal control for anti-braking system," in *Proc. IEEE Int. Symp. Control and Automation Mediterrean Conf Intelligent Control*, 2005, pp. 581–585.

[33] R. Morselli and R. Zanasi, "Self-tuning control strategy for antilock braking systems," in *Proc. American Control Conf*, 2006.

[34] S. Armeni and E. Mosca, "ABS with constrained minimum energy control law," in *Proc. IEEE Conf. Control Applications CCA 2003*, vol. 1, 2003, pp. 19–24.

[35] Z. Xin, L. Yuanyuan, and Y. Xiufang, "Study of control logic for automobile anti-lock braking system," in *Proc. Int Intelligent Computation Technology and Automation (ICICTA) Conf*, vol. 1, 2008, pp. 493–497.

[36] W. K. Lennon and K. M. Passino, "Intelligent control for brake systems," *IEEE Transactions on Control Systems Technology*, vol. 7, no. 2, pp. 188–202, 1999.

[37] R. Zhang, L. Weng, W. Cai, and Y. D. Song, "Neuro-adaptive control method for antilock braking systems," in *Proc. 7th World Congress Intelligent Control and Automation WCICA 2008*, 2008, pp. 2859–2863.

[38] W.-Y. Wang, I.-H. Li, M.-C. Chen, S.-F. Su, and S.-B. Hsu, "Dynamic slip-ratio estimation and control of antilock braking systems using an observer-based direct adaptive fuzzy–neural controller," *IEEE Transactions on Industrial Electronics*, vol. 56, no. 5, pp. 1746–1756, 2009.

[39] A. V. Topalov, E. Kayacan, Y. Oniz, and O. Kaynak, "Neuro-fuzzy control of antilock braking system using variable-structure-systems-based learning algorithm," in *Proc. Int. Conf. Adaptive and Intelligent Systems ICAIS '09*, 2009, pp. 166–171.

[40] C.-K. Chen and Y.-C. Wang, "Fuzzy control for the anti-lock brake system," in *Proc. Asian Fuzzy Systems Symp. 'Soft Computing in Intelligent Systems and Information Processing'*, 1996, pp. 67–72.

[41] C.-M. Lin and C.-F. Hsu, "Self-learning fuzzy sliding-mode control for antilock braking systems," *IEEE Transactions on Control Systems Technology*, vol. 11, no. 2, pp. 273–278, 2003.

[42] R. E. Precup, S. Preitl, M. Balas, and V. Balas, "Fuzzy controllers for tire slip control in anti-lock braking systems," in *Proc. IEEE Int Fuzzy Systems Conf*, vol. 3, 2004, pp. 1317–1322.

[43] J. A. Cabrera, A. Ortiz, J. J. Castillo, and A. Simon, "A fuzzy logic control for antilock braking system integrated in the inmma tire test bench," *IEEE Transactions on Vehicular Technology*, vol. 54, no. 6, pp. 1937–1949, 2005.

[44] A. Mirzaei, M. Moallem, B. M. Dehkordi, and B. Fahimi, "Design of an optimal fuzzy controller for antilock braking systems," *IEEE Transactions on Vehicular Technology*, vol. 55, no. 6, pp. 1725–1730, 2006.

[45] J.-M. Zhang, B.-Y. Song, and G. Sun, "An advanced control method for abs fuzzy control system," in *Proc. Int Intelligent Computation Technology and Automation (ICICTA) Conf*, vol. 1, 2008, pp. 845–849.

[46] K. Yang, J. Li, Y. Li, H. Wan, Z. Wang, C. Li, and S. Tan, "Simulation of fuzzy pi controller for abs based on electromechanical brake system," in *Proc. IEEE Int. Conf. Vehicular Electronics and Safety ICVES 2006*, 2006, pp. 407–412.

[47] J. Davis, L. I., G. V. Puskorius, F. Yuan, and L. A. Feldkamp, "Neural network modeling and control of an anti-lock brake system," in *Proc. Intelligent Vehicles '92 Symp.*, 1992, pp. 179–184.

[48] F. Yuan, G. V. Puskorius, L. A. Feldkamp, and J. Davis, L. I., "Neural network control of a four-wheel abs model," in *Proc. 37th Midwest Symp. Circuits and Systems*, vol. 2, 1994, pp. 1503–1506.

[49] W. Ning and Z. Chongyang, "A neuron controller with self-tuning gain for anti-lock braking systems," in *Proc. 3rd World Congress Intelligent Control and Automation*, vol. 2, 2000, pp. 1018–1021.

[50] C.-M. Lin and C.-F. Hsu, "Neural-network hybrid control for antilock braking systems," *IEEE Transactions on Neural Networks*, vol. 14, no. 2, pp. 351–359, 2003.

[51] K.-S. Park and J.-T. Lim, "Wheel slip control for abs with time delay input using feedback linearization and adaptive sliding mode control," in *Proc. Int. Conf. Control, Automation and Systems ICCAS 2008*, 2008, pp. 290–295.

[52] J. O. Pedro, O. T. C. Nyandoro, and S. John, "Neural network based feedback linearisation slip control of an anti-lock braking system," in *Proc. 7th Asian Control Conf. ASCC 2009*, 2009, pp. 1251–1257.

[53] A. Poursamad, "Adaptive feedback linearization control of antilock braking systems using neural networks," *Mechatronics*, vol. 19, no. 5, pp. 767 – 773, 2009.

[54] F. Chikhi, A. El Hadri, and J. C. Cadiou, "ABS control design based on wheel-slip peak localization," in *Proc. Fifth Int. Workshop Robot Motion and Control RoMoCo '05*, 2005, pp. 73–77.

[55] H. Yu and U. Ozguner, "Extremum-seeking control strategy for abs system with time delay," in *Proc. American Control Conf the 2002*, vol. 5, 2002, pp. 3753–3758.

[56] C. Zhang and R. Ordonez, "Non-gradient extremum seeking control of feedback linearizable systems with application to abs design," in *Proc. 45th IEEE Conf. Decision and Control*, 2006, pp. 6666–6671.

[57] ——, "Numerical optimization-based extremum seeking control with application to abs design," *IEEE Transactions on Automatic Control*, vol. 52, no. 3, pp. 454–467, 2007.

[58] S. B. Choi, "Antilock brake system with a continuous wheel slip control to maximize the braking performance and the ride quality," *IEEE Transactions on Control Systems Technology*, vol. 16, no. 5, pp. 996–1003, 2008.

[59] Y. Oniz, E. Kayacan, and O. Kaynak, "A dynamic method to forecast the wheel slip for antilock braking system and its experimental evaluation," *IEEE Transactions on Systems, Man, and Cybernetics, Part B: Cybernetics*, vol. 39, no. 2, pp. 551–560, 2009.

[60] H. Tan and Y. Chin, "Vehicle traction control: variable structure control approach," *Journal of Dynamic Systems, measurement and Control*, vol. 113, pp. 223–230, 1991.

[61] A. Cavallo and C. Natale, "High-order sliding control of mechanical systems: theory and experiments," *Control Engineering Practice*, vol. 12, no. 9, pp. 1139 – 1149, 2004.

[62] S. Drakunov, V. Utkin, S. Zarei, and J. Miller, "Sliding mode observers for automotive applications," in *Proc. IEEE Int Control Applications Conf*, 1996, pp. 344–346.

[63] S. Drakunov and V. Utkin, "Sliding mode observers. tutorial," in *Proc. 34th IEEE Conf. Decision and Control*, vol. 4, 1995, pp. 3376–3378.

[64] J. Davila, L. Fridman, and A. Levant, "Second-order sliding-mode observer for mechanical systems," *IEEE Transactions on Automatic Control*, vol. 50, no. 11, pp. 1785–1789, 2005.

[65] J. Davila, L. Fridman, and A. Poznyak, "Observation and identification of mechanical systems via second order sliding modes," in *Proc. VSS'06 Variable Structure Systems Int. Workshop*, 2006, pp. 232–237.

[66] H. Shraim, B. Ananou, L. Fridman, H. Noura, and M. Ouladsine, "Sliding mode observers for the estimation of vehicle parameters, forces and states of the center of gravity," in *Proc. 45th IEEE Conf. Decision and Control*, 2006, pp. 1635–1640.

[67] N. K. M'sirdi, A. Rabhi, L. Fridman, J. Davila, and Y. Delanne, "Second order sliding mode observer for estimation of velocities, wheel sleep, radius and stiffness," in *Proc. American Control Conf*, 2006.

[68] M. Bouteldja, A. El Hadri, J. C. Cadiou, J. A. Davila, and L. Fridman, "Observation and estimation of dynamics performance of heavy vehicle via second order sliding modes," in *Proc. VSS'06 Variable Structure Systems Int. Workshop*, 2006, pp. 280–285.

[69] G. Baffet, A. Charara, and D. Lechner, "Experimental evaluation of a sliding mode observer for tire-road forces and an extended kalman filter for vehicle sideslip angle," in *Proc. 46th IEEE Conf. Decision and Control*, 2007, pp. 3877–3882.

[70] H. Imine, L. Fridman, H. Shraim, and M. Djemai, *Sliding Mode Based Analysis and Identification of Vehicle Dynamics (Lecture Notes in Control and Information Sciences)*, 1st ed. Springer, 8 2011.

[71] Y.-K. Chin, W. C. Lin, D. M. Sidlosky, D. S. Rule, and M. S. Sparschu, "Sliding-mode ABS wheel-slip control," in *Proc. American Control Conf*, 1992, pp. 1–8.

[72] H. Ebrahimirad, M. J. Yazdanpanah, and R. Kazemi, "Sliding mode four wheel slip-ratio control of anti-lock braking systems," in *Proc. IEEE Int. Conf. Industrial Technology IEEE ICIT '04*, vol. 3, 2004, pp. 1602–1606.

[73] A. Harifi, A. Aghagolzadeh, G. Alizadeh, and M. Sadeghi, "Designing a sliding mode controller for slip control of antilock brake systems," *Transportation Research Part C: Emerging Technologies*, vol. 16, no. 6, pp. 731 – 741, 2008.

[74] C. Unsal and P. Kachroo, "Sliding mode measurement feedback control for antilock braking systems," *IEEE Transactions on Control Systems Technology*, vol. 7, no. 2, pp. 271–281, 1999.

[75] M. Schinkel and K. Hunt, "Anti-lock braking control using a sliding mode like approach," in *Proc. American Control Conf the 2002*, vol. 3, 2002, pp. 2386–2391.

[76] S. Baek, J. Song, D. Yun, H. Kim, and K. Boo, "Application of a sliding mode control to anti-lock brake system," in *Proc. Int. Conf. Control, Automation and Systems ICCAS 2008*, 2008, pp. 307–311.

[77] S. Zhang, S. Zhou, and J. Sun, "Vehicle dynamics control based on sliding mode control technology," in *Proc. Chinese Control and Decision Conf. CCDC '09*, 2009, pp. 2435–2439.

[78] L. Junwei and W. Jian, "Design of antilock braking system based on variable structure control," in *Proc. IEEE Int. Conf. Intelligent Computing and Intelligent Systems ICIS 2009*, vol. 2, 2009, pp. 411–415.

[79] T. Kawabe, M. Nakazawa, I. Nostu, and Y. Watanabe, "A sliding mode controller for anti-lock brake system: usage of sluggish actuators," in *Proc. 35th IEEE Decision and Control*, vol. 3, 1996, pp. 2769–2770.

[80] S. Drakunov, U. Ozguner, P. Dix, and B. Ashrafi, "ABS control using optimum search via sliding modes," *IEEE Transactions on Control Systems Technology*, vol. 3, no. 1, pp. 79–85, 1995.

[81] N. Patel, C. Edwards, and S. K. Spurgeon, "Optimal braking and estimation of tyre friction in automotive vehicles using sliding modes," *International Journal of Systems Science*, vol. 38, pp. 901–912, 2007.

[82] A. Hadri, J. Cadiou, and N. MSirdi, "Adaptive sliding mode control for vehicle traction," in *IFAC World Congress, Barcelona, Spain*, July 22-26 2002.

[83] W.-Y. Wang, K.-C. Hsu, T.-T. Lee, and G.-M. Chen, "Robust sliding mode-like fuzzy logic control for anti-lock braking systems with uncertainties and disturbances," in *Proc. Int Machine Learning and Cybernetics Conf*, vol. 1, 2003, pp. 633–638.

[84] J. K. Hwang, K. H. Oh, and C. K. Song, "Sliding mode control with disturbance observer for antilock braking systems," in *Proc. Conf. IEEE/ASME Int Advanced Intelligent Mechatronics*, 2005, pp. 277–281.

[85] T. Shim, S. Chang, and S. Lee, "Investigation of sliding-surface design on the performance of sliding mode controller in antilock braking systems," *IEEE Transactions on Vehicular Technology*, vol. 57, pp. 747–759, 2008.

[86] J. Song, "Performance evaluation of a hybrid electric brake system with a sliding mode controller," *Mechatronics*, vol. 15, no. 3, pp. 339 – 358, 2005.

[87] M.-C. Wu and M.-C. Shih, "Simulated and experimental study of hydraulic anti-lock braking system using sliding-mode pwm control," *Mechatronics*, vol. 13, no. 4, pp. 331 – 351, 2003.

[88] M. Amodeo, A. Ferrara, R. Terzaghi, and C. Vecchio, "Wheel slip control via second-order sliding-mode generation," *IEEE Transactions on Intelligent Transportation Systems*, vol. 11, no. 1, pp. 122–131, 2010.

[89] A. Alleyne, "Improved vehicle performance using combined suspension and braking forces," in *Proc. American Control Conf*, vol. 3, 1995, pp. 1672–1676.

[90] Y. M. Sam, J. H. S. Osman, and M. R. A. Ghani, "A class of proportional-integral sliding mode control with application to active suspension system," *Systems & Control Letters*, vol. 51, no. 3-4, pp. 217 – 223, 2004.

[91] W.-Y. Wang, Y.-H. Chien, M.-C. Chen, and T.-T. Lee, "Control of uncertain active suspension system with anti-lock braking system using fuzzy neural controllers," in *Proc. IEEE Int. Conf. Systems, Man and Cybernetics SMC 2009*, 2009, pp. 3371–3376.

[92] J. Lin and W. Ting, "Nonlinear control design of anti-lock braking systems with assistance of active suspension," *IET Control Theory & Applications*, vol. 1, no. 1, pp. 343–348, 2007.

[93] C. Clover and J. Bernard, "Longitudinal tire dynamics," *Vehicle System Dynamics*, vol. 29, pp. 231–259, 1998.

[94] I. Novozhilov, P. Kruchinin, and M. Magomedov, "Contact force relation between the wheel and the contact surface," *Collection of scientific and methodic papers Teoreticheskaya mekhanika, MSU*, vol. 23, pp. 86–95, 2000, (In Russian).

[95] P. Kruchinin, M. Magomedov, and I. Novozhilov, "Mathematical model of an automobile wheel for antilock modes of motion." *Mechanics of Solids*, vol. 36, no. 6, pp. 52–57, 2001.

[96] I. Petersen, A. Johansen, J. Kalkkuhl, and J. Ludemann, "Wheel slip control in ABS brakes using gain scheduled constrianed LQR," in *Proc. European Contr. Conf., Porto.*, 2001.

[97] M. Magomedov, V. Alexandrov, and K. Pupkov, "Robust adaptive stabilization of moving a car under braking with ABS in control circuit," in *Automotive and Transportation Technology Congress and Exposition Proceedings Chassis and Total Vehicle, Barcelona, SPAIN.*, S. S. ATTCE, Ed., vol. 6, 2001.

[98] E. Bakker, H. Pacejka, and L. Lidner, "A new tire model with application in vehicle dynamic studies," *SAE Paper No. 890087*, vol. 01, pp. 101–113, 1989.

[99] V. I. Utkin, *Sliding Modes in Control and Optimization.* Springer-Verlag, Berlin, 1992.

[100] W. Perruquetti and J.-P. Barbot, *Sliding Mode Control In Engineering (Automation and Control Engineering)*, 1st ed. CRC Press, 1 2002.

[101] V. Utkin, J. Guldner, and J. Shi, *Sliding Mode Control in Electro-Mechanical Systems, Second Edition (Automation and Control Engineering)*, 2nd ed. CRC Press, 5 2009.

[102] A. G. Loukyanov and V. I. Utkin, "Methods of reducing equations for dynamic systems to a regular form," *Automation and Remote Control*, vol. 42, no. 4, pp. 413–420, 1981.

[103] S. V. Drakunov, D. B. Izosimov, A. G. Lukyanov, V. A. Utkin, and V. Utkin, "The block control principle I," *Automation and Remote Control*, vol. 51, pp. 601–608, 1990.

[104] ——, "The block control principle II," *Automation and Remote Control*, vol. 51, pp. 737–746, 1990.

[105] A. Adhami-Mirhosseini and M. J. Yazdanpanah, "Robust tracking of perturbed nonlinear systems by nested sliding mode control," in *Proc. Int. Conf. Control and Automation ICCA '05*, vol. 1, 2005, pp. 44–48.

[106] P. K. Rashevskii, *Geometrical Theory of Partial Differential Equations.* Gostekhiizdat, Moscow, 1947, in Russian.

[107] V. I. Utkin, S. V. Drakunov, and D. B. Izosimov, "Hierarchical principle of the control system decomposition based on motion separation," in *The 9th World IFAC Congress, Budapest, Hungary*, July 2-6 1984.

[108] V. Utkin, *Sliding Modes in Control and Optimization (Communications and Control Engineering).* Springer, 2 1992.

[109] B. Drazenovic, "The invariance conditions in variable structure systems," *Automatica*, vol. 5, no. 3, pp. 287–295, 1969.

[110] A. Isidori, *Nonlinear Control Systems (Communications and Control Engineering)*, 3rd ed. Springer, 1995.

[111] M. Krstic, I. Kanellakopoulos, and P. V. Kokotovic, *Nonlinear and Adaptive Control Design (Adaptive and Learning Systems for Signal Processing, Communications and Control Series)*, 1st ed. Wiley-Interscience, 5 1995.

[112] C. Edwards and S. Spurgeon, *Sliding Mode Control: Theory And Applications (Series in Systems and Control)*, 1st ed. CRC Press, 1998.

[113] J. E. Hernandez, A. G. Loukianov, B. Castillo-Toledo, and V. I. Utkin, "Observer based decomposition control of linear delayed systems," in *Proc. 40th IEEE Conf. Decision and Control*, vol. 2, 2001, pp. 1867–1872.

[114] O. Espinosa-Guerra, A. G. Loukianov, and B. Castillo-Toledo, "Block predictor sliding mode control of linear time delay sytems," in *Proc. Int. Conf. Control and Automation ICCA '05*, vol. 1, 2005, pp. 20–25.

[115] A. Loukianov, "Nonlinear block control with sliding mode," *Automation and Remote Control*, vol. 59, no. 7, pp. 916–933, 1998.

[116] V. I. Utkin, D.-S. Chen, and H.-C. Chang, "Block control principle for mechanical systems," *Journal of dynamic systems, measurement, and control*, vol. 122, no. 1, pp. 1–10, 2000.

[117] A. G. Loukianov, B. Castillo-Toledo, and S. Dodds, "Robust stabilization of a class of uncertain system via block decomposition and vsc," *International Journal of Robust and Nonlinear Control*, vol. 12, no. 15, pp. 1317–1338, December 2002.

[118] S. Rao, H. Brandtstadter, V. Utkin, and M. Buss, "Generalized block control principle," in *Proceedings of the 16th IFAC World Congress*, 2005.

[119] M. I. Galicia, A. G. Loukianov, and J. Rivera, "Second order sliding mode sensorless torque regulator for induction motor," in *Proc. 49th IEEE Conf. Decision and Control (CDC)*, 2010, pp. 78–83.

[120] A. G. Loukianov, S. J. Dodds, W. Hosny, and J. Vittek, "A robust automotive controller design," in *Proc. IEEE Int Control Applications Conf*, 1997, pp. 806–811.

[121] E. N. Sanchez, A. G. Loukianov, and R. A. Felix, "Stepper motor trajectory tracking via dynamic block form neural networks," in *Proc. IEEE Int Intelligent Control Symp*, 2000, pp. 267–272.

[122] R. A. Felix, E. N. Sanchez, and A. G. Loukianov, "Neural block control with input constraints for induction motors," in *Proc. 29th Annual Conf. of the IEEE Industrial Electronics Society IECON '03*, vol. 3, 2003, pp. 3007–3012.

[123] E. Sanchez, A. Loukianov, and R. Felix, "Recurrent neural block form control," *Automatica*, vol. 39, no. 7, pp. 1275–1282, 2003.

[124] V. H. Benitez, E. N. Sanchez, and A. G. Loukianov, "Neural block control for a synchronous electric generator," in *Proc. IEEE Int Neural Networks Joint Conf*, vol. 4, 2004, pp. 2919–2924.

[125] A. G. Loukianov, J. M. Canedo, V. I. Utkin, and J. Cabrera-Vazquez, "Discontinuous controller for power systems: sliding-mode block control approach," *IEEE Transactions on Industrial Electronics*, vol. 51, no. 2, pp. 340–353, 2004.

[126] A. G. Loukianov, J. M. Canedo, L. M. Fridman, and A. Soto-Cota, "High-order block sliding-mode controller for a synchronous generator with an exciter system," *IEEE Transactions on Industrial Electronics*, vol. 58, no. 1, pp. 337–347, 2011.

[127] A. Y. Alanis, E. N. Sanchez, A. G. Loukianov, and M. A. Perez-Cisneros, "Real-time discrete neural block control using sliding modes for electric induction motors," *IEEE Transactions on Control Systems Technology*, vol. 18, no. 1, pp. 11–21, 2010.

[128] A. Estrada and L. M. Fridman, "Quasi-continuous HOSM control for systems with unmatched perturbations," *Automatica*, vol. 11, pp. 1916–1919, 2010.

[129] ——, "Integral HOSM semiglobal controller for finite-time exact compensation of unmatched perturbations," *IEEE Transactions on Automatic Control*, vol. 55, no. 11, pp. 2645–2649, 2010.

[130] A. Sabanovic, L. Fridman, and S. Spurgeon, *Variable Structure Systems: From Principles to Implementation (IEE Control Engineering)*. The Institution of Engineering and Technology, 2004.

[131] A. Polyakov and A. Poznyak, "Reaching time estimation for "super-twisting" second order sliding mode controller via Lyapunov function designing," *IEEE Transactions on Automatic Control*, vol. 54, no. 8, pp. 1951–1955, 2009.

[132] J. A. Moreno and M. Osorio, "A Lyapunov approach to second-order sliding mode controllers and observers," in *Proc. 47th IEEE Conf. Decision and Control CDC 2008*, 2008, pp. 2856–2861.

[133] A. G. Loukianov, "Robust block decomposition sliding mode control design," *Mathematical Problems in Engineering*, vol. 8, no. 4-5, pp. 349–365, 2002.

[134] L. González-Jiménez and A. Loukianov, "Integral nested sliding mode control for robotic manipulators," in *Proc.of the 17th IFAC World Congress pp. 9899-9904, Seoul, Korea, July 6-11*, 2008.

[135] H. Huerta-Avila, A. G. Loukianov, and J. M. Canedo, "Nested integral sliding modes of large scale power system." in *Proc. 46th IEEE Conf. Decision and Control*, 2007, pp. 1993–1998.

[136] H. Huerta, A. Loukianov, and J. Cañedo, *Systems, Structure and Control*, August 2008, ch. Integral Sliding Modes with Block Control and its Application to Electric Power Systems, pp. 83–110.

[137] H. Huerta, A. G. Loukianov, and J. M. Canedo, "Multimachine power-system control: Integral-sm approach," *IEEE Transactions on Industrial Electronics*, vol. 56, no. 6, pp. 2229–2236, 2009.

[138] H. K. Khalil, *Nonlinear Systems (3rd Edition)*, 3rd ed. Prentice Hall, 12 2001.

[139] W. M. Wonham, *Linear Multivariable Control: A Geometric Approach*, 2nd ed. Springer, 1979.

Appendices

Publications

Published articles

- Vazquez, Ivan., Galicia, Marcos I., Sánchez-Torres, Juan Diego., Loukianov, Alexander G., Kruchinin, Pavel A., "Integral Nested Sliding Mode Control for Antilock Brake System" *Proc. of 6th IFAC Symposium Advances in Automotive Control*, Munich, Germany, July 11, 2010.

- Galicia, Marcos I., Sánchez-Torres, Juan Diego., Loukianov, Alexander G., Rivera, Jorge, "Sliding mode control for Antilock Brake System" *7th International Conference on Electrical Engineering Computing Science and Automatic Control (CCE)*, pp. 87 92, Tuxtla Gutierrez México, 8-10 Sept. 2010

Accepted for publication

- Sánchez-Torres, Juan Diego., Loukianov, Alexander G., Galicia, Marcos I., Rivera, Jorge, "A Sliding Mode Regulator for Antilock Brake System" *Proc. of the 18th IFAC World Congress*, August 28 - September 2, 2011, Milano, Italy

- Sánchez-Torres, Juan Diego., Loukianov, Alexander G., Ruiz, Javier., Rivera, Jorge, "ABS + Active Suspension Control via Sliding Modes and Linear Geometric Methods for Disturbance Attenuation" *IEEE Conference in Decision and Control*, December 12-15, 2011, Orlando, Florida.

Submitted

- Sánchez-Torres, Juan Diego., Loukianov, Alexander G., Galicia, Marcos I., Rivera, Jorge, "Robust Nested Sliding Modes Integral Control for Antilock Brake System"

Paper submitted for the: International Journal of Vehicle Design Special Issue on Variable Structure System in Automotive Application.

CENTRO DE INVESTIGACIÓN Y DE ESTUDIOS AVANZADOS DEL I.P.N.
UNIDAD GUADALAJARA

"2011, Año del Turismo en México"

El Jurado designado por la Unidad Guadalajara del Centro de Investigación y de Estudios Avanzados del Instituto Politécnico Nacional aprobó la tesis

Control robusto por modos deslizantes de un sistema ABS
Robust sliding mode control of antilock brake system

del (la) C.

Juan Diego SÁNCHEZ TORRES

el día 22 de Agosto de 2011.

Dr. Edgar Nelson Sánchez Camperos
Investigador CINVESTAV 3D
CINVESTAV Unidad Guadalajara

Dr. Alexander Georgievich Loukianov
Investigador CINVESTAV 3C
CINVESTAV Unidad Guadalajara

Dr. José Javier Ruíz León
Investigador CINVESTAV 3B
CINVESTAV Unidad Guadalajara